# CHARACTERIZATION OF *VIBRIO FISCHERI* MUTANTS WITH ALTERED AMINO ACID METABOLISM AND PEPTIDOGLYCAN BIOSYNTHESIS

by

RICHARD M. JONES, JR.

(Under the Direction of ERIC V. STABB)

## ABSTRACT

Bacteria generate and catabolize a number of non-proteinogenic amino acids, which serve many functions and some are best known as constituents of the peptidoglycan (PG) cell wall. PG is a distinctive, highly conserved Prokaryote-specific structure, and Eukaryotes have evolved to recognize PG along with other microbe-associated molecular patterns (MAMPs). For example, in the monospecific symbiotic relationship between the marine bacterium *Vibrio fischeri* and its squid host *Euprymna scolopes*, *V. fischeri* PG is important for triggering normal host development. While PG structure is largely conserved, there is natural variation among bacteria, and the identity of the non-proteinogenic amino acids in PG can affect the pathways by which this MAMP elicits responses in the host. In this dissertation, I describe a strategy to alter *V. fischeri*'s PG by generating auxotrophic mutants that require PG-specific amino acids and selecting spontaneous suppressor mutants able to overcome this auxotrophy. I report the characterization of two distinct types of suppressor mutants; one that had induced a novel pathway to generate wild-type PG and another that had evolved a new PG structure. In the former case, suppression of the D-Glu auxotrophy exhibited by a glutamate racemase (*murI*) mutant led me to discover a D-Asp

responsive transcriptional regulator, DarR. I provide evidence that mutation of *darR* can render its encoded protein active in the absence of effector and compensate for the *murI* mutation by increasing expression of an Asp racemase gene with cryptic Glu racemase activity. In the second case, I describe a mutant of *V. fischeri* that has replaced diaminopimelate with lanthionine in the peptide side chain structure of its PG, a feature that appears to be enabled by alterations in cysteine metabolism. Despite this change in PG structure, cell surface fractions from the mutant with lanthionine-containing PG still induced morphogenesis in the host. Together, these data broaden our understanding of D-amino acid catabolism, PG evolution, and the flexibility of PG recognition in a model symbiosis.

INDEX WORDS: *Aliivibrio*, *Photobacterium*, signaling, peptidoglycan, D-aspartate

# CHARACTERIZATION OF *VIBRIO FISCHERI* MUTANTS WITH ALTERED AMINO ACID METABOLISM AND PEPTIDOGLYCAN BIOSYNTHESIS

by

RICHARD M. JONES, JR.

B.S., Clemson University, 2010

A Dissertation Submitted to the Graduate Faculty of The University of Georgia in Partial Fulfillment of the Requirements for the Degree

DOCTOR OF PHILOSOPHY

ATHENS, GEORGIA

2017

# CHARACTERIZATION OF *VIBRIO FISCHERI* MUTANTS WITH ALTERED AMINO ACID METABOLISM AND PEPTIDOGLYCAN BIOSYNTHESIS

by

RICHARD M. JONES, JR.

| | |
|---|---|
| Major Professor: | Eric V. Stabb |
| Committee: | Anna Karls |
| | Ellen Neidle |
| | Lawrence Shimkets |

Electronic Version Approved:

Suzanne Barbour
Dean of the Graduate School
The University of Georgia
May 2017

# DEDICATION

I dedicate this work to my godchildren, Mary Catherine Wilkinson and Jamani Travion Rodgers.

May they grow to love learning.

ACKNOWLEDGEMENTS

First and foremost, I want to acknowledge my wife, Mellisa Roskosky. She has been the most supportive, patient, and loving partner I could have ever dreamed of throughout this entire process. I want to also thank my family and friends for their continued support. My committee members, Anna Karls, Ellen Neidle, and Larry Shimkets, have been incredibly helpful. I must especially thank Anna for serving as my teaching mentor and sponsoring me for the Future Faculty Program. I also want to thank my advisor, Eric Stabb, and current and past members of the Stabb Lab for their continued help, feedback, and support.

TABLE OF CONTENTS

Page

ACKNOWLEDGEMENTS ..... v

LIST OF TABLES ..... viii

LIST OF FIGURES ..... ix

LIST OF ABBREVIATIONS ..... xi

CHAPTER

1 Introduction and Literature Review ..... 1

Overview ..... 1

*Vibrio-Euprymna* symbiosis as a model system ..... 2

Colonization of the light organ ..... 3

Developmental signals during colonization ..... 6

Effect of LPS on light organ morphogenesis ..... 7

Effect of PG-derived TCT on light-organ morphogenesis ..... 9

PG biosynthesis and recycling in *V. fischeri* ..... 10

Variations in PG structure ..... 11

Lanthionine-containing PG in *Fusobacterium nucleatum* ..... 13

Roles of free D-amino acids ..... 15

Rationale and scope of this work ..... 17

2 *Vibrio fischeri* DarR directs responses to D-aspartate and represents a wider group of LysR-type transcriptional regulators ..... 21

Abstract ..... 22
Importance ..... 22
Introduction ..... 23
Results ..... 25
Discussion ..... 35
Materials and methods ..... 41
Acknowledgements ..... 52
3 Suppression of diaminopimelic acid auxotrophy via lanthionine substitution in the peptidoglycan side chain of *Vibrio fischeri* ..... 53
Abstract ..... 54
Introduction ..... 55
Results ..... 56
Discussion ..... 62
Materials and methods ..... 68
Acknowledgements ..... 74
4 Conclusions and Future Directions ..... 75
Discovery of a D-Asp-associated LTTR ..... 76
Generation of Lantionine-containing PG mutant ..... 80
D-Ala auxotroph suppressors ..... 82
Conclusions ..... 83
REFERENCES ..... 84

LIST OF TABLES

Page

Table 1.1: Modifications to the PG side chain.....12

Table 2.1: Bacterial strains, plasmids, and oligonucleotides used in this study .....41

Table 3.1: Bacterial strains, plasmids, and oligonucleotides used in this study .....69

LIST OF FIGURES

Page

Figure 1.1: TUNEL-stained *E. scolopes* light organ....4

Figure 1.2: TCT structure ....8

Figure 1.3: Activity of a CysK homologue from *Fusobacterium nucleatum* ....14

Figure 1.4: Overview of research approach....17

Figure 2.1: Restoration of prototrophy to the D-Glu auxotroph AN3 by *darR*(M202I) or by multi-copy *racD in trans* ....26

Figure 2.2: The *V. fischeri darR* locus....27

Figure 2.3: Effect of *darR* and D-Asp on expression of $P_{racD}$-*gfp* reporter ....28

Figure 2.4: Dose dependence and specificity of $P_{racD}$-*gfp* reporter response to D-Asp....29

Figure 2.5: Evidence of DarR autorepression....30

Figure 2.6: Synteny of *darR* homologs in diverse Proteobacteria ....31

Figure 2.7: Requirement of *racD* and *darR* for growth on D-Asp ....32

Figure 2.8: Biolayer interferometry analysis of DarR DNA target binding ....33

Figure 2.9: Biolayer interferometry response of DarR to wild-type and scrambled target DNA..34

Figure 3.1: HPLC and mass spectroscopy analysis of PG isolated from wild-type strain ES114 or RMJ1S1. ....58

Figure 3.2: Mutant *cysK* alleles *in trans* overcome DAP auxotrophy of RMJ1 ....60

Figure 3.3: Decreased salt tolerance of strain RMJ1S1 ....61

Figure 3.4: Cell morphology of RMJ1S1 ....62

Figure 3.5: Counts of TUNEL+ cells after exposure to wild-type and lanthionine-containing cell-surface factions .....63

Figure 3.6: Amino acids that can replace DAP in PG biosynthesis.....64

# LIST OF ABBREVIATIONS

| | |
|---|---|
| BHI | brain-heart infusion |
| BLI | biolayer interferometry |
| CEA | ciliated epithelial appendage |
| Cm | chloramphenicol |
| CSF | cell-surface fraction |
| D-AA | D-amino acid |
| DAP | diaminopimelic acid |
| EBD | effector-binding domain |
| Em | erythromycin |
| FMM | fischeri minimal media |
| Km | kanamycin |
| LB | Luria broth |
| LBP | lipopolysaccharide binding proteins |
| LBS | Luria broth with salt added |
| LPS | lipopolysaccharide |
| LTG | lytic transglycosylase |
| LTTR | LysR-type transcriptional regulator |
| MAMP | microbe-associated molecular pattern |
| NMDA | N-methyl-D-aspartate |
| OMV | outer membrane vesicle |
| PAMP | pathogen-associated molecular pattern |
| PG | peptidoglycan |
| PGRP | peptidoglycan recognition protein |
| PIMT | protein L-isoaspartyl O-methyltransferase |
| SOE | splicing by overlap extension |
| TCT | tracheal cytotoxin |
| TUNEL | terminal deoxynucleotidyl transferase (TdT) dUTP nick-end labeling |

CHAPTER 1

# INTRODUCTION AND LITERATURE REVIEW

## OVERVIEW

Eukaryotes evolved in a sea of Prokaryotes, and have associations with microbes that are integrated into their normal biology. These host-associated microorganisms can perform beneficial functions, such as contributing to host metabolism and stimulating development (6). Beneficial bacteria can be recognized by hosts as non-self just as pathogens are. In the context of the innate immune system, bacteria are typically recognized through the presence of microbial-associated molecular patterns (MAMPs), which are conserved across both pathogens and mutualists. One such MAMP is the peptidoglycan (PG) structure that comprises the cell wall of most bacteria. PG is not found in Eukaryotes, and its structure is conserved in Bacteria, traits that make it both an ideal MAMP and a target for antibacterial drugs. Another MAMP is lipopolysaccharide (LPS), which forms the outer layer of the outer membrane of Gram-negative Bacteria and has a relatively conserved lipid A moiety anchoring it to the membrane. MAMPs such as PG and LPS have often been investigated through the lens of pathogenic relationships, and given this viewpoint they are usually called PAMPs for pathogen-associated molecular patterns. However, it is clear that these microbial structures play critical roles not only in immune recognition of potential invaders but also in beneficial symbiotic contexts.

The symbiosis between *Vibrio fischeri* and the Hawaiian bobtail squid, *Euprymna scolopes*, is an experimentally tractable association that serves as a powerful model for investigating inter-kingdom signals, including PG (7). *V. fischeri* possess a cell wall PG typical of

most Gram-negative organisms, but this bacterium is unusual in that it releases large amounts of PG fragments, which can trigger host development. The simplified immune system of the squid host is under investigation (8), and putative receptors for LPS (9) and PG (10, 11) have been identified. Model bacteria such as *V. fischeri* allow careful investigation into the biosynthesis and evolution of MAMPs. Using this natural marine symbiosis as a model system for host-microbe interactions will more broadly reveal signals and processes necessary for the establishment and maintenance of beneficial interactions.

## *VIBRIO-EUPRYMNA* SYMBIOSIS AS A MODEL SYSTEM

The *Vibrio-Euprymna* symbiosis is ideal for experimental laboratory-based study. In this monospecific relationship only the bacterium *V. fischeri* is able to colonize the light-producing organ of its squid host (12). The symbionts are transmitted horizontally, meaning that hatchling juvenile squid are aposymbiotic (without symbionts) and initiation of symbiosis can be controlled experimentally (13). The wild-type *V. fischeri* used in most symbiotic studies is strain ES114, a squid isolate that readily infects juvenile squid (14). Because the light organ is essentially external, and bathed in seawater, researchers can also expose the hatchlings to specific molecules, either synthetic or natural products, and readily track their effects on light organ development. Additionally, the *V. fischeri* genome has been sequenced and the organism can be cultured and genetically manipulated. For these reasons and others, this relationship lends itself well to controlled investigation of the mechanisms involved in establishing a productive symbiosis. The symbiotic colonization of *E. scolopes* as well as the contribution of *V. fischeri* to host development have been carefully studied, and these findings will be reviewed in the following sections.

## COLONIZATION OF THE LIGHT ORGAN

*E. scolopes* has a dedicated light-emitting organ that is located on the ventral side of the animal below the ink sac. It is hypothesized that the bioluminescent bacteria provide a counter-illumination effect to obscure the squid's silhouette from predators or prey beneath it in the water column (15-17). When the squid hatch, this organ contains appendages lined with ciliated epithelial cells used to increase water flow toward pores on the surface of the light organ, apparently to increase the likelihood of bacterial colonization (12, 18-21). For one hour after hatching, the light organ is in a "permissive" stage during which multiple types of bacteria and even polystyrene beads can be drawn into the light organ (21). After this first hour, any bacteria that were sampled are readily cleared from the light organ (21), including any *V. fischeri* cells that may have been drawn in. After the permissive stage, the juvenile squid produce mucus on the light-organ surface (20). *V. fischeri* cells in the surrounding seawater are drawn into the mantle and are able to form a biofilm "aggregate" on this mucus surface, where it can effectively outcompete close relatives such as *Vibrio parahaemolyticus* and *Photobacterium leiognathi*. Thus, mucus secretion and the aggregation of bacteria in this mucus constitute the first step in establishing the specificity of this host-microbial interaction (21, 22).

After establishment of mucus-associated aggregates on the epithelium-lined surface of the light organ, *V. fischeri* must traverse through the pores (**Figure 1.1**) and pass through ducts into the light organ crypts, where it grows to establish a symbiotic population (20, 23). Upon initial colonization of the first few cells, broad transcriptional changes are induced in the host, including the expression of an endochitinase enzyme (24). This enzyme hydrolyzes chitin in the mucus to generate a chitobiose gradient that promotes migration of *V. fischeri* into the deep crypts (24). Full colonization requires that the bacteria are motile (25), as they must be able to move inward through

ducts containing cilia that beat outwards (19). *V. fischeri* can also recognize *N*-acetylneuraminic acid, a component of squid mucus, as a chemoattractant (26). Multiple studies indicate that motility and chemotaxis contribute to efficient infection (27-30). Bacteria other than *V. fischeri* also may aggregate on the light organ surface and migrate to the pores, but they are not often found in the ducts or crypts of the light organ (20). After reaching the crypts, *V. fischeri* cells multiply rapidly, stop producing flagella, and eventually begin to bioluminesce (31).

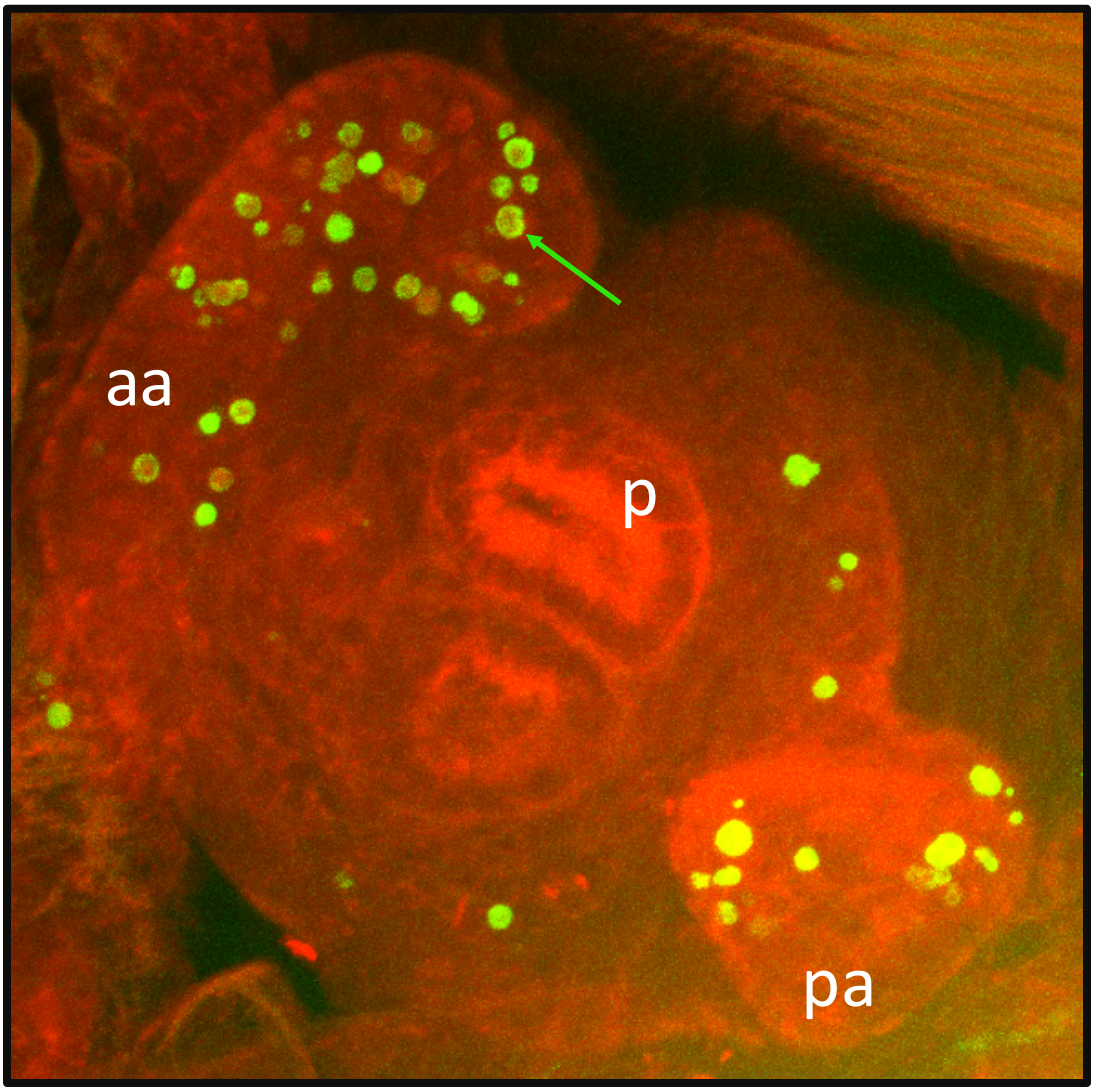


**Figure 1.1** Terminal deoxynucleotidyl transferase (TdT) dUTP Nick-End Labeling (TUNEL) stained *E. scolopes* light organ, after 24 h exposure to ES114 cell-surface fractions. Shown are the posterior (pa) and anterior appendages (aa) and pores (p). TUNEL+ cells undergoing apoptosis are green (green arrow). Over the course of four days, both appendages will regress as a result of the apoptosis seen here. (RM Jones, unpublished image).

As is the case in pathogenic interactions, the immune response of the squid is activated by the presence of bacteria. Invertebrates such as *E. scolopes* have immune systems that lack adaptive components but have the capacity for an innate response (32). In these animals, hemocytes are the macrophage-like cells that mediate innate immune responses such as phagocytosis (33, 34). Upon initiation of symbiosis, squid hemocytes migrate to sinuses inside of the ciliated epithelial appendages (CEAs) described above that are found on the surface of the light organ (35). The CEAs are infection-promoting structures that are only present in juvenile squid (**Figure 1.1**) (36). Their absence in adults is due to normal host development triggered by bacterially-derived signals, the details of which will be discussed below. Hemocyte infiltration into the CEA sinuses does not induce CEA regression, but studies with strains that delay hemocyte trafficking suggest that high numbers of these cells in CEAs may facilitate regression (35). Further along in the colonization process, hemocytes in the crypts selectively phagocytize other bacteria while bypassing *V. fischeri*, a discriminatory ability that is not present in hosts that lack *V. fischeri* symbionts (37). These intriguing data suggest that the host's immune system is modulated by the presence of the symbiont. Indeed, the proteome of host hemocytes is affected by the colonization state of the host, as the presence of symbionts alters the abundance of certain proteins associated with the cytoskeleton, lysosomes, and immune recognition (38, 39).

The squid also has receptor proteins dedicated to recognizing various bacterial components. For example, four members of the peptidoglycan recognition protein (PGRP) family are expressed in the squid light organ (8). One of these, EsPGRP1, localizes to nuclei of squid epithelial cells, and is lost from the nuclei of the light-organ epithelium in response to either *V. fischeri* or a combination of MAMPs (10). A different PGRP, EsPGRP2, is released into the light organ crypts and acts as an amidase capable of degrading PG fragments (11). Additionally, genes

encoding three putative lipopolysaccharide binding proteins (LBPs) and one Toll-like receptor (TLR) have been identified in an *E. scolopes* expressed sequence tag database (8). Characterization of squid innate immunity and its role in the symbiosis is an active area of investigation. It is clear that through immune recognition and by other means, several signals are passed between the partners in order to establish and maintain the symbiosis.

## DEVELOPMENTAL SIGNALS DURING COLONIZATION

Upon hatching and subsequent infection with symbionts, a number of developmental changes take place in the squid light organ that are triggered by *V. fischeri*. These include changes in epithelial cell structure, a decrease in nitric oxide production, and an increase in filamentous actin (40-43). The most obvious change is visible regression of the CEAs on the light organ surface. Between 4 and 6 hours after infection with *V. fischeri*, the DNA in the CEAs begins to condense, causing the development of pyknotic nuclei (44), which are indicative of apoptotic, programmed cell death. The number of intact cells in the appendages then decreases over the next 72 to 96 hours (36), resulting in complete regression of the CEA by day 4 or 5 (45). Exposing juvenile squid to *V. fischeri* for 4 hours or less does not induce CEA regression; however, if squid are exposed for 12 hours, regression is irreversible even if symbionts are cleared with antibiotics (12, 36).

*V. fischeri*-derived outer membrane vesicles (OMVs) can deliver a portion of this developmental signal, as OMVs are sufficient to induce early-stage hemocyte trafficking (46). OMVs are released in other organisms, and can carry signals that trigger host responses, including virulence factors (47-52). In the plant pathogen *Xylella fastidiosa* OMVs serve to block the organism's attachment to the walls of xylem vessels (48). The production of OMVs in *X. fastidiosa*

is controlled through a quorum-sensing signal, and the resulting signal network serves to modulate the colonization of the plant (48). The regulation and cargo of *V. fischeri*'s OMVs are still open questions, though there is evidence that they do not contain PG derivatives (46).

Independent of any involvement in OMV-mediated signaling, PG and LPS from *V. fischeri* can induce developmental changes when introduced directly to juvenile squid (53, 54). Bacterially-derived signals such as these are not novel, as LPS and PG-based signals have been shown to induce host developmental programs in both pathogenic and symbiotic interactions (55, 56). For example, gut bacteria-derived, low-immunogenic LPS has been proposed as a therapeutic for inflammatory bowel disease (56). Additionally, the O-antigen portion of LPS has been identified as a symbiotic factor in bacterial associations with legumes and insects (57, 58). The next two sections will review the roles of LPS and PG in the *V. fischeri – E. scolopes* symbiosis.

## EFFECT OF LPS ON LIGHT-ORGAN MORPHOGENESIS

LPS, often called endotoxin in the world of pathogenic interactions, has been implicated as an important MAMP for eukaryotic organism recognition. LPS can trigger an innate immune response in many systems, and is also important for recognition of bacteria in certain mutualisms (59). In the squid symbiosis LPS alone effectively induces apoptosis in the CEAs, although it does not trigger CEA regression (53). When added to seawater, LPS purified from *Haemophilus influenza* can also stimulate apoptosis in the light organ, an effect that is weakened by altering the lipid A acylation pattern (53). Secondary acylations on lipid A are important for toxicity toward mammalian cells, and therefore could be important in triggering changes in squid morphology (53). *V. fischeri* strains lacking secondary acyltransferase genes *htrB2* or *msbB* have phenotypes commonly associated with disruption of lipid A in other Gram-negative bacteria (60), including

reduced motility, increased luminescence, and increased membrane permeability in culture (61). Conversely, an *htrB1* mutant behaves like wild-type in culture, but is attenuated in initiating the symbiosis when compared to the parent strain (61). These data suggest that lipid A modifications affect the MAMP-mediated signaling between *V. fischeri* and host cells. *V. fischeri* lipid A structure was elucidated through multistage mass spectrometry (62), revealing a unique phosphoglycerol moiety that may play a role in establishing this specific symbiosis (62). The search for the enzyme responsible for the addition of this moiety, and other lipid A and LPS-modifying enzymes in both partners is ongoing.

Recently, the rotation of *V. fischeri*'s sheathed flagella was shown to mediate the release of LPS from *V. fischeri* (63). As mentioned above, the squid has putative LBPs, presumably in

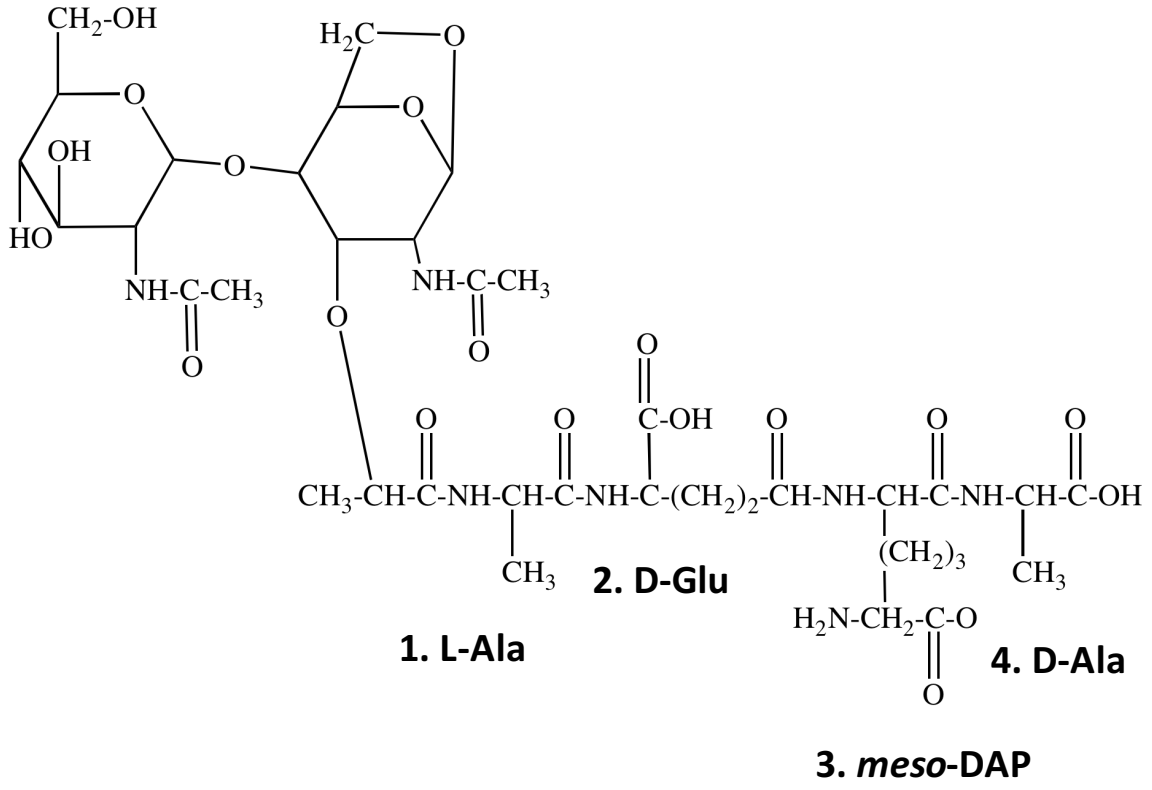


**Figure 1.2** Tracheal cytotoxin (TCT) structure. Shown are the amino acids that constitute the tetrapeptide in *V. fischeri*. This is the identity of the PG peptide in most Gram-negative organisms.

order to bind LPS. There is evidence that the host expresses one of these LBPs, EsLBP1, in response to colonization, and that it binds *V. fischeri* LPS with high affinity (9). Interestingly, expression of the *eslbp1* transcript is induced by PG derivatives rather than by LPS, and the protein is localized to the apical surface of host epithelial cells, suggesting a general role in LPS binding (9).

## EFFECT OF PG-DERIVED TRACHEAL CYTOTOXIN (TCT) ON LIGHT-ORGAN MORPHOGENESIS

Through the release of large amounts of PG monomer, a different signal is passed from *V. fischeri* to the host, in this case triggering appendage regression. The PG monomer from *V. fischeri* has the structure *N*-acetylglucosaminyl-1,6-anhydro-*N*-acetylmuramylalanyl-γ-glutamyl-diaminopimelylalanine (**Figure 1.2**) commonly called tracheal cytotoxin (TCT). Its name derives from its role in the pathogenic bacterium *Bordetella pertussis*, where it triggers the death of ciliated cells in the trachea of its human hosts, resulting in whooping cough (64). *Neisseria gonorrhoeae* also releases TCT, which is cytotoxic toward ciliated cells in the fallopian tubes of humans (65). These similar effects across hosts and tissues may reflect a conserved mechanism of action for TCT. In the two pathogenic cases, the methods of *in vivo* research typically rely on cell culture, although in some cases researchers can use cadavers and animal models. The *Vibrio*-squid model allows for precise manipulation and testing of the TCT structural components in a natural infection involving whole animals and intact tissues, providing an avenue to determine how the structure of the molecule relates to its biological function. Though TCT structure is known to cause death of ciliated host cells in the three cases above, the structural specificity of this signal is unknown.

Moreover, despite PG structure being largely conserved, as discussed below, small deviations from TCT structure could lead to major effects on PG's activity as an inter-kingdom signal.

## PG BIOSYNTHESIS AND RECYCLING IN *V. FISCHERI*

PG biosynthesis has been studied extensively in model bacteria, in part because the cell wall is a target for many important antibiotics. PG is a dynamic structure that must be constantly broken apart and reassembled to accommodate growth and division of bacterial cells. As part of this process, PG monomers are often released from the wall in the periplasm but recycled in the cytoplasm and eventually reused as the wall is re-laid.

This important process is accomplished through the action of a suite of enzymes present in most Gram-negative bacteria. Lytic transglycosylase (LTG) enzymes cleave the *N*-acetylmuramic acid-*β*-1,4-*N*-acetylglucosamine linkage in peptidoglycan and catalyze the formation of a 1,6-anhydro bond on the *N*-acetylmuramic acid to make TCT (66). In most organisms, the TCT is normally recycled back into the cytoplasm once freed from the native PG structure (67). To do so, cleaved fragments must pass through the AmpG permease, which forms a channel in the cytoplasmic membrane (68). In *B. pertussis*, the increase in TCT release can be attributed to the disruption of AmpG synthesis due to the insertion of an IS element upstream of the *ampG* gene (69, 70). By contrast, *N. gonorrhoeae* possesses a functional and expressed AmpG, and instead the action of two LTGs apparently produces so much TCT that some escapes the cell (71). The disruption of both types of proteins had effects on the net TCT release in *V. fischeri*. A *V. fischeri ampG* mutant released 100-fold more TCT than wild type, while a *ltgA ltgD ltgY* triple mutant had 10% of the normal accumulation of TCT in culture (72). In squid colonization assays, the *ampG* mutant not only induced light-organ morphogenesis even when the Δ*ampG* allele was placed in a

non-motile background, which otherwise prevents the induction of morphogenesis (72). The *ltgADY* mutant was still able to induce morphogenesis, though squid exposed to the *ltgADY* strain were more susceptible to subsequent infection suggesting that the decrease in TCT production leads to attenuated regression of the infection-promoting CEAs (72). None of the mutants completely prevented the release of the 921-Da PG monomer known as TCT.

## VARIATIONS IN PG STRUCTURE

Though PG structure is well-conserved, PG variations exist among Prokaryotes, and can affect PG's activity as a MAMP. The glycan chain that forms the basis of PG can vary in length in addition to being subject to modifications such as O-acetylation, N-deacetylation and N-glycosylation (73). However, most of the variation is present in the peptide stem. The peptide portion of PG is characterized by non-proteinogenic amino acids, particularly D-amino acids (D-AAs), and there are examples of variation at each position of the peptide stem. The greatest variation is found at position three, which is typically occupied by a diamino acid added by MurE. Most Gram-negative organisms and *Bacillus* species have *meso*-diaminopimelic acid (DAP) in this position, while most Gram-positive organisms have L-Lys. There are exceptions to this rule, and some species have other diamino (L-ornithine, *meso*-lanthionine) or even monoamino acids in this position. Examples of PG-peptide variability can be found in **Table 1.1,** which is taken largely from Vollmer and Blanot, 2008 (1). Though there are many possible variations listed, some structures are due to the activity of the organisms' PG biosynthetic pathway, while others are modifications that occur to intact PG, replacing some fraction of the canonical AA in the peptide stem after PG synthesis.

**Table 1.1** Modifications to the PG side chain, modified from Vollmer *et al*. (1)

| **Amino acid and position in *V. fischeri*** | **Alternatives** | **Examples** |
|---|---|---|
| 1. L-Ala | Gly | *Mycobacterium leprae* |
| | L-Ser | *Butyribacterium rettgeri* |
| 2. D-Glu* | D-Gln | Many Gram-positives, *Mycobacteria* |
| | 3-OH-Glu | *Microbacterium lacticum* |
| 3. *meso*-DAP | L-Lys | Most Gram-positives |
| | Lanthionine | *Fusobacterium nucleatum* |
| | L-Orn | Spirochetes |
| | L-homoserine | *Corynebacterium poinsettiae* |
| 4. D-Ala* | Gly | *Microbispora* |
| | D-Ser | |
| | D-Met | *Vibrio cholerae* |
| 5. N/A | D-Ala | Most bacteria |
| | D-Ser | *Enterococcus gallinarum* |
| | D-Lac | *Lactobacillus casei,* Vancomycin-resistant *Enterococci* |

*Alteration occurs after incorporation of D-Glu or D-Ala

There is also diversity in the length, location, and makeup of the cross-link between peptide stems. The most common is a linkage between the amino group of the AA in position 3 (usually DAP or Lys) to the carboxyl group of the D-Ala at position 4 of another peptide stem. Some species have crosslinks between peptide positions 2 and 4, and there is often variability in the number of amino acids in the bridge between stems (1, 73). The size of the bridge can range from one to seven amino acids in length. The extent to which PG is crosslinked also differs between bacterial species, ranging from approximately 20% in *E. coli* to 93% in *S. aureus* (74, 75).

Variations like those discussed above can affect PG's ability to act as a MAMP. *Drosophila melanogaster*, like *E. scolopes* and other invertebrates, relies on innate immunity to recognize and respond to invading bacteria. *D. melanogaster* has evolved the ability to detect both DAP-type PG, which is typical of Gram-negative organisms, and Lys-type PG, typical of Gram-positives, through the activity of distinct PGRPs (76). PGRP-LE and PGRP-LC each recognize DAP-type PG in *D. melanogaster*. However, they have distinct roles, as PGRP-LE acts intracellularly to recognize PG monomer such as TCT, while PGRP-LC acts extracellularly (77). Both of these PGRPs activate the Imd pathway, an innate immunity regulatory cascade in *Drosophila* that leads to production of antimicrobials such as *Diptericin* that act against Gram-negative bacteria. Conversely, PGRP-SA and PGRP-SD recognize the Lys-type PG typical of Gram-positive bacteria. These proteins serve to activate the Toll immune pathway, which leads to the production of Gram-positive specific antimicrobials such as *Drosomycin* (78). The substrate specificity of the PGRPs in *E. scolopes* is not known, though it is clear that they can recognize and respond to DAP-type PG and TCT (10, 11). Any variations in PG structure may well have roles in *V. fischeri*'s ability to signal morphogenesis to the host.

## LANTHIONINE-CONTAINING PG IN *FUSOBACTERIUM NUCLEATUM*

One organism that has evolved a PG structure containing a unique amino acid component is *Fusobacterium nucleatum*. *F. nucleatum* is a Gram-negative anaerobe and a widespread oral bacterium. This organism is of particular interest because it has been recently associated with a number of different types of infections (79). While *F. nucleatum* has been known to be a commensal of the mouth, it is now often cited as an opportunistic pathogen, though there is some debate over whether this organism is causal or simply associated with such infections (80). The

PG of *F. nucleatum* is similar to that of most other Gram-negatives, with the notable exception that *F. nucleatum* contains a lanthionine residue in the third position of its PG peptide stem where DAP or Lys are typically found (2). Variation in the amino acid identity at this position is high in the genus *Fusobacterium*. Traditional DAP- and Lys-type PG can be found, and in *Fusobacterium mortiferum* both DAP and Lanthionine can be found in the third position (2).

A study aimed at the negative effects of *F. nucleatum* on the host serendipitously uncovered a connection to its unusual PG structure. Specifically, *F. nucleatum* was studied for its ability to produce $H_2S$, a virulence factor for oral pathogens, and one of the $H_2S$-producing enzymes is a homolog of O-acetylserine sulfhydrylase, also called CysK (81). In most Gram-negative organisms, CysK catalyzes the final step in cysteine biosynthesis – the conversion of O-acetylserine to cysteine. However, researchers demonstrated that a CysK homolog, Fn1220, in *F. nucleatum* was able to condense two L-cysteines to lanthionine, producing $H_2S$ in the process (**Figure 1.3**) (82). This activity has not been demonstrated for CysK in *E. coli*, however, cysteine dehsulfhydrase activity has been shown, suggesting that CysK does have the ability to degrade

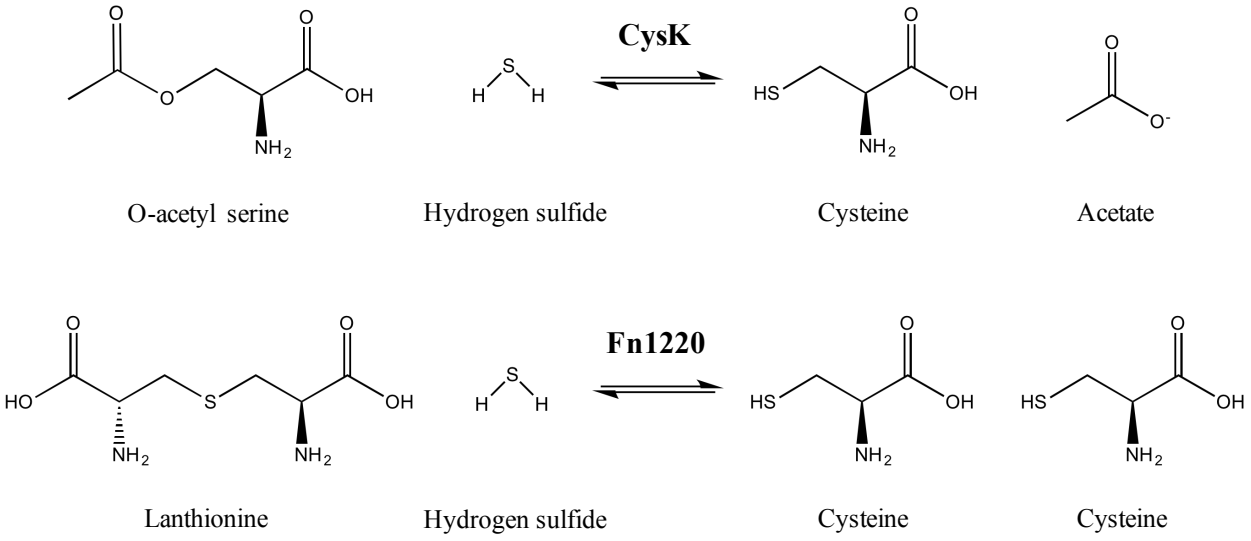


**Figure 1.3** Activities of CysK enzymes from *Fusobacterium nucleatum*. Adapted from Yoshida *et al.*

cysteine (83). The activity of *F. nucleatum* Fn1220 may raise the pool of lanthionine available to its MurE protein, allowing lanthionine to replace DAP in its PG side chain. The $H_2S$-producing enzymes from *F. nucleatum* are an area of active study, and therefore more light is likely to be shed on the mechanism of lanthionine biosynthesis and its incorporation into the PG structure.

## ROLES OF FREE D-AMINO ACIDS

The presence of D-AAs has been long recognized as one of the distinguishing features of PG structure; however, additional roles in signaling for non-proteinogenic stereoisomers of various amino acids have begun to emerge. It has become clear that bacteria produce, encounter, and direct responses to a variety of D-AAs in the environment. Bacteria may incorporate unusual D-AAs into their PG (84, 85), catabolize them (86, 87), or perhaps most intriguingly use them as signals (88). Where and why bacteria encounter D-AAs, as well as the biological significance of D-AAs for bacteria, are active areas of research, but a pattern has emerged of their involvement in developmental processes (88, 89).

D-AAs can influence bacteria through their introduction into cellular structures. For example, a new family of broad-spectrum racemases that contributes to bacterial cell-wall remodeling during stationary phase has been described (90), and these racemases generate a variety of D-AAs that are released into the environment or incorporated into PG, providing a signal that is both auto- and paracrine in nature (91). Subsequent studies have shown that D-AA-induced changes in *V. cholerae* are dependent upon RpoS, a stress-associated sigma factor, suggesting that these changes may be in response to multiple environmental cues including but not limited to the onset of stationary phase in their growth cycle (88).

D-Asp is one example of a D-AA that has an emerging role as a signal. D-Asp has been widely studied as a neural signal in mammals (92-94). It has been found in a variety of mammalian tissues, including the central nervous and endocrine systems, and has been implicated in the development and neurogenesis of the brain (95). D-Asp binds the L-Glu binding site of the *N*-methyl-D-aspartate (NMDA) receptor and therefore has been suggested as a drug for the treatment of NMDA receptor-related diseases, including depression and schizophrenia (96, 97).

In addition to their incorporation into PG, if unusual D-AAs have a role as cues or signals they would have to direct regulatory responses, and it seems likely these would be transcriptional. There are only a few examples of D-AA-responsive transcriptional regulators, but one is DsdC, which is a LysR-type transcriptional regulator (LTTR) expressed in uropathogenic *E. coli*. DsdC responds to D-Ser and acts in concert with cyclic AMP receptor protein to activate transcription of the *dsdXA* operon (98), which encodes a D-Ser transporter (DsdX) and D-Ser deaminase (DsdA). DcdX and DcdA have been proposed to act on high levels of D-Ser present in human urine (99), however a *dcdA* mutant was unimpaired in colonizing the mouse urinary tract (100). Recently, a second D-Ser-responsive LTTR was shown to sense and respond to D-Ser in enterohaemorrhagic *E. coli*. In this case, the LTTR YhaJ directly regulates an important pathogenicity island called the locus of enterocyte effacement (101). Interestingly, strains carrying both the *dsdXA* and the this pathogenicity island that are modulated by D-Ser are extremely rare, suggesting that these loci are "evolutionarily incompatible" (102). This observation shows the delicate balance between metabolic and pathogenic genes that host-associated organisms must achieve to proliferate.

Another example of a transcriptional regulator that responds to a D-AA is DguR, which was discovered in *Pseudomonas aeruginosa* PAO1. DguR was recently characterized as a D-Glu

responsive LTTR that directs the breakdown of D-Glu (87). Because D-Glu is a standard component of PG, this pathway may simply reflect a means for catabolizing bacterial cell wall fragments, which are presumably plentiful in environments with high bacterial populations and turnover.

## RATIONALE AND SCOPE OF THIS WORK

The conserved nature of the bacterial cell wall structure has long been exploited by hosts to recognize and respond to bacteria. The appropriate response may be to attack the PG to kill a pathogenic invader, or rather to begin a developmental program associated with benign bacterial colonization. Either way, the host must be able to recognize the bacterial glycan-peptide sacculus, or fragments of it. The goal of this dissertation work was to force the bacterium to adopt a new PG structure, and observe the effects of this new PG on its role as an inter-kingdom signal.

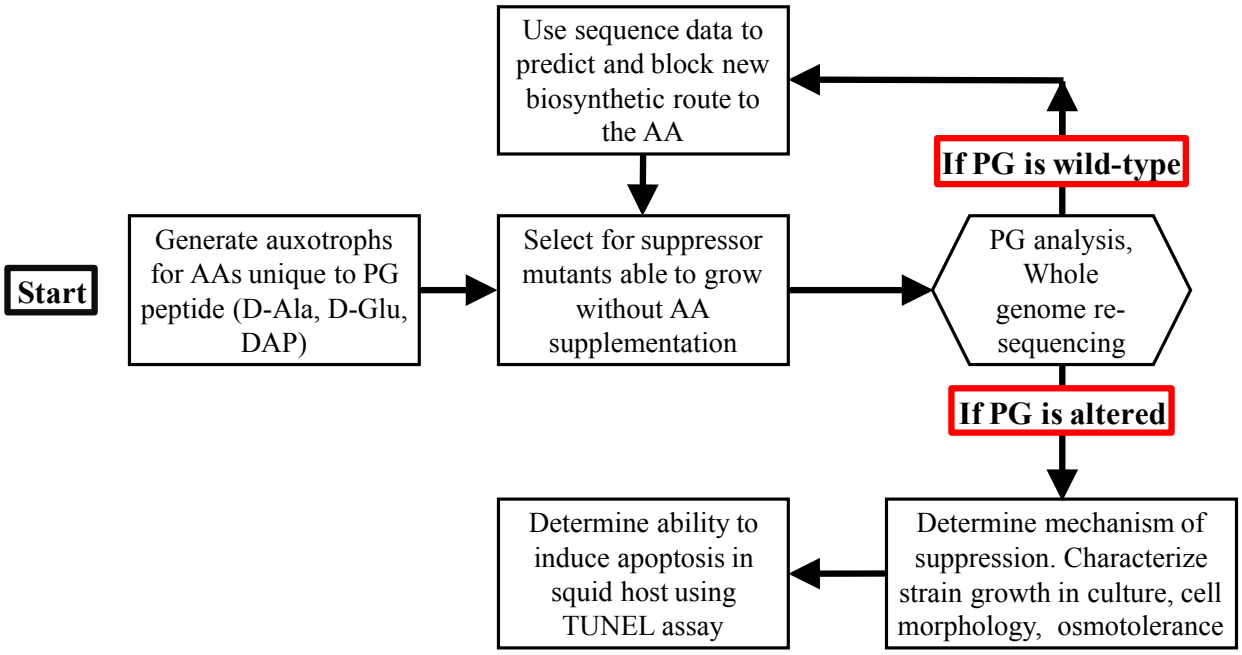


**Figure 1.4** Overview of research approach. Hexagon represents a key branch point, red boxes represent alternate outcomes.

D-Amino acids present in the PG side chain and the enzymes that generate them are deemed essential. However, somewhat paradoxically, the composition and sequence of the peptide side chain is diverse (**Table 1.1**). It seems that organisms are able to circumvent the "essentiality" of certain D-AAs by modifying their PG structure. Likely, the selective forces driving this evolution are determined by the organism's external and metabolic environments. Indeed, even within a single bacterium, the structure of PG can vary with growth conditions (1). More research into how bacterial PG peptide side chains evolve, and the capacity of an organism to adopt a new PG structure is needed, as this structure is integral to bacterial recognition in a number of systems.

In order to reveal the evolvability of the PG peptide structure in *V. fischeri,* we designed a screen for spontaneous suppressors of auxotrophs that normally require components of PG to grow. In *V. fischeri*, the three PG-specific AAs are D-Ala, D-Glu, and DAP. We started by generating strains auxotrophic for each of these D-amino acids, and proceeded to use growth as a selection mechanism for spontaneous suppressors of auxotrophy (**Figure 1.4**). Suppression could come from one of two workarounds: 1) The strain found a novel metabolic route to generate the D-AA or 2) The strain altered its PG structure in the absence of the D-AA in question. By utilizing a combination of PG analysis and whole-genome re-sequencing, we determined if the PG structure was altered and genetically defined the mutations responsible for suppression. In order to assess the impact of altered PG, we characterized the ability of an altered strain to grow, infect, and trigger normal development in the context of the *V. fischeri-E. scolopes* model symbiosis. In Chapter 2, I describe an instance of a new metabolic route to D-Glu, while Chapter 3 describes the replacement of DAP with lanthionine in a suppressor strain. Our research has allowed for a greater understanding of the capacity for change in PG, and the work discussed in Chapter 3 provides insight into how changes can have effects on PG's role as an integral structure and signal.

In one attempt to alter the PG, we began with a strain lacking a functional glutamate racemase and used the above approach to generate suppressors (**Figure 1.4**). After biochemical and genetic analysis, we determined that the suppressors analyzed generated wild-type PG, and contained single point mutations in a gene encoding an uncharacterized LTTR, VF_1545. In Chapter 2, I describe how we used these initial findings to inform further characterization of the LTTR, which we determined is responsive to D-Asp and regulates a putative aspartate racemase that can supply D-Glu when expressed at high levels. The LTTR variant in the suppressor mutant raises expression of the racemase to a level sufficient to generate enough D-Glu for incorporation into PG and restoration of prototrophy. Insight into the function of this D-Asp-responsive LTTR in *V. fischeri* may inform further study in other organisms. Indeed, homologs for the regulator are found in a wide range of bacteria.

Chapter 3 is the study of a DAP auxotroph suppressor that was generated through a similar screen (**Figure 1.4**). In this case the PG analysis revealed non-wild-type PG. Further analysis showed that this strain incorporated lanthionine into the third position of its PG side chain. Re-sequencing of the mutant's genome revealed that the basis for suppression was a single-nucleotide polymorphism in the organism's *cysK* gene. While CysK is traditionally studied for its role as the final enzyme in cysteine biosynthesis, as noted above, a CysK homolog from the oral pathogen *F. nucleatum* generates lanthionine, which is found in this bacterium's PG. Chapter 3 discusses the impact of the lanthionine-containing PG on the structure's role in growth, osmotolerance, and as a developmental trigger. Previous studies have knocked-down *V. fischeri*'s ability to orchestrate the host's developmental program (72), but by changing the PG directly we have made a strain which does not produce any true TCT.

The bacterial cell wall has long been studied as a target for antibiotics, and recognition by host PRRs. Partly, the conserved nature of PG is what makes this structure a good target for recognition. However, the variation that is present suggests that the PG structure is at least somewhat variable. This research has broadened the study of the bacterial cell wall in the areas of PG biosynthesis, D-AA-producing and responsive enzymes, and the role of PG as a MAMP in symbiotic associations. In the last chapter, I discuss the implications of this research, and suggest areas for further study.

# CHAPTER 2

# *VIBRIO FISCHERI* DARR DIRECTS RESPONSES TO D-ASPARTATE AND REPRESENTS A WIDER GROUP OF LYSR-TYPE TRANSCRIPTIONAL REGULATORS[1]

[1]Richard M Jones, Mareena M.Whisby, David L. Popham, Alicia L. Schmidt, Jonathan L. McMurry, Ellen L. Neidle, and Eric V. Stabb. To be submitted to mBio.

**ABSTRACT**

D-amino acids (D-AAs) play previously underappreciated roles in a broad spectrum of organisms. In bacteria, even D-AAs that are absent from canonical peptidoglycan (PG) may act as growth substrates, as signals, or in other functions. Given these roles and the ubiquity of D-AAs, the paucity of known D-AA-responsive transcriptional control mechanisms in bacteria suggests that such regulation awaits discovery. We made the serendipitous discovery of a LysR-type transcriptional regulator (LTTR), DarR, which activates transcription in response to D-Asp. The D-Glu auxotrophy of a *Vibrio fischeri murI*::Tn mutant could be suppressed, with wild-type PG structure maintained, by a point mutation in *darR*. This *darR* mutation resulted in overexpression of an adjacent operon encoding a putative aspartate racemase, RacD, which compensated for loss of *murI*. Using transcriptional reporters, we found that wild-type DarR activated transcription *in vivo* from the *racD* promoter in response to exogenous D-Asp, but not upon addition of L-Asp, L-Glu, or D-Glu. His-tagged DarR showed specific binding to the region between *darR* and the *racD* operon, and this binding correlated with a putative LTTR binding site. Genes encoding DarR homologs are present in several Proteobacteria, and most *darR* homologs are linked to genes annotated as having roles in D- and/or L-Asp metabolism. Functional similarities between the *V. fischeri* and *Acinetobacter baylyi* orthologs are suggested by the requirement in both bacteria for *darR* and *racD* to grow on D-Asp. Our results suggest that several bacteria have the ability to sense and respond to D-Asp.

**IMPORTANCE**

D-amino acids (D-AAs) can be found throughout the environment, and they are generated by all domains of life. Some biological roles for D-AAs are understood, but in other cases their

function or utility remain uncertain. Given the ubiquity of D-AAs, it seems likely that bacteria will mount transcriptional responses to them, and finding D-AA-responsive regulators along with the genes they control will help elucidate bacterial uses of D-AAs. Here, we report the discovery of DarR, a LysR-type transcriptional regulator (LTTR) in *Vibrio fischeri* that mediates a transcriptional response to environmental D-Asp. DarR represents a group of bacterial transcriptional regulators that shows homology and synteny across species. Based on our experimental and bioinformatic analyses, we hypothesize that many bacteria respond to D-Asp and/or to D-Asp-containing peptides. Our data suggest that *V. fischeri* DarR underpins the scavenging and catabolism of D-Asp, and other possible roles for DarR homologs are discussed.

## INTRODUCTION

There is a growing appreciation for the breadth of D-amino acids (D-AAs) found in the biosphere and a likewise burgeoning interest in their metabolism and functions. D-AAs can form spontaneously from L-AAs (103, 104), and in cells they are often generated enzymatically through the activity of AA racemases, which are found in all domains of life and interconvert the D- and the proteinogenic L- forms of AAs (105). Asp racemases, for example, have been purified from mammalian cells (106), amphibians (107), invertebrates (108, 109), and bacteria (110). In bacteria there are well-established roles of D-Glu and D-Ala, along with their respective racemases, in generating the conserved canonical structure of peptidoglycan (PG) cell wall, and D-Glu is also commonly found in spore coats (111). However, bacteria encounter and produce a variety of other less well-known D-AAs too (88, 110).

The biological significance of these D-AAs for bacteria is an active area of research. D-AAs encountered in the environment can be catabolized (86, 87), and in some cases their presence

may serve as indirect indicators of where the bacteria are. In addition to PG remnants, bacteria may encounter several other sources of D-AAs. Consistent with D-AA production by a broad range of organisms, as well as their slow but significant spontaneous interconversion with L-AAs (103, 104), D-AAs have been found at substantial levels in natural settings ranging from rhizosphere soils to the mouse gut (89, 112, 113). There has been particular interest in the presence of D-AAs in the marine environment, where several D-AAs are actively released and consumed by Bacteria and Archaea (114-116).

Several D-AAs endogenously produced by bacteria have also been explored. In addition to the D-Ala and D-Glu found in PG, these D-AAs can be incorporated into antibiotics, surfactants, or non-canonical PG (84, 117). D-AAs may be used as signals or in other roles as well (88). Intriguingly, D-AAs have shown involvement in developmental processes (88, 110), including spore germination (118) and cell-wall remodeling during stationary phase (90). The latter of these phenomena is underpinned by a newly discovered family of broad-spectrum racemases responsible for generating a variety of D-AAs that are both released into the environment and incorporated into the cell's own PG, thus providing a signal that is both auto- and paracrine in nature (91).

Whether produced as signals or scavenged as catabolites, one might expect D-AAs to elicit transcriptional responses; however, there are few known D-AA-responsive transcriptional regulators. One example is the LysR-type transcriptional regulator (LTTR) DsdC from *Escherichia coli*. DsdC responds to D-Ser and functions in concert with cyclic AMP receptor protein to activate transcription of the *dsdXA* operon (98), which encodes a D-Ser transporter (DsdX) and D-Ser deaminase (DsdA). Together, DsdC and DsdA may act in response to high levels of D-Ser in human urine (99). Another D-AA-responsive LTTR is DguR in *Pseudomonas*

*aeruginosa* PAO1, which directs the catabolism of D-Glu in response to D-Glu (87) and may underpin a mechanism for scavenging bacterial PG fragments in the environment.

In this study, we describe a D-Asp-responsive LTTR that induces transcription of a putative Asp racemase in the marine bacterium *V. fischeri*. This locus was uncovered in a screen for spontaneous suppressor mutants that restore prototrophy to a *murI* mutant, which is a D-Glu auxotroph. We named the gene for this LTTR *darR*, for D-aspartate responsive regulator. Bioinformatic analyses revealed several bacteria that have *darR* homologs genetically linked to genes with predicted functions in D-AA and/or aspartate metabolism, and we propose that *V. fischeri* DarR represents a larger family of D-AA-responsive LTTRs with varied ecological roles.

## RESULTS

**A mutation in *darR* suppresses the D-Glu auxotrophy of a *murI* mutant.** In many bacteria, *murI* (*glr*) encodes a glutamate racemase necessary to generate D-Glu for peptidoglycan biosynthesis. In a recent search for transposon insertions in conditionally essential genes we recovered the *murI*::miniTn*5*-erm mutant AN3 (119), which requires D-Glu supplementation for growth. We selected spontaneous suppressors of D-Glu auxotrophy in AN3 by plating on LBS medium without D-Glu. The frequency of suppression was approximately $10^{-7}$, based on dilution plating in parallel on LBS supplemented with D-Glu (data not shown). We analyzed three suppressor mutants, but these may have been siblings, as they were indistinguishable from each other in the amino acid content of their PG, in growth assays, and in whole-genome re-sequencing analyses. We therefore report the characterization of AN3S2 as a representative of these suppressor mutants. The growth defect of parent strain AN3 (*murI*::miniTn*5*-erm) in the absence of D-Glu was significantly reversed in suppressor AN3S2 (**Figure 2.1**), yet the PG of AN3S2 was

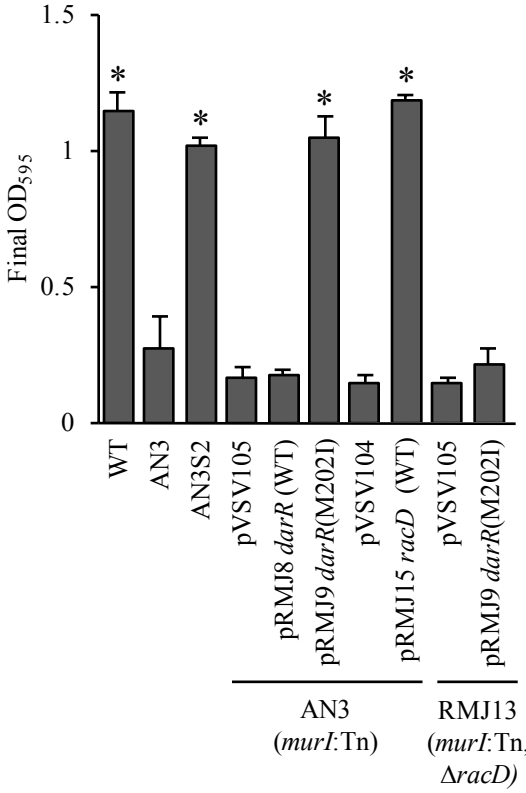


**Figure 2.1** Restoration of prototrophy to the D-Glu auxotroph AN3 by *darR*(M202I) or by multi-copy *racD in trans*. Strains were sub-cultured (1:1000) from broth cultures at an $OD_{595}$ of 0.6, grown for 14 hours in LBS, and final $OD_{595}$ was recorded. Asterisks indicate a significant difference relative to AN3 (*murI*::Tn) as determined by Student's t-test ($P < 0.01$). Error bars indicate standard error ($n$=3). Data from one representative experiment among three is shown.

indistinguishable from wild type in its amino acid and muropeptide content based on HPLC analysis (data not shown). These biochemical PG analyses cannot rule out the unprecedented substitution of L-Glu for D-Glu, but they more likely indicate a restoration of wild-type PG.

The genome sequence of AN3S2 revealed a point mutation in gene VF_1545 (*darR*), which encodes a previously uncharacterized LTTR (**Figure 2.2A**). The mutation (G606A) results in a single amino acid replacement (M202I) in the putative effector-binding domain of the protein (**Figure 2.2A**). To determine whether the point mutation found in *darR* was responsible for suppression of D-Glu auxotrophy, we tested whether this allele restored prototrophy to strain AN3 *in trans*. When added on a plasmid, the variant version of *darR* (M202I) reversed the D-Glu auxotrophy of AN3, whereas a plasmid carrying the wild-type *darR* or an empty-vector control did not (**Figure 2.1**), indicating that the mutant *darR* allele could account for the suppression phenotype.

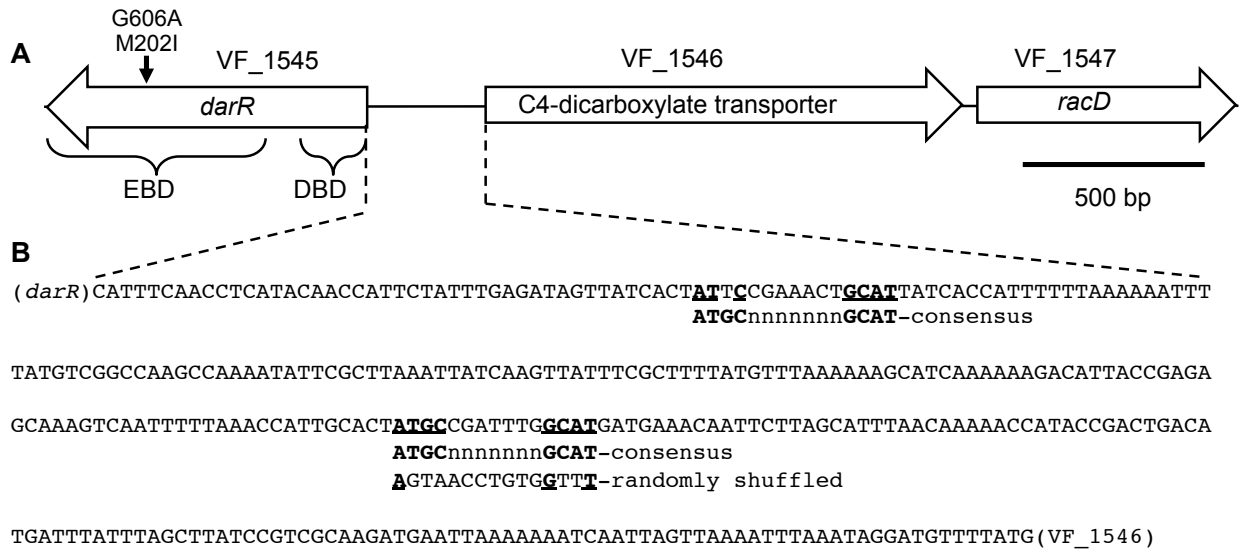


**Figure 2.2** The *V. fischeri darR* locus. (A) Horizontal arrows represent ORFs VF_1545 (*darR*), VF_1546, and VF_1547 from *V. fischeri* ES114 chromosome 1. Shown on *darR* are the site of the G606A mutation (causing M202I amino acid substitution in DarR) in suppressor mutant AN3S2, the effector-binding domain (EBD), and the DNA-binding domain (DBD). (B) intergenic region between and including the ATG start codons for *darR* (reverse strand) and VF_1546. Two putative DarR-binding sites are shown, one a perfect match to the proposed consensus and another with a 1-bp mismatch. The sequence used to randomly shuffle the exact-consensus site in control experiments is indicated.

**Overexpression of a putative Asp racemase suppresses the D-Glu auxotrophy of a *murI* mutant.** As illustrated in **Figure 2.2A**, the *darR* gene is divergently oriented adjacent to a putative two-gene operon annotated as encoding a C4-dicarboxylic acid transporter (VF_1546) and an Asp racemase (*racD*; VF_1547). Given that LTTRs are often adjacent to the genes they control, and that Glu and Asp are similar amino acids, we hypothesized that DarR activates expression of an Asp racemase (RacD) thereby compensating for loss of the Glu racemase encoded by *murI*. Three lines of evidence support this hypothesis. First, introducing a Δ*racD* mutation abolished the ability of the *darR*(M202I) allele to restore prototrophy in a *murI* mutant (compare AN3 and RMJ13 in **Figure 2.1**). Second, overexpression of *racD* from a multi-copy plasmid was itself sufficient to restore D-Glu prototrophy to AN3 (**Figure 2.1**). Third, a $P_{racD}$-*gfp* reporter showed increased expression in the *darR*(M202I) mutant but decreased expression in a Δ*darR*

mutant (**Figure 2.3**). This $P_{racD}$-*gfp* reporter (pRMJ11) was constructed by cloning the intergenic region between *darR* and ORF VF_1546 (**Figure 2.2**) into a reporter plasmid upstream of *gfp*. There are only 41 bp between VF_1546 and *racD* (VF_1547), suggesting this cloned fragment is likely to include the transcriptional promoter for *racD.* Together, these data indicate that *racD* expression is responsible for suppression of D-Glu auxotrophy, and that DarR regulates the expression of the *racD* operon.

**Dose-dependent stimulatory effect of exogenous D-Asp on a $P_{racD}$-*gfp* reporter.** Because *racD* encodes a putative Asp racemase, we hypothesized that DarR regulates *racD* in response to L- or D-Asp. Consistent with our hypothesis the $P_{racD}$-*gfp* reporter displayed dose-

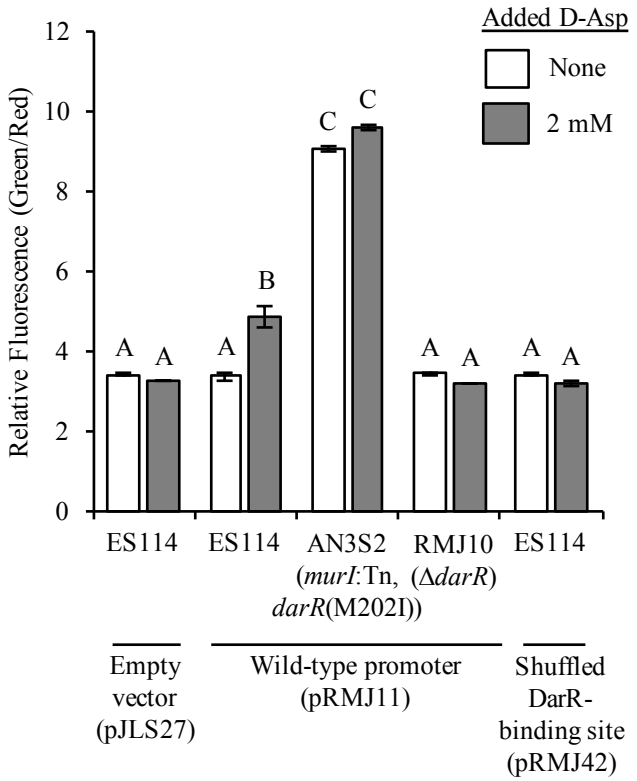


**Figure 2.3** Effect of *darR* and D-Asp on expression of $P_{racD}$-*gfp* reporter. Relative $P_{racD}$-*gfp* reporter activity is presented as GFP expression (green fluorescence) normalized to constitutive mCherry (red fluorescence) expression for strains grown in LBS (open bars) or LBS supplemented with 2 mM D-Asp (filled bars). Strains carry either a reporter with the wild-type promoter sequence (pRMJ11) or a version where a putative DarR binding site has been randomly shuffled (see Fig. 1B) in pRMJ42. Values with the same letter are not statistically significantly different ($P > 0.05$), whereas different letters indicate significant differences ($P < 0.01$), based on a one-way analysis of variance (ANOVA) and Tukey's multiple comparison test. Error bars indicate standard error (n=3). Data from one representative experiment among three is shown.

dependent expression with increasing D-Asp, showing a significant response ($p<0.01$) to as little as 125 μM exogenous D-Asp (**Figure 2.4**). This response is *darR*-dependent, as a Δ*darR* strain showed no response to D-Asp (**Figure 2.3**); however, activation of the $P_{racD}$-*gfp* reporter does not require RacD (**Figure 2.3**), which if present might interconvert D- and L-Asp. Moreover, expression of this reporter was not altered detectably by the addition of 16 mM L-Asp, D-Glu, or L-Glu (**Figure 2.4**), indicating specificity for D-Asp.

**Evidence of autorepression by DarR.** In addition to regulating other nearby genes, LTTRs often repress their own expression, even in the absence of an activating effector, to maintain regulator homeostasis (120). To determine the effect of DarR on its own expression, we constructed a $P_{darR}$-*gfp* reporter (pRMJ10). This $P_{darR}$-*gfp* reporter showed a small but significant ($p<0.01$) increase in expression in a Δ*darR* background, consistent with the DarR protein repressing *darR* transcription (**Figure 2.5**). Moreover, in the suppressor strain AN3S2

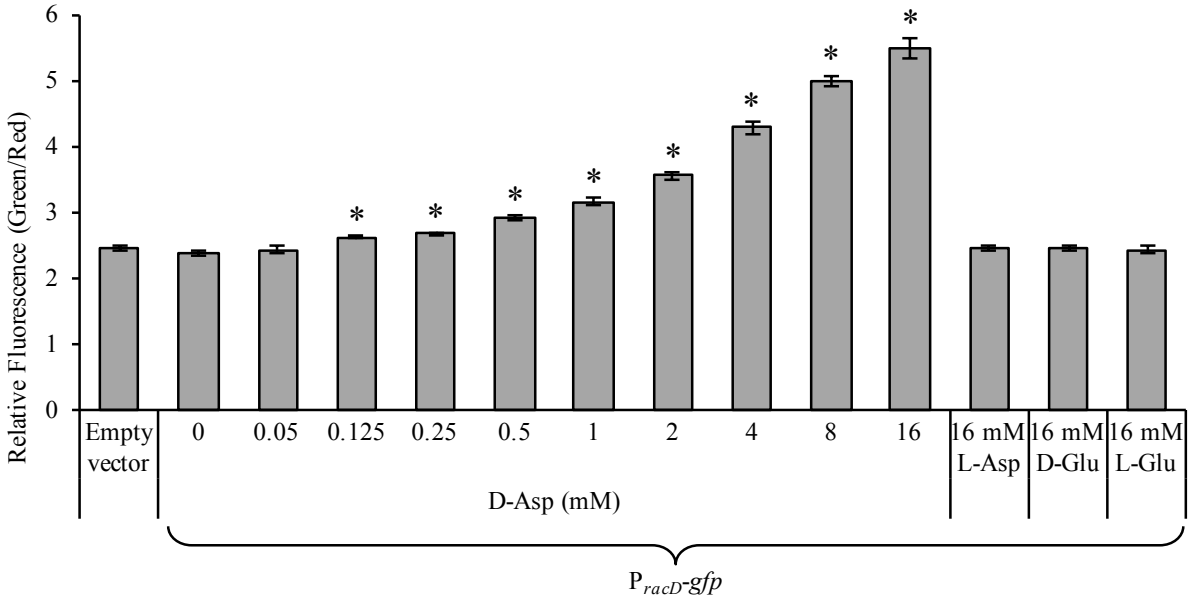


**Figure 2.4** Dose dependence and specificity of $P_{racD}$-*gfp* reporter response to D-Asp. $P_{racD}$-*gfp* reporter activity is presented as GFP expression (green fluorescence) normalized to constitutive mCherry expression (red fluorescence) for wild-type strain ES114 carrying the $P_{racD}$-*gfp* reporter (pRMJ11) or the empty vector control (pJLS27) grown in LBS or LBS supplemented with the indicated concentration (mM) of specific amino acids (D-Asp, L-Asp, D-Glu, or L-Glu). Asterisks indicate significantly more expression relative to empty vector control, as determined by one-tailed Student's t-test ($P<0.01$). Error bars indicate standard error ($n=6$).

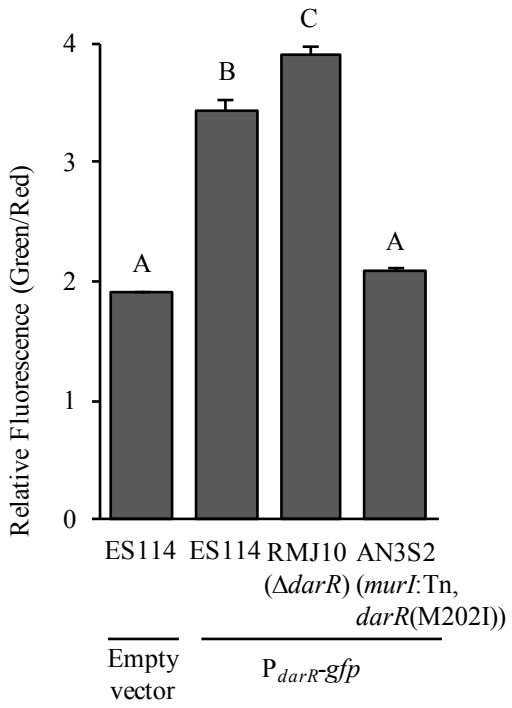


**Figure 2.5** Evidence of DarR autorepression. GFP expression (green fluorescence) from the $P_{darR}$-*gfp* reporter on pRMJ10 normalized to constitutive mCherry expression (red fluorescence) is shown when the reporter is carried by ES114 (wild type), RMJ10 (Δ*darR*), or AN3S2 (*murI*::Tn *darR*(M202I)). Cultures were grown in LBS, and the promoterless parent vector pJLS27 (indicated as "empty vector") in wild type is shown for comparison. Values with the same letter are not statistically significantly different ($P > 0.05$), whereas different letters indicate significant differences ($P < 0.01$), based on a one-way analysis of variance (ANOVA) and Tukey's multiple comparison test. Error bars indicate standard error ($n$=3).

(*darR*(M202I)), $P_{darR}$-*gfp* expression drops significantly below wild-type levels (**Figure 2.5**). Although expression of the $P_{darR}$-*gfp* reporter is repressed to the point of being indistinguishable ($p>0.05$) from background levels in AN3S2 (*darR*(M202I)) (**Figure 2.5**), this does not necessarily mean that the *darR*(M 202I) mutation actually prevents expression of DarR(M202I), which seems unlikely. In each of these backgrounds, the expression of this $P_{darR}$-*gfp* reporter does not show a consistent response to D-Asp, L-Asp, D-Glu or L-Glu (data not shown). Thus, *darR* appears to mediate regulation of the $P_{darR}$-*gfp*, without the obvious D-Asp dependence that was seen on activation of the $P_{racD}$-*gfp* reporter.

**DarR homologs are encoded in similar genetic contexts in diverse Proteobacteria.** We searched sequence databases for DarR homologs and found several genes encoding putative LTTRs with more than 25% identity to DarR. The genetic contexts of these genes often suggested functional connections to Asp metabolism and/or racemase activity. Specifically, *darR*-like genes were often linked to genes predicted to encode one of five types of products; (1) aspartate

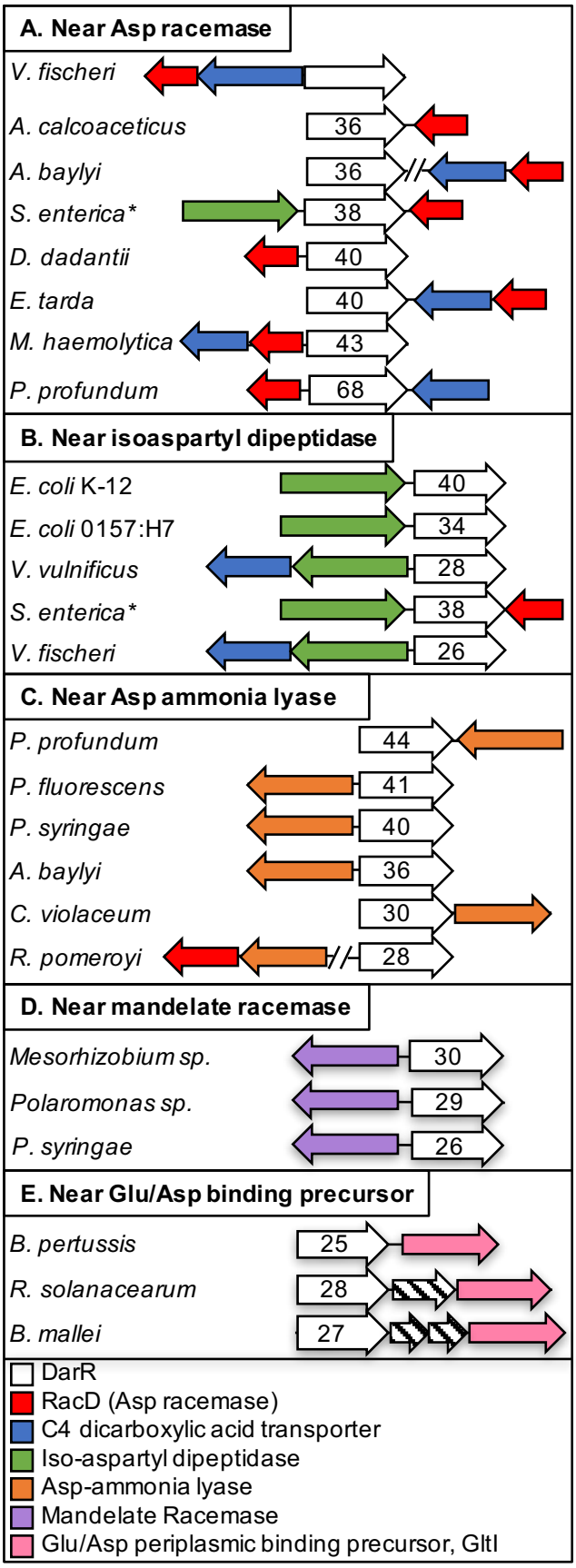


**Figure 2.6.** Synteny of *darR* homologs in diverse Proteobacteria. White arrows represent *darR* homologs with numbers indicating the percent identity to the DarR sequence from ES114. Homologs are grouped by their proximity to genes annotated as encoding (A) aspartate racemase (RacD), (B) isoaspartyl dipeptidase, (C) Aspartate-ammonia lysase, (D) mandelate racemase, or (E) glutamate/aspartate periplasmic binding precursor, GltI. Arrows with same color represent genes with the same functional annotation (see color legend at bottom) and striped arrows indicate ORFs that do not fall into any of the groups described above. Asterisks indicate that the same DarR homolog in *S. enterica* is listed in panels A and B, because it is flanked by both Asp racemase and isoaspartyl dipeptidase gene homologs.

racemase, (2) isoaspartyl dipeptidase, (3) aspartate-ammonia lyase, (4) mandelate racemase, or 5) GltI, which is involved in Glu/Asp periplasmic binding and uptake. Out of one hundred and fifty-five *darR* homologs examined, one hundred and twenty-three (79%) were within a 16-kbp window of one or more genes annotated in these five categories. To put this observation in perspective, we examined how often homologs of two other LTTRs from *V. fischeri* (VF_1974 and VF_2606) fell within a 16-kbp window of the same five gene groups listed above, and a similar genetic proximity occurred in only 0% and 4% of the

100 genomes examined, respectively. Potential aspartate transporters are also common in the regions near *darR* homologs, including the predicted C4-dicarboxylic acid transporter (VF_1546) adjacent to *darR* mentioned above. **Figure 2.6** shows a representative subset of these common genomic arrangements. Notably, some bacteria have more than one *darR* homolog, including *V. fischeri* ES114, which has a second *darR*-like gene adjacent to an isoaspartyl-dipeptidase gene.

***darR* and *racD* are required for catabolism of D-Asp.** The combination of a D-Asp-responsive regulator activating expression of Asp racemase might allow bacteria to recognize environmental D-Asp and convert it to L-Asp, thereby enabling its catabolism. We tested this possibility using both *V. fischeri* ES114 and another bacterium with *darR* linked to *racD*, *Acinetobacter baylyi*

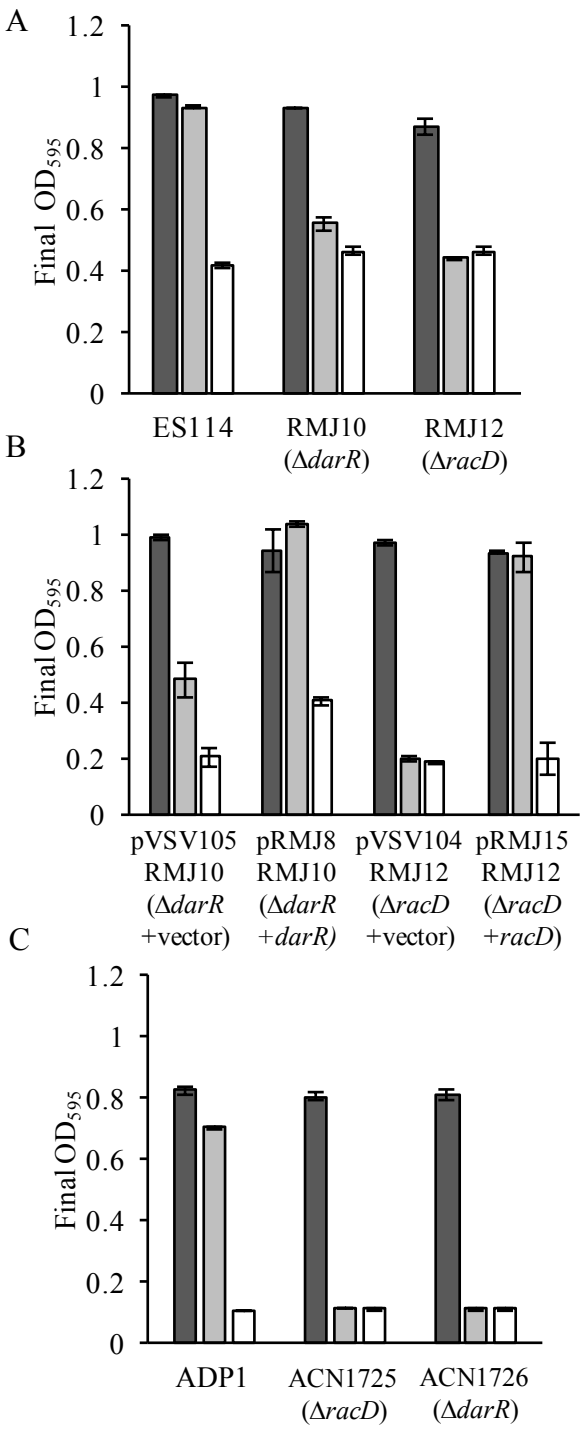


**Figure 2.7.** Requirement of *racD* and *darR* for growth on D-Asp. Shown are final $OD_{595}$ readings for *V. fischeri* (A&B) and *A. baylyi* (C) cultures grown with 20 mM L-Asp, D-Asp, or no added aspartate. For *V. fischeri* cultures, Asp was used as an additional nitrogen source with 1g/L casamino acids in FMM minimal medium and 40 mM glycerol was provided as a carbon source. For *A. baylyi*, Asp was used as the carbon source and 15 mM ammonium sulfate was added as a nitrogen source. Cultures were grown with shaking for 24h before reading final $OD_{595}$. Error bars indicate standard error ($n$=6).

ADP1 (**Figure 2.6**). In addition to *darR* and *racD* being genetically linked in each of these bacteria, reciprocal genomic BLAST searches suggest that DarR and RacD in ES114 are orthologs of DarR and RacD in ADP1, respectively (121). *V. fischeri* ES114 can use L- or D-Asp as a sole nitrogen source; however, loss of *racD* or *darR* reduces or eliminates the ability to use D-Asp (**Figure 2.7**). This effect can be complemented by adding either gene back on a plasmid (**Figure 2.7 B**). Similarly, *A. baylyi* ADP1 can grow on L- or D-Asp as a sole carbon source, but the ability to grow on D-Asp is lost in *racD* and *darR* mutants (**Figure 2.7**). The *darR* and *racD* genes in ES114 and ADP1 can be classified as orthologs via reciprocal best blast (121). Thus, at least in these two bacteria, *darR* and *racD* underpin D-Asp catabolism.

**Purified DarR binds specifically to a site in the intergenic region between *darR* and the *racD* operon.** We used the analysis of *darR* homologs above (**Figure 2.6**) as the basis for a search for a DarR binding site (see Materials and

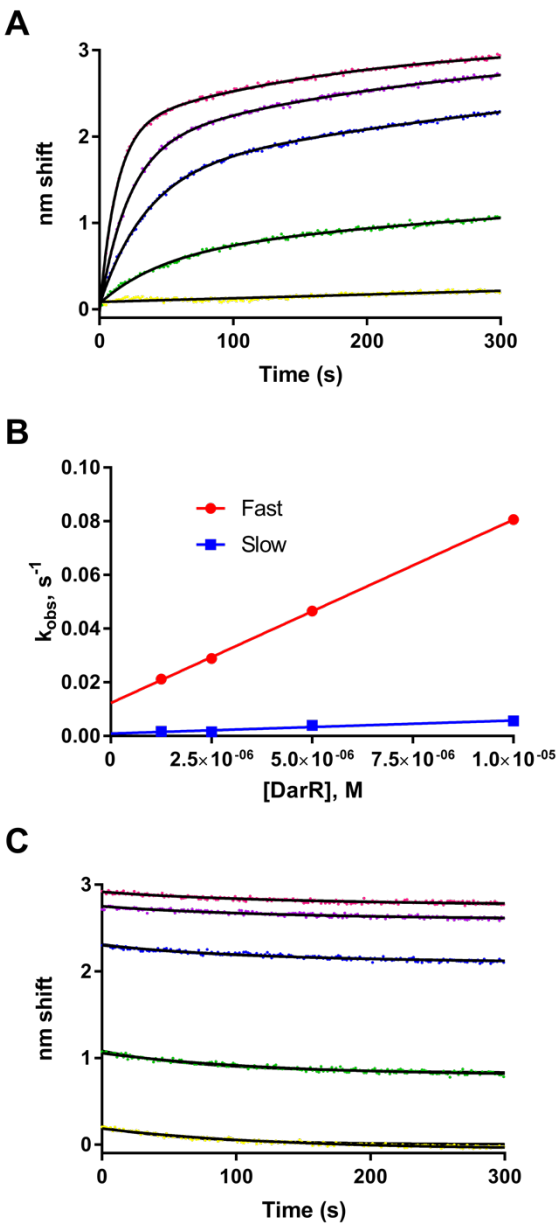


**Figure 2.8.** Biolayer interferometry analysis of DarR DNA target binding. (A) Association phase. Analyte DarR at 10 (magenta), 5 (purple), 2.5 (blue), 1.25 (green) and 0.63 µM (yellow) was exposed to sensor-tethered target DNA for 5 min. Fits (black lines) are shown to a parallel two-state model. (B) $k_{obs}$ for fast and slow states as determined from data in panel A plotted against analyte concentration yield $k_{on}$ (slope). (C) Dissociation phase shown with fits to two-state parallel model. Colors are the same as panel A.

Methods below). In short, we aligned putative promoter sequences upstream from genes we speculated might be regulated by DarR homologs, searched these sequences for a conserved sequence with the canonical 5'-T-$N_{11}$-A-3' motif and dyad symmetry typical of LTTR binding sites (122). In this way, we identified a putative DarR binding site; 5'-ATGC-$N_7$-GCAT-3'. The same sequence (5'-ATGC-$N_7$-GCAT-3') was independently identified as a predicted LTTR-binding site upstream of an Asp-ammonia lyase in *Acinetobacter baylyi* ADP1 by Craven and colleagues (123), and there is a divergently transcribed *darR* homolog upstream of this gene, further implicating this sequence as the recognition site for DarR. There is one perfect match to this putative DarR binding site upstream of VF_1546, and another site with a one-bp mismatch closer to *darR* (**Figure 2.2B**). Allowing for a 1-bp mismatch from the putative DarR binding site, there are two thousand and seventy-six potential binding sites within the *V. fischeri* ES114 genome; however, there are only five occurrences of two such sites in the same intergenic region, including the sequence between *darR* and VF_1546, and similarly only eight out of ninety perfect matches to the DarR-binding sequence fall in intergenic regions (data not shown).

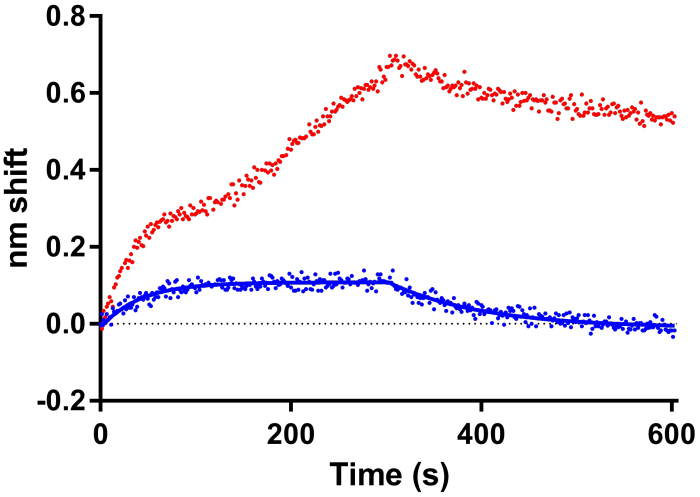


**Figure 2.9** Biolayer interferometry response of DarR to wild-type and scrambled target DNA. DarR at 10 µM is shown binding to wild-type target DNA (red) or target DNA with the putative binding site scrambled (blue). Association was allowed to proceed for 300s followed by dissociation from 300 to 600s. A fit to a one-state binding model is shown.

6x-His-tagged DarR was used in DNA-binding experiments using biolayer interferometry (BLI). Biotin-tagged PCR products were analyzed for DarR binding after they were loaded onto streptavidin-coated sensors. The wild-type DNA target was a 216-bp fragment upstream of the *racD* operon containing the predicted consensus DarR target site (5'-ATGCCGATTTGGCAT-3'; see **Figure 2.2B**). DarR protein bound this wild-type target with high affinity (**Figure 2.8**). Interestingly, instrument response to analyte was of negative amplitude, which has been observed for BLI previously and may indicate a change in shape of the target bound to the sensor (124). In this case, for example, a binding-induced bending in DNA might account for the negative amplitude of the response. When all data were multiplied by -1, sensorgrams fit well to a parallel two-state binding model, and the $k_{obs}$ values were determined accordingly by fitting the association phase (**Figure 2.8A**). For each state, $k_{obs}$ plotted against DarR concentration yields $k_{on}$ as the slope (**Figure 2.8B**), revealing "fast" and "slow" $k_{on}$ values of 6800 and 490 $M^{-1}s^{-1}$, respectively, for the two states. A global two-state dissociation model yielded off rates of 0.01 $s^{-1}$ and 8.3 x $10^{-5}$ $s^{-1}$ (**Figure 2.8C**). The vast majority of the BLI binding amplitude (90% or more in every sample) was represented in the slow-off state. Hypothesizing that fast-on, slow-off is the most biologically relevant interaction, $K_D$ is 12 nM (see Discussion). When the putative DarR target site in this fragment was randomly shuffled (to 5'-AGTAACCTGTGGTTT-3'), binding was negligible (**Figure 2.9**), and the same shuffled control sequence eliminated D-Asp-responsive activity in the $P_{racD}$-*gfp* reporter (**Figure 2.3**).

## DISCUSSION

D-AAs are widespread in nature, and there is growing appreciation of the roles they play in organisms, so it may be somewhat surprising that few regulatory responses to D-AAs have been

described. Here, we report the discovery of DarR, which directs transcriptional responses to D-Asp (e.g. **Figures 2.3 and 2.4**), and we show that DarR homologs are encoded in many bacterial genomes (**Figure 2.6**). Three lines of evidence suggest functional similarity of these DarR homologs to DarR. First, most *darR* homologs are oriented near genes predicted to be involved in Asp metabolism. Second, a conserved 5'-ATGC-$N_7$-GCAT-3' motif required for high-affinity DarR binding was identified upstream of such genes in multiple organisms. In one case, Craven et al. previously and independently predicted the binding sites for LTTRs in *Acinetobacter baylyi* ADP1 and identified a sequence between genes encoding a *darR* homolog and an aspartate lyase that exactly matches our predicted DarR binding site (123). Finally, functional similarity is evident in the observation that *darR* mutants of *V. fischeri* and *A. baylyi* were defective in using D-Asp to support growth (**Figure 2.7**). We therefore posit that *V. fischeri* DarR represents a larger group of LTTRs that warrant further investigation.

**Role of the *darR-racD* locus in *V. fischeri.*** The manner in which *darR* was discovered immediately suggested something about the function of this locus. We had attempted to alter the PG of *V. fischeri* by selecting spontaneous suppressors of D-Glu auxotrophy in a *murI* mutant; however, rather than replacing the D-Glu in their PG, the suppressors apparently used an alternative route to synthesize wild-type PG. Suppression was achieved by a single point mutation in *darR*, and further data indicated that restoration of prototrophy was mediated by overexpression of *racD*, which encodes a putative Asp racemase. The most parsimonious explanation consistent with our data is that *V. fischeri* RacD has some ability to interconvert L- and D-Glu and thereby substitute for MurI. A gene upstream of *racD* encodes a putative C4-dicarboxylic acid transporter (VF_1546), which we speculate transports D-Asp. Wild-type DarR mediates transcriptional

activation of this transporter gene and *racD* in response to D-Asp, and we can imagine at least two possible roles for this two-gene operon.

One possibility is that *V. fischeri* uses this locus to catabolize the D-Asp that it encounters in the marine environment. This function is supported by the observation that *darR* and *racD* are required for *V. fischeri* to grow on D-Asp as a nitrogen source (**Figure 2.7**), although it cannot grow on D- or L-Asp as a sole carbon source (data not shown). D-Asp has been found in marine habitats at levels in the hundreds of micromolar range (114), which is enough to induce the $P_{racD}$-*gfp* reporter (**Figure 2.4**). *V. fischeri* might also respond to D-Asp from animal cells, which have been shown to release D-Asp in the presence of apoptotic inducers (125). Preliminary experiments showed no evidence that the $P_{racD}$-*gfp* reporter was induced during colonization of *V. fischeri*'s host squid, *Euprymna scolopes* (data not shown), but this possibility merits further investigation.

Alternatively, or in addition to, D-Asp catabolism, bacteria including *V. fischeri* may generate D-Asp as a signaling molecule, with a response directed by DarR. If RacD activity resulted in a net production of D-Asp, this setup would resemble the positive-feedback signaling circuit comprised by *V. fischeri* LuxI and LuxR, which generate and respond to *N*-3-oxo-hexanoyl-homoserine lactone, respectively. One observation inconsistent with a role in signaling is that the suppressor mutant with a hyperactive DarR, which appears to increase RacD activity, did not release enough D-Asp to trigger a response in nearby cells (data not shown). Still, we cannot rule out signaling or other possible functions for the locus.

Future work should further help to test possible roles for the *darR-racD* locus. Investigating the enzyme kinetics and specificity of RacD would not only test whether it is capable of generating D-Glu, as we hypothesize, but it might help resolve its function for *V. fischeri*. An Asp/Glu racemase in *E. coli* was described that favors the conversion of L- to D-Glu (126), and such

unidirectional (or biased) interconversion could speak to the enzyme's role. For example, bias in the D- to L-Asp direction would be consistent with catabolism of environmental D-Asp and its incorporation into central metabolism (e.g., into proteins) but would not support the idea that this operon generates D-Asp as a signaling molecule. On the other hand, if D-Asp generated by RacD underlies a signaling mechanism, presumably DarR will control other genes, which could be assessed in global transcriptomic experiments.

**Role of DarR homologs in other bacteria. Figure 2.6** illustrates some of the many *darR* homologs found in bacteria, and the genomic contexts of these genes reveal patterns that may reflect conserved function(s). Genes encoding DarR homologs tend to be found at loci that also encode Asp racemases, isoaspartyl dipeptidases, Asp-ammonia lyases, mandelic acid racemases or the periplasmic Glu/Asp binding precursor, GltI. Thus, as noted above, most DarR homologs are encoded near genes involved in some way with Asp metabolism. We speculate that many of these gene clusters respond to D-Asp encountered in the environment and in some way direct its metabolism, although some that encode racemases may alternatively generate D-AA signals.

We also hypothesize that the DarR homologs encoded near isoaspartyl dipeptidase genes respond to D-Asp linked to other amino acids rather than to free D-Asp. These DarR homologs are widespread and even include one DarR paralog in *V. fischeri* (**Figure 2.6B**). Given the function of isoaspartyl dipeptidase, we speculate these LTTRs respond to D-iso-Asp in peptides originating from damaged proteins. Isoaspartate residues are created in aging proteins when Asp residues become isomerized. Isomerization, deamidation and racemization of Asp and Asn make up a large portion of the damage caused when proteins age (127), with isomerization being the most common form of damage and leading to the generation of iso-Asp residues (128). These damaged residues

are resolved to either D- or L-Asp through a succinimide intermediate. The accumulation of iso-Asp residues is countered through the activity of protein L-isoaspartyl O-methyltransferase (PIMT), which is found in both Eukaryotes and Bacteria (129). PIMT is responsible for protein-damage repair and recovery from long-term stationary phase (130). In *Salmonella typhimurium*, PIMT is important for survival under oxidative stress conditions like those found upon infection of macrophages (131). Through PIMT activity, methylation of the iso-Asp residue favors regeneration of the succinimide intermediate thereby favoring resolution to L- or D-Asp. Thus, this damage and repair process can ultimately result in the acquisition of D-Asp or D-iso-Asp residues in proteins. Isoaspartyl-dipeptidases can cleave linkages between iso-Asp and adjacent amino acids when these damaged proteins are turned over. We speculate that the DarR homologs encoded near isoaspartyl-dipeptidase genes may respond to D-iso-Asp-containing dipeptides and underpin their turnover and recycling by the cell.

Interestingly, one DarR homolog encoded near an isoaspartyl-dipeptidase gene has been characterized: HypT in *E. coli*. This LTTR mediates a transcriptional response to hypochlorite (132) and is activated by methionine oxidation (133). Although hypochlorite may directly induce HypT's regulatory activity, it is tempting to speculate that hypochlorite also results in protein damage and accumulation of D-iso-Asp-X dipeptides, which might act as the effector or co-effector. Although HypT was previously identified as an ortholog of DarR, it is more likely an ortholog of DarR's paralog (VF_1510) as they share the genetic context of proximity to an isoaspartyl dipeptidase gene (**Figure 2.6B**). Further study is needed to determine if VF_1510 in *V. fischeri* responds similarly to HOCl, which is among the reactive oxygen species *V. fischeri* encounters when it infects the light organ (41, 134).

**Biochemistry of DarR.** Our initial characterization of DarR indicates that it behaves similarly to other characterized LTTRs. Binding assays place the $K_D$ ~12 nM for binding near the *racD* promoter, which is an affinity high enough to be consistent with DarR having a physiologically relevant activity as a transcriptional regulator. DarR binding occurred without added D-Asp; however LTTRs typically do not require effectors for specific DNA binding, and instead such effectors elicit transcriptional effects from LTTRs in more subtle ways (120). The major components of DarR binding to target DNA were the fast-on and slow-off states in two-state parallel fits (**Figure 2.8**). This complexity may reflect biologically important components such as cooperativity or oligomeric changes. Alternatively, the secondary components may be biologically irrelevant, perhaps reflecting non-homogeneity of the analyte population or other confounding parameters. The 12 nM $K_D$ underscores the high affinity nature of the binding, largely due to a very slow dissociation rate constant.

**A broader view of D-AAs.** Our unforeseen discovery of a D-Asp-responsive regulator in *V. fischeri* has opened a window on a number of similar bacterial genes that may likewise direct responses to D-Asp, and it suggests that transcriptional responses to other D-AAs may exist but remain unknown. D-AAs can be formed either through the activity of dedicated racemase enzymes or through unavoidable spontaneous chemical reactions, and they may serve bacteria either as signals or as carbon sources to be scavenged. The functional roles of D-AAs, the transcriptional responses to them, and how they relate to bacterial ecology should be interesting topics for future research.

## MATERIALS AND METHODS

**Bacterial strains and culture conditions.** The strains used in this study are listed in **Table 2.1**. When added to LB medium (135) for selection of *E. coli*, chloramphenicol (Cm) and kanamycin (Km) were used at concentrations 20 and 40 μg $ml^{-1}$, respectively. For selection of *E. coli* with erythromycin (Em), 150 μg $ml^{-1}$ was added to BHI medium (Difco, Sparks, MD). *A. baylyi* strains were grown in minimal medium with 20 mM pyruvate, 20 mM L-aspartate, or 20 mM D-aspartate added as the carbon source (136). When added for selection of *A. baylyi*, Km was added at a concentration of 25 μg $ml^{-1}$. Unless otherwise noted, *E. coli* and *A. baylyi* were incubated at 37°C. *V. fischeri* was grown at 28°C in LBS medium (137) or FMM minimal medium (72) with Asp replacing $NH_4Cl$. When added to LBS for selection of *V. fischeri*, Cm, Km, and Em were used at concentrations of 2, 100 and 5 μg $ml^{-1}$ respectively. D-Glu was added at a final concentration of 400 μg $ml^{-1}$ for D-Glu auxotrophs unless otherwise indicated. Agar was added to a final concentration of 1.5% for solid media.

**Table 2.1:** Bacterial strains, plasmids, and oligonucleotides used in this study

| **Strain, plasmid, or oligonucleotide** | **Relevant characteristics**[a] | **Source or reference** |
|---|---|---|
| ***A. baylyi*** | | |
| ACN1720 | Δ*racD*::*sacB-kanR51720* | This study |
| ACN1721 | Δ*darR*::*sacB-kanR51721* | This study |
| ACN1725 | Δ*racD51725* | This study |
| ACN1726 | Δ*darR51726* | This study |
| ADP1 | Wild-type *Acinetobacter baylyi* (BD413) | (138, 139) |
| | | |

| | | |
|---|---|---|
| ***E. coli*** | | |
| BL21-CodonPlus(DE3)-RIPL | *E. coli* B $F^-$ *ompT hsdS* ($r_B^-$ $m_B^-$) $dcm^+$ $Tet^r$ gal λ(DE3) *endA* Hte [*argU proL* $Cam^r$] [*argU ileY leuW* Strep/$Spec^r$] | Agilent Technologies, Santa Clara, CA |
| CC118λ*pir* | Δ**(***ara-leu***)** *araD* Δ*lac74 galE galK phoA20 thi-1 rpsE rpsB argE*(Am) *recA* λ*pir* | (140) |
| DH5α | φ80d*lacZ*ΔM15 Δ(*lacZYA-argF*)U169 *deoR supE44 hsdR17 recA1 endA1 gyrA96 thi-1 relA1* | (141) |
| DH5αλ*pir* | DH5α lysogenized with λ*pir* | (142) |
| | | |
| ***V. fischeri*** | | |
| AN3 | *murI*::miniTn*5*-erm , D-Glu auxotroph | (119) |
| AN3S2 | AN3 spontaneous suppressor, *murI*::miniTn*5*-erm, *darR* point mutant (M202I) | This study |
| ES114 | Wild-type isolate from *E. scolopes* | (14) |
| RMJ10 | Δ*darR* | This study |
| RMJ12 | Δ*racD* | This study |
| RMJ13 | *murI*:: miniTn*5*-erm , Δ*racD* (VF_1547) | This study |

| | | |
|---|---|---|
| **Plasmids**[b] | | |
| pBAC1289 | *ampR*, *kanR*; *A. baylyi* Δ*racD*::*sacB-kanR51720; sacB-kanR* cassette inserted in XhoI site of pBAC1291 | This study |

| | | |
|---|---|---|
| pBAC1291 | *ampR*; *A. baylyi* Δ*racD51725* in pUC19 | This study |
| pBAC1296 | *ampR*; *A. baylyi* Δ*darR1726* in pUC19 | This study |
| pBAC1297 | *ampR*, *kanR*; *A. baylyi* Δ*darR*::*sacB-kanR51721; sacB-kanR* cassette inserted in XhoI site of pBAC1296 | This study |
| pCR-Blunt II-TOPO | *ori*$V_{ColE1}$, *kanR* | Thermo Fisher |
| pET28b(+).SapKO−CH.BspQ | Modified pET28b(+) vector for BspQI cloning; *ori*$V_{ColE1}$, *kanR* | (143) |
| pEVS94 | *ori*$V_{R6K}$ *ori*$T_{RP4}$, *ermR* | (140) |
| pEVS104 | conjugative helper plasmid; *ori*$V_{R6K}$, *oriT*$_{RP4}$, *kanR* | (140) |
| pEVS118 | *ori*$V_{R6K}$ *ori*$T_{RP4}$, *camR* | (142) |
| pJLS27 | *ori*$V_{R6K}$, *ori*$V_{pES213}$, *ori*$T_{RP4}$, *mCherry*, *kanR*, promoterless-*camR-gfp* | (144) |
| pRMJ1 | *ampR*, *kanR*; source of *sacB-kanR* cassette | (145) |
| pRMJ8 | *darR* from ES114 cloned into pVSV105 | This study |
| pRMJ9 | *darR*(M202I) from AN3S2 cloned into pVSV105 | This study |
| pRMJ10 | $P_{darR}$-*gfp* reporter plasmid | This study |
| pRMJ11 | $P_{racD}$-*gfp* reporter plasmid | This study |
| pRMJ15 | *racD* from ES114 cloned into pVSV104 | This study |
| pRMJ16 | Region upstream of VF_1546 ES114 cloned into pCR-Blunt II-TOPO | This study |
| pRMJ17 | Synthetic altered DarR target cloned into pCR-Blunt II-TOPO | This study |

| | | |
|---|---|---|
| pRMJ26 | Δ*racD* allele in pCR-Blunt II-TOPO | This study |
| pRMJ27 | pRMJ26 ligated to pEVS94 | This study |
| pRMJ30 | Δ*darR* allele in pCR-Blunt II-TOPO | This study |
| pRMJ31 | pRMJ30 ligated to pEVS118 | This study |
| pRMJ34 | pET28b(+).SapKO−CH.BspQ-based vector to express 6x-His-DarR | This study |
| pRMJ42 | Altered target $P_{racD}$-*gfp* reporter plasmid | This study |
| pUC19 | *ori*$V_{ColE1}$ *ampR*; cloning vector | (146) |
| pVSV104 | *ori*$V_{R6K}$, *ori*$V_{pES213}$, *oriT*$_{RP4}$, *kanR*, *lacZ*α | (147) |
| pVSV105 | *ori*$V_{R6K}$, *ori*$V_{pES213}$, *oriT*$_{RP4}$, *camR*, *lacZ*α | (147) |

| **Oligonucleotides**[c] | | |
|---|---|---|
| MTV395 | GAGTCAGAGCTCGACATCTTAAAAAAAGCGCATGTG | This study |
| MTV396 | GATCATCTGCAGTGATTCCCTGGATAACGAATTTGAC | This study |
| MTV397 | CCACGATACTGTCTAGGATCATCTCGAGCATTCACCATTTTTTGAATTGCCTA | This study |
| MTV398 | TAGGCAATTCAAAAATGGTGAATGCTCGAGATGATCCTAGACAGTATCGTGG | This study |
| MTV399 | GAGTCAGAGCTCAAATTGACTGGAAAACATGGTGTTG | This study |
| MTV400 | GATCATCTGCAGCACTTGCTTAGGTACACCAAATT | This study |
| MTV401 | CTAATAAATATCTTAGATTACAGGTAAAACTCATGCTCGAGATGAAGGTTCATGCATTTTGTG | This study |

| | | |
|---|---|---|
| MTV402 | CACAAAATGCATGAACCTTCATCTCGAGCATGAGTTTTACCTGTAATCTAAGATATTTATTAG | This study |
| RJ24 | GATGCATGCATCATGTCAGTCGGTATGGT | This study |
| RJ25 | CTAGTCGACTTCAACCTCATACAACCATTCT | This study |
| RJ26 | GATGCATGCTTCAACCTCATACAACCATTCTA | This study |
| RJ27 | CTAGTCGACAAAACATCCTATTTAAATTTTAACTAATTGATTTT | This study |
| RJ35 | CGGTAATAATTGAAATCTCAGTAGT | This study |
| RJ36 | AATGCTAGCCATAATATTTACTCCTTTAAATGAAATACGC | This study |
| RJ37 | ATTGCTAGCTAACGATTTCTTCTTACTGAATTCACC | This study |
| RJ38 | CCATATTCATTGGTAGTTCAGTTAT | This study |
| RJ41 | TTTTAATAATACGATCCGGATGAAT | This study |
| RJ42 | AGCGTCGACCATTTCAACCTCATAC | This study |
| RJ43 | CGTGTCGACTAGCTTACGGCATTAT | This study |
| RJ44 | ACTTTTTACCTCTGTTTTCCCACC | This study |
| RJ55 | GGGCTCTTCCATGAATGTAGAAAGTAAATGGCTAGA | This study |
| RJ56 | CCGCTCTTCGGTGAGTATCTAAATTACATAGAATACTCCATACC | This study |
| RJ57 | TAACCTAGGAATGGTTGTATGAGGTTGAAATG | This study |

| | | |
|---|---|---|
| RJ58 | AATGGTACCAAGCAAATAATGCCGTAAGCTA | This study |
| RJ60 | AGTCTCGAGGGTGAATTCAGTAAGAAGAAATCG | This study |
| RJ61 | TCACTCGAGGCACTTACTACAACGCGTATTTC | This study |
| RJ65 | ATCAAGTTATTTCGCTTTTATGTTT | This study |
| RJ81[d] | *-AAAACATCCTATTTAAATTTTAACTAATTGATTTT | This study |

[a] Drug resistance abbreviations used: *camR*, chloramphenicol resistance (*cat*); *ermR*, erythromycin resistance; *kanR*, kanamycin resistance (*aph*), and *ampR*, ampicillin resistance.
[b] Alleles cloned in this study are from *V. fischeri* strain ES114 or *A. baylyi* strain ADP1. Replication origin(s) (*oriV*) on each vector are listed as R6Kγ, ColE1, and/or pES213. Plasmids based on pES213 are stable in *V. fischeri* and do not require antibiotic selection for maintenance (147).
[c] All oligonucleotides are shown 5' to 3'. Underlined regions highlight restriction enzyme recognition sites; a 3-base overhang is generated at the double-underlined sequence when cut with BspQI, the dashed underlined regions correspond to complementary sequences for SOE PCR.
[d] asterisk indicates 5' biotinylation.

**Molecular genetics and sequence analysis.** Plasmids (**Table 2.1**) were constructed using standard genetic techniques. Oligonucleotides used for PCR and cloning are listed in **Table 2.1** and were synthesized by Integrated DNA Technologies (Coralville, IA). DNA ligase and restriction enzymes were obtained from New England BioLabs (Beverly, MA). PCR was conducted with Phusion DNA polymerase, except in the production of biotinylated probes, which were generated using *Taq* polymerase (New England BioLabs, Beverly, MA). Plasmids used for cloning were isolated with the Zymo plasmid miniprep kit (Zymo Research, Irvine, CA). DNA was repurified between cloning steps with the DNA Clean and Concentrator-5 kit (Zymo Research, Irvine, CA). Cloned PCR products were sequenced at the University of Michigan DNA Sequencing Core Facility, except *A. baylyi* alleles, which were sequenced by GeneWiz (South Plainfield, NJ). Sequences were analyzed using Geneious version 8.1 (148). Genome resequencing was performed as described previously (149). Resulting assemblies were analyzed for SNPs using Geneious version 8.1 (148).

Plasmids were generated in *E. coli* and conjugated into *V. fischeri* through triparental

mating using the helper plasmid pEVS104 (140) in strain CC118*λpir* (150). Transcriptional reporters pRMJ10 ($P_{darR}$-*gfp*) and pRMJ11 ($P_{racD}$-*gfp*) were constructed by PCR amplifying the 346-bp intergenic region between VF_1545 and VF_1546 and cloning it between SphI and SalI sites upstream of *gfp* in pJLS27 (144) using SphI and SalI sites on primer pairs RJ24 and RJ25 (pRMJ10) or RJ26 and RJ27 (pRMJ11) (**Table 2.1**). Complementation plasmids pRMJ8 and pRMJ9 were constructed by amplifying *darR* from ES114 or AN3S2, respectively, with primers RJ57 and RJ58. The resulting PCR products were digested with AvrII and KpnI, and ligated into KpnI- and XbaI-digested pVSV105 (147). Complementation plasmid pRMJ15 was constructed by amplifying *racD* from ES114 with primers RJ60 and RJ61. The resulting PCR product was XhoI-digested and ligated into XhoI-digested pVSV104. Plasmid pRMJ16 was constructed by PCR-amplifying the 346-bp region upstream of *racD* using primers RJ26 and RJ27 and cloning this fragment into pCR-Blunt II TOPO (ThermoFisher, Waltham, MA). Plasmid pRMJ17 was generated from pRMJ16 by replacing the fragment between SphI and SalI restriction sites with a synthesized "BioBrick" DNA fragment (IDT, Coralville, IA) identical to the 346-bp sequence upstream of the VF_1546 translational start site, except that the putative DarR-binding site (5'-ATGCCGATTTGGCAT-3') from 120- to 135-bp upstream of the gene is replaced with a randomly shuffled sequence (5'-AGTAACCTGTGGTTT-3'), which was arrived at using the Sequence Manipulation Suite (51). Plasmid pRMJ42 was constructed by PCR amplifying the altered intergenic region from pRMJ17 using primers RJ26 and RJ27, digesting this amplicon with SphI and SalI, and cloning into the same sites upstream of *gfp* in pJLS27.

To generate *V. fischeri* mutants, gene deletions were constructed on plasmids and the corresponding mutants were generated using allelic exchange. A Δ*racD* allele was constructed by amplifying regions upstream and downstream of *racD* with primer pairs RJ35 and RJ36, or RJ37

and RJ38, respectively. The resulting PCR products were digested with NheI, ligated together, gel-purified, and cloned into pCR-Blunt II-TOPO to generate pRMJ26. To facilitate mobilization into *V. fischeri*, pEVS94 (140) and pRMJ26 were each digested with SpeI and ligated together to generate pRMJ27. Plasmid pRMJ27 was conjugated into strains ES114 and AN3, and allelic exchange was confirmed via PCR, resulting in mutants RMJ12 and RMJ13, respectively. A Δ*darR* allele was similarly constructed by amplifying regions upstream and downstream of *darR* with primer pairs RJ41 and RJ42, or RJ43 and RJ44, respectively. The resulting PCR products were digested with SalI, ligated together, gel purified, and cloned into pCR-Blunt II-TOPO to generate pRMJ30. To facilitate allelic exchange in *V. fischeri*, pEVS118 (142) and pRMJ30 were each digested with XbaI, and ligated together to generate pRMJ31. Plasmid pRMJ31 was conjugated into strain ES114 and allelic exchange was confirmed via PCR, resulting in Δ*darR* mutant RMJ10.

Mutants of *A. baylyi* ADP1 were constructed using standard methods (151). In some cases, Splicing by Overlap Extension (SOE) PCR (152) was used with the Expand High Fidelity PCR system (Roche) to join DNA fragments. Indicated genomic sequence coordinates for ADP1 correspond to GenBank CR543861. To delete *racD* (ACIAD0318), PCR was used to amplify wild-type DNA upstream (with primers MTV399 with MTV402) and downstream (with MTV400 with MTV401) of *racD*. These fragments were joined by SOE PCR, and the combined product was digested with SacI and PstI and ligated to similarly digested pUC19. The resulting plasmid, pBAC1291, contains an XhoI site in place of the deleted *racD* sequence. A *sacB-kanR* cassette, excised by digestion with SalI from pRMJ1 (145), was ligated to pBAC1291 digested with XhoI to create pBAC1289. The same process was used to delete *darR* (ACIAD0323), using primer pairs MTV396 with MTV397, and MTV395 with MTV398, to generate pBAC1296. The *sacB-kanR* cassette was introduced into the XhoI site of pBAC1296, which replaced the deleted *darR*

sequence, to create pBAC1297.

To introduce the plasmid-borne *A. baylyi* DNA into the chromosome by allelic replacement, naturally competent recipients were transformed with plasmids that were linearized by restriction enzyme digestion, as described (153-155). Strains were selected either for resistance to Km or for the loss of the *sacB* gene in the presence of sucrose (5%). Genotypes were confirmed by PCR and regional DNA sequencing. Linearized pBAC1289 transformed ADP1 to create ACN1720 (Δ*racD*::*sacB-kanR*). Linearized pBAC1291 transformed recipient ACN1720 to obtain ACN1725 (Δ*racD*). Similarly, transformation of ADP1 by linearized pBAC1297 yielded ACN1721 (Δ*darR*::*sacB-kanR*), and transformation of ACN1721 by linearized pBAC1296 yielded ACN1726 (Δ*darR*).

**GFP transcriptional-reporter assays.** Strains harboring GFP-expressing reporter plasmids were grown in 200 μL of media in Greiner 96-well flat bottom black-walled plates (Sigma-Aldrich, St. Louis, MO) with shaking (200 RPM) at 28°C. Optical density at 595 nm ($OD_{595}$) and red and green fluorescence were measured using a Synergy 2 plate reader (Biotek, Winooski, VT). Data presented are from samples where $OD_{595}$ was between 0.9 and 1.1.

**Screen for spontaneous suppressors of D-Glu auxotrophy**. Strain AN3 (*murI*::miniTn*5*-erm) was grown to an $OD_{595}$ of 0.5 in LBS supplemented with 400 μg $ml^{-1}$ D-Glu, and then dilution plated on LBS without D-Glu. Cultures were dilution plated in parallel on LBS supplemented with D-Glu to determine the total population density. Plates were incubated at 28°C and colonies were counted at 48h. Colonies were streak purified, stocked in LBS, and checked for Em resistance to ensure the presence of the original *murI*::mini-Tn5-erm allele.

**Peptidoglycan preparation and analysis.** To isolate PG, cells were grown to an $OD_{595}$ of ~0.6 in LBS medium, chilled on ice for 10 min and centrifuged at 4°C and 15,000 x g for 10 min.

After resuspension in 4 ml cold water, cell suspensions were dripped into 50 ml boiling, 4% SDS with continuous stirring, boiled for 30 min, and allowed to cool to room temperature. Samples were then centrifuged at 130,000 x g for 60 min at room temperature, resuspended in 20 ml 50°C water, and washed twice more in 20 mL water. The pellet was resuspended in 20 ml water, heated at 100°C for 2 min to dissolve precipitated SDS and washed twice more as above. Before resuspension, the supernatant was assayed for SDS using methylene blue and chloroform (156). When SDS was undetectable, the pellet was resuspended in 1 ml 100 mM Tris HCl pH 7.5, and subsequently treated with α-amylase (Sigma-Aldrich, St. Louis, MO), DNase I (Sigma-Aldrich, St. Louis, MO), RNase (Sigma-Aldrich, St. Louis, MO) and Trypsin (Worthington Biochemical, Lakewood, NJ). SDS was added to 1%, the solution was boiled for 15 min, diluted into 20 ml warm water, and centrifuged at 130,000 x g for 10 min at 20°C. The resulting pellet was washed twice in water, once in 8 M LiCl, and twice more in water. The final pelleted PG was resuspended in 100 µl of water and stored at -80°C. Amino acid (157) and muropeptide analyses (158) were performed by HPLC as previously described.

**Purification of 6x-His-tagged VF_1545.** The *darR* gene was PCR amplified using primers RJ55 and RJ56 and cloned into the pET28b(+).SapKO−CH.BspQ expression vector using the BspQI method described elsewhere (143) to generate expression vector pRMJ34. Expression was performed using *E. coli* BL21-CodonPlus(DE3)-RIPL cells (Agilent Technologies, Santa Clara, CA) grown overnight in autoinduction medium at 30°C (159). Cells were harvested via centrifugation and lysed using a French pressure cell at 110 MPa. The cell lysate was centrifuged for 30 min at 39,000 x g and the supernatant was loaded onto a 5-ml HisTrap metal-chelate column (GE Healthcare, Chicago, IL) charged with $Ni^{2+}$ and equilibrated with binding buffer (20 mM Tris, 10% glycerol, 10 mM 2-mercaptoethanol, pH 8.0) supplemented with 500 mM NaCl and 5 mM

imidazole. Purification was performed at room temperature with an ÄKTA (Pharmacia) system. The protein was eluted with a linear gradient of imidazole (5 mM to 500 mM) in binding buffer with 500 mM NaCl. Purified protein was dialyzed into binding buffer with 100 mM NaCl, and further dialyzed into binding buffer with no added NaCl. Dialyzed protein was loaded onto a HiTrap Q HP ion exchange column (GE Healthcare, Chicago, IL). The protein was eluted with a linear gradient of NaCl (0 to 500 mM). Purified fractions showing a single band on Coomasie-stained SDS-PAGE gels were pooled and dialyzed in storage buffer (20 mM Tris pH 8.0, 10 mM 2-mercaptoethanol).

**Biolayer Interferometry.** Biolayer interferometry (BLI) was used to analyze the binding kinetics of purified 6x-His-tagged DarR protein to target and control DNA. Biotin-tagged PCR fragments (216 bp) were amplified from upstream of the *racD* operon using Taq polymerase and primers RJ81 and RJ65. Either purified pRMJ16 (wild-type sequence) or pRMJ17 (altered binding site) was used as template. BLI was conducted using a FortéBio OctetQK instrument (FortéBio, Menlo Park, CA). Streptavidin biosensors were initially hydrated in HBS-T buffer (10 mM HEPES, 150 mM NaCl, 0.1% Tween), then loaded in HBS-T containing 1.4 nM biotinylated dsDNA probe for 15 minutes. Baseline response was established for 5 min in buffer, after which loaded sensors were exposed to varying concentrations of 6x-His-DarR for a 5 min association phase. Sensors were again moved to buffer only and dissociation was monitored for 15 min. Reference-subtracted raw data were analyzed using GraphPad Prism 5.03.

**Bioinformatic analyses.** Putative promoters were predicted using the BPROM tool from Softberry (160) for sequences upstream from *racD*, *darR*, and genes from other bacteria that were near *darR* homologs. The top scoring potential promoters were annotated, and the sequences were trimmed to the -10 region, aligned, and queried for canonical T-$N_{11}$-A sites using Geneious (148).

A visual inspection for dyad symmetry led to selection of a new query (5'-ATG-$N_9$-CAT-3'). This sequence appeared upstream of all six putative promoters examined, including the putative DarR binding site in *V. fischeri* described above. Further examination of these sequences led to the proposed 5'-ATGC-$N_7$-GCAT-3' binding site, and this site was queried against genome databases (sometimes allowing a 1-bp mismatch) using Pattern Locator (161). The genomic context of *darR* homologs was found by searching The RAST database for genes similar to *darR* using The SEED Viewer version 2.0 with a window of 16 kbp (162). The DarR homologs depicted beneath *V. fischeri* DarR (VF_1545) in **Figure 2.6** from top to bottom correspond to the following annotated open reading frames: BDGL002587 (*Acinetobacter calcoaceticus*), ACIAD0323 (*A. baylyi* ADP1), STM4511 (*Salmonella enterica*), Dd586_2631 (*Dickeya dadantii*), ETAE_0919 (*Edwardsiella tarda*), F382_06960 (*Mannheimia haemolytica*), PBPRA2355 (*Photobacterium profundum*), B4327 (*E. coli* MG1655 K-12), Z5926 (*E. coli* 0157:H7), VV2_1132 (*Vibrio vulnificus*), STM4511 (*Salmonella enterica*), VF_1510 (*V. fischeri*), PBPRB1351 (*P. profundum*), Pfl01_5624 (*Pseudomonas fluorescens*), Psyr_5050 (*Pseudomonas syringae*), ACAID1745 (*A. baylyi* ADP1), CV_4113 (*Chromobacterium violaceum*), SPO2668 (*Ruegeria pomeroyi*), Meso_4540 (*Mesorhizobium sp.* BNC1), Bpro_3905 (*Polaromonas sp.* JS666), Psyr_2713 (*Pseudomonas syringae*), BP0764 (*Bordetella pertussis*), RSc0479 (*Ralstonia solanacearum*), and BMA2440 (*Burkholderia mallei*).

**ACKNOWLEDGEMENTS**

We thank Cory Momany, Nickolaus R. Galloway, Chris Moxley, and Jonathan Visick for technical assistance and helpful conversations.

# CHAPTER 3

# SUPPRESSION OF DIAMINOPIMELATE AUXOTROPHY VIA LANTHIONINE SUBSTITUTION IN THE PEPTIDOGLYCAN OF *VIBRIO FISCHERI*[2]

[2]Richard M. Jones, David L. Popham and Eric V. Stabb. To be submitted to PLoS One.

**ABSTRACT**

Bacterial peptidoglycan (PG) is among the conserved microbe-associated molecular patterns (MAMPs) that Eukaryotic hosts have evolved to recognize. Although some motifs in PG are considered essential, examples of natural variation show that these structures are not immutable. Understanding how PG structural variety can arise and the impact of these changes on MAMP-elicited responses will help elucidate interkingdom signaling mechanisms and the evolution of PG. In the model symbiosis between the Hawaiian bobtail squid and the bioluminescent bacterium *Vibrio fischeri*, PG can trigger developmental morphogenesis in the symbiotic light organ. We sought to test whether *V. fischeri* could evolve a new PG structure and how this would affect signaling. We utilized a mutant auxotrophic for the PG-specific amino acid diaminopimelic acid (DAP) and selected spontaneous suppressor mutants able to restore prototrophy. One of the strains we investigated, RMJ1S1, displayed an altered PG structure, replacing DAP in its PG peptide chain with the sulfur-containing amino acid lanthionine. Whole genome re-sequencing of RMJ1S1 revealed a point mutation in the *cysK* gene encoding O-acetyl serine sulfhydrylase, the final step in cysteine synthesis, and a 340-bp deletion in *yecC*, which encodes a cystine transporter. RMJ1S1 also displayed decreased growth rate, altered cellular morphology, and decreased salt tolerance. However, PG-containing cell fractions isolated from RMJ1S1 maintained the ability to trigger late-stage apoptosis in juvenile squid light organs. The results illustrate how PG structure can evolve, and indicate that DAP is not required for PG-dependent responses by the host squid.

## INTRODUCTION

Bacterial peptidoglycan (PG) is highly conserved, and its structure presumably is constrained both by the requirement that it provide mechanical strength and by the number of different cellular structures that must interface with it. Because PG varies little and is specific to Prokaryotes, it is both an attractive target for antibiotics and a key microbe-associated molecular pattern (MAMP) that plants and animals exploit to detect and respond to bacteria. Some variation in PG structure has evolved across species, and variations in the amino acids that constitute the crosslinking peptide are more common than changes to the core glycan polymer backbone (1). In the best-known PG-peptide variation, the third residue in this chain is Lys in most Gram-positive bacteria but diaminopimelic acid (DAP) for most Gram-negative bacteria. Other mono and diamino acids can be found in this PG position as well (1), with lanthionine having evolved to take the place of DAP in the oral bacterium *Fusobacterium nucleatum* for example (2). The occurrence of such PG variation is unusual though, and for most bacteria with DAP-containing PG, DAP biosynthesis is considered essential (163-165). How novel PG structures arose remains somewhat mysterious, but it seems plausible that PG-targeting antibiotics and MAMP-stimulated innate immunity could have provided important selective pressures underlying PG evolution.

In its role as a MAMP, PG triggers host responses to both pathogenic and beneficial bacteria in a range of associations (166), including the tractable model mutualism between the Hawaiian bobtail squid *Euprymna scolopes* and its bioluminescent light-organ symbiont *Vibrio fischeri*. During initial infection by *V. fischeri*, developmental changes are triggered in the squid's symbiotic light organ. Specifically, ciliated epithelial appendages extending from the light organ serve to facilitate infection (12, 18, 72) but undergo apoptotic cell death and regress through a series of programmed events after *V. fischeri* has colonized (44, 54). MAMPs, including a

monomer of PG called tracheal cytotoxin (TCT), can mimic these effects of colonization, triggering apoptosis and tissue remodeling in the infection-promoting ciliated epithelial appendages (53, 54). TCT's common name derives from its role in whooping cough, which is caused by *Bordetella pertussis*, where TCT triggers the death of ciliated cells in the trachea (64). The same PG monomer released by *Neisseria gonorrhoeae* kills ciliated cells in fallopian tubes (167). Like these two pathogens, and in contrast to most Gram-negative bacteria, *V. fischeri* releases high amounts of TCT from the cell, and addition of TCT to juvenile squid causes regression of ciliated appendages both alone and synergistically with LPS (54).

In this study, we experimentally investigated the evolvability of PG biosynthesis in *V. fischeri*. We targeted the peptide stem of PG, given its documented natural and experimental variation (1, 3-5, 84), and because the PG peptide structure can affect how a host detects and responds to PG (76, 77). A previous attempt to eliminate TCT release from *V. fischeri* was unsuccessful (72), but isolating mutants with altered PG structure should either serve a similar experimental function by eliminating TCT-based signaling or at least provide insight into the structural flexibility in PG detection by *E. scolopes*. Our study started with an approach previously used by others with *Mycobacterium smegmatis* (3), generating a DAP auxotroph and selecting suppressors that no longer require DAP. In this way, we were able to isolate and characterize mutants with lanthionine replacing DAP in their PG.

## RESULTS

We isolated a DAP auxotroph, strain RMJ1, by deleting most of the *dapE* gene, which encodes *N*-succinyl-L,L-diaminopimelic acid desuccinylase. RMJ1 was generated via allelic exchange by growing cells on DAP-supplemented minimal salts medium (DAP medium), after we

were unexpectedly unable to isolate a mutant on DAP-supplemented LBS medium. This observation is corroborated by a recent screen for *V. fischeri* mutants isolated on supplemented LBS, which likewise failed to identify any DAP auxotrophs using this complex base medium (168).

RMJ1 was grown in DAP medium and plated on DAP-free plates, resulting in the appearance of spontaneous suppressors of DAP auxotrophy at a rate of ~$10^{-8}$ (data not shown). Three mutants able to grow without DAP supplementation were subjected to PG analysis and whole-genome resequencing. Two of the suppressor mutants grew better than the third in liquid media, and for these two mutants HPLC analysis of the PG amino acid content revealed the typical 2:1:1 ratio of Ala, DAP, and Glu (data not shown). Genome sequencing revealed that mutant RMJ1S3 contained a missense mutation (G484A/E162K) in VFA_1086, which is annotated as encoding a subtilisin-like serine protease. The other mutant, RMJ1S2 had a nonsense (G1144A) mutation in VF_1349, which encodes a LysR-type transcriptional regulator. Because these two mutants had PG that was indistinguishable from that of wild type, they were not analyzed further.

The third suppressor mutant did not grow as well as the other two, and the provenance of this lineage deserves description. Initially, the isolate did not grow in broth culture and was quickly stocked in the freezer by scraping cells off plates, resulting in strain RMJS0. However, a broth culture derived from this suppressor eventually did grow and was stocked as mutant RMJS1. Later we discovered that RMJS0 and RMJS1 are genetically distinct, as described below. However, most characterization was performed on RMJS1.

PG analysis of RMJ1S1 revealed an Ala:DAP:Glu ratio of 2:0:1. Although there was no evidence of DAP, a new peak appeared that did not correspond to any of our amino acid standards. We also analyzed muramidase-digested PG from ES114 (**Figure 3.1A**) and RMJ1S1 (**Figure 3.1**

**B**), finding that peaks corresponding to the mono- and di-murosaccharide peaks of wild type PG are absent in the mutant, while two peaks similarly altered in their retention time appear in their place. These data suggest the presence of mono- and di-murosaccharide peaks in the mutant, which would indicate the PG peptide chain is still able to cross-link in RMJ1S1. Fractions corresponding to the mono-murosaccharide structures were collected and analyzed via mass spectroscopy

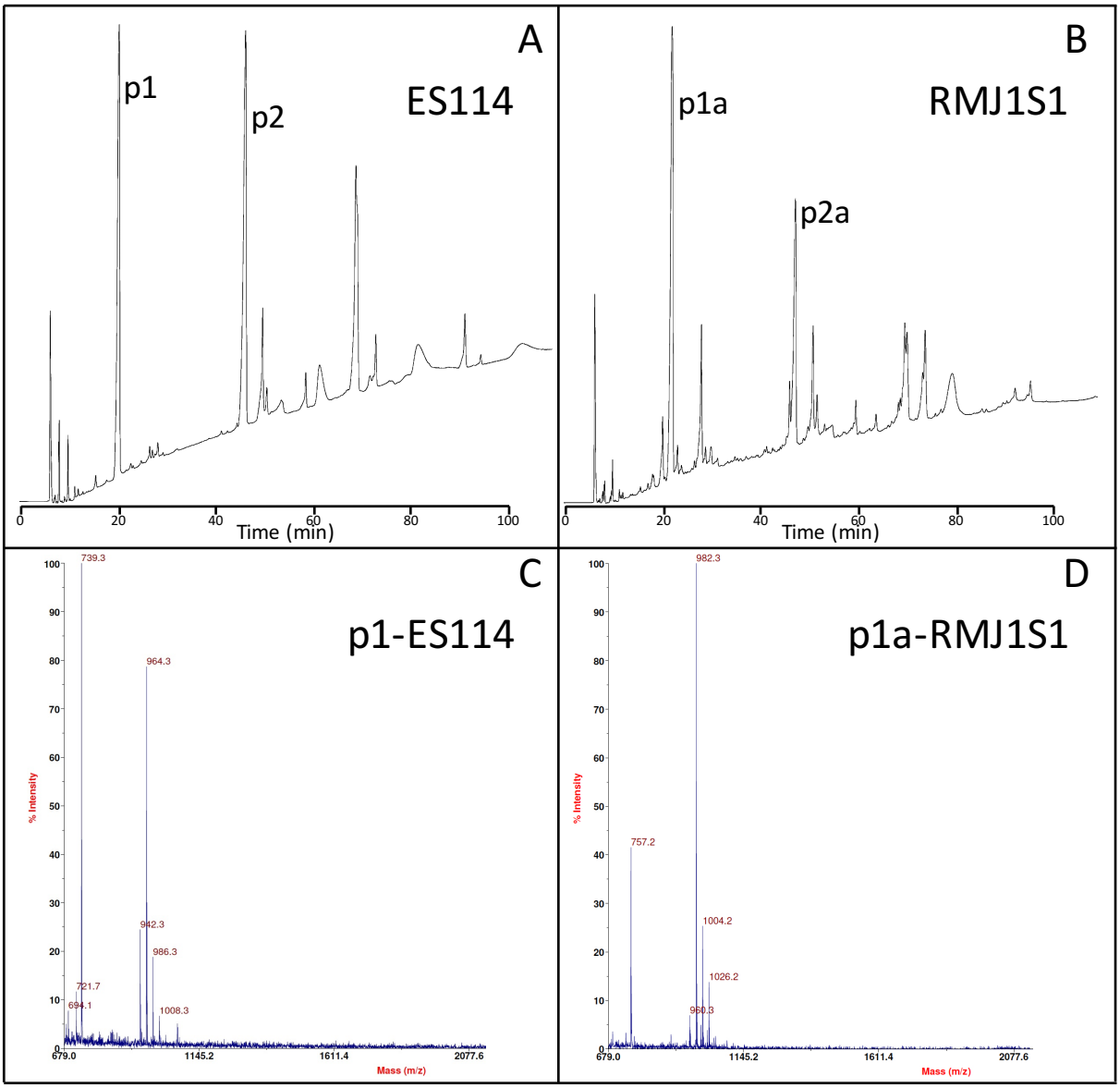


**Figure 3.1** HPLC and mass spectroscopy analysis of PG isolated from wild-type strain ES114 (A & C) or RMJ1S1 (B & C). Panels A and B show HPLC traces from muramidase digested PG. Labeled are the mono-muropeptide (p1) and di-muropeptide (p2) structures from wild type, and what appear to be modified but analogous peaks from RMJ1S1 (p1a, p2a). Panels C and D show mass spectroscopy for collected peaks p1 and p1a, respectively.

(**Figure 3.1 C and D**). The difference in molecular weight between the wild-type and mutant PG fragment is approximately 18 Da, which would be consistent with the replacement of DAP with lanthionine. Lanthionine is structurally similar to DAP with the difference being a sulfur atom (32 Da) replacing a $–CH_2-$ (14 Da) in the center of the molecule (the C4 position). Amino acid analysis was repeated with the addition of a lanthionine standard, which had a retention time identical to that of the unknown amino acid in the RMJ1S1 PG. Taken together, these data indicate that lanthionine replaces DAP in mutant RMJ1S1.

Sequencing the genome of RMJ1S1 revealed a single nucleotide polymorphism in the *cysK* gene (VF_1893), which encodes the O-acetyl serine sulfhydrylase serving as the final step in cysteine biosynthesis. The T419G mutation resulted in a L140R change in CysK. There was also a 340-bp deletion (bp 97-437) in the *yecC* gene (VF_0006), which encodes a putative cystine transporter. In attempting to determine whether one of these mutations preceded the other, we explored clones in our original stock and discovered that RMJ1S0 has wild-type *yecC* and is a *cysK* mutant. However, RMJ1S0 has a different *cysK* mutation (G290A) than does RMJ1S1, resulting in a G232S replacement in CysK. The possible origins of RMJS0 and RMJS1 are discussed below, but the latter strain was characterized owing to its superior growth.

To test whether the CysK variants in RMJS0 and RMJS1 are responsible for restoring prototrophy to strain RMJ1, the respective mutant *cysK* alleles were cloned and expressed *in trans* in RMJ1 (**Figure 3.2**). Both alleles show some capacity to restore DAP-independent growth to RMJ1, with the L140R variant from RMJ1S1 supporting more robust growth than did the G232S variant from RMJ1S0. However, neither CysK variant was able to restore growth to the level of wild type (ES114) or strain RMJ1S1 (**Figure 3.2**). Wild-type *cysK* did not support growth of RMJ1 in DAP-free media (**Figure 3.2**).

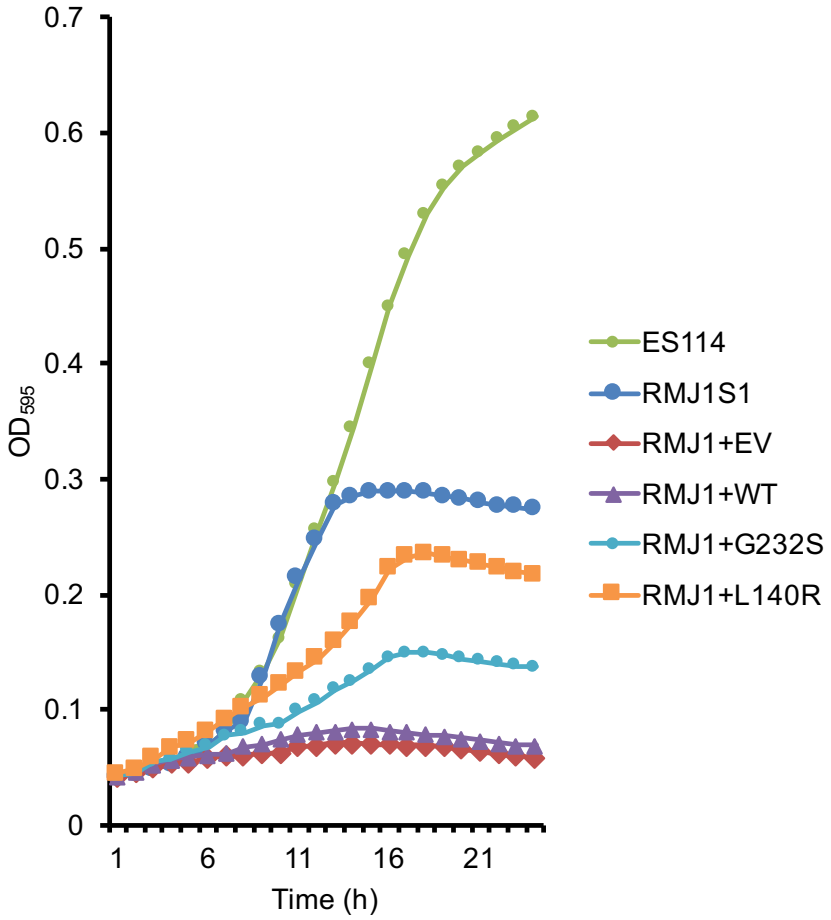


**Figure 3.2** Mutant *cysK* alleles *in trans* overcome DAP auxotrophy of RMJ1**.** Growth in DAP-free minimal medium was assessed for RMJ1 (Δ*dapE*) carrying pVSV104 (RMJ1+EV; red diamonds) or derivatives of this plasmid expressing wild-type *cysK* (+WT; purple triangles), the G232S mutant *cysK* from RMJ1S0 (RMJ1+G232S; light blue circles), or the L140R mutant *cysK* from RMJ1S1 (RMJ1+L140R; orange squares). Growth of strains ES114 (green circles) and RMJ1S1 (dark blue circles) is shown for comparison. Strains were grown overnight, and subcultured (1:1000) into 200 µL of minimal salts medium in a 96-well plate, grown with shaking (200 RPM) at 28°C, and $OD_{595}$ was measured every hour. One of three representative experiments is shown.

Despite growing much better in broth than did RMJ1S0, strain RMJ1S1 showed obvious differences from wild type. When attempting to infect squid with RMJ1S1, we noticed that colony-forming units for this strain decreased orders of magnitude upon dilution into Instant Ocean. We subsequently found that RMJ1S1 is substantially less tolerant of NaCl than is wild type (**Figure 3.3**). RMJ1S1 also has a larger and more spherical cell morphology relative to the small rods

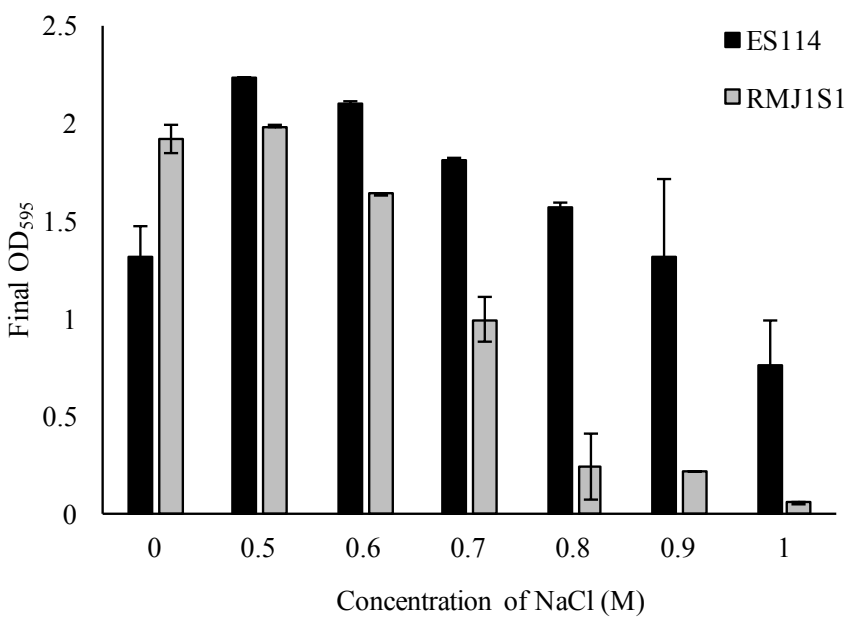


**Figure 3.3** Decreased salt tolerance of strain RMJ1S1. Overnight cultures of ES114 (black bars) or RMJ1S1 (gray bars) grown in Tris-buffered minimal salts medium were adjusted to an $OD_{595}$ of 1.0, subcultured 1:1000 into media with varying NaCl concentrations, incubated at 28 degrees for 24 h, and the final $OD_{595}$ is shown. Bars show standard error ($n$=3)

typical of wild-type cells (**Figure 3.4**). The morphology of the Δ*dapE* parent (RMJ1) grown in DAP medium was indistinguishable from wild type (data not shown).

Given the intolerance of RMJ1S1 to the Instant Ocean in which squid are kept, we were effectively unable to evaluate this mutant's symbiotic proficiency; however, we were still able to investigate whether the replacement of DAP with lanthionine in RMJ1S1's PG affected the ability of cell-surface fractions (CSF) to trigger late-stage apoptosis in developing juvenile squid. CSFs contain both LPS and PG, and they trigger changes in the infection-promoting ciliated epithelial cells on the surface of the light organ that are similar to the synergistic effect of LPS and PG combined, which is itself similar to the effect of normal symbiotic infection. The most readily quantified effect is apoptosis of cells in the ciliated epithelial appendages, which can be assessed after TUNEL staining by counting the number of TUNEL+ cells per appendage. CSFs prepared from either wild type or RMJ1S1 induced indistinguishable levels of late-stage apoptosis, as measured by TUNEL+ cells, and both treatments induced significantly more apoptosis than was seen in untreated control animals (**Figure 3.5**).

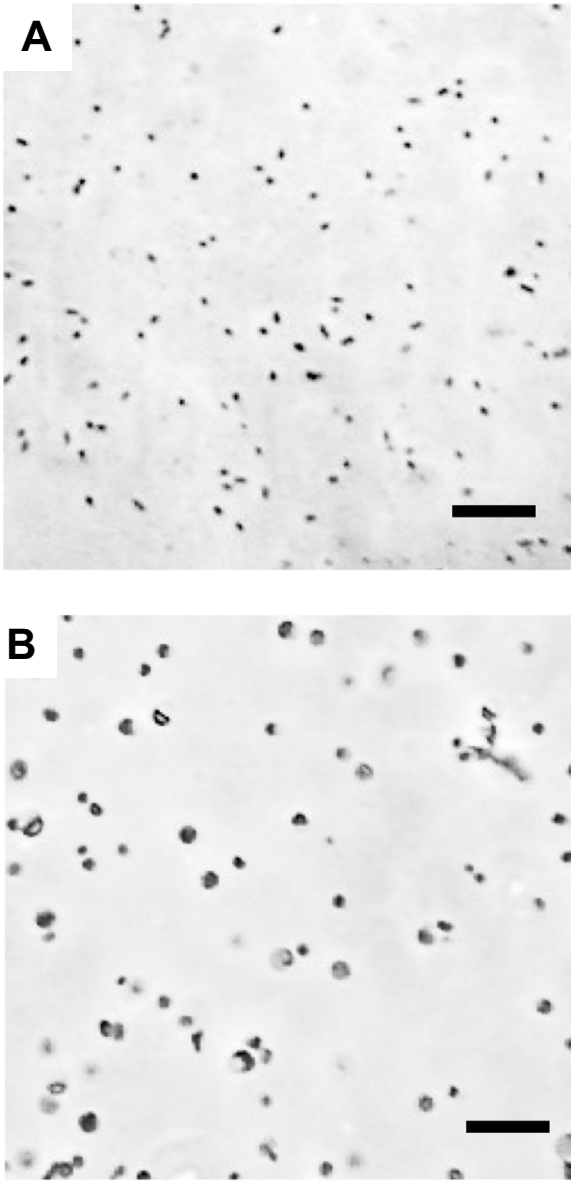


**Figure 3.4** Cell morphology of RMJ1S1. Phase-contrast images show the wild-type strain ES114 (A) and the lanthionine-containing mutant strain RMJ1S1 (B). Bars indicate standard size of 10 µm. Cells were grown to mid-log phase in minimal salts medium at 28°C with shaking at 200 rpm.

## DISCUSSION

### *Role of PG in the* V. fischeri-E. scolopes *symbiosis*

In the monospecific, horizontally-acquired mutualism between *V. fischeri* and its squid host *E. scolopes*, PG plays an important role in the well-studied infection process leading to a stable symbiosis (32), serving as a developmental signal to the host (54). The recognition of PG and other *V. fischeri*-specific signals alerts the host to the presence of the symbiont, and triggers

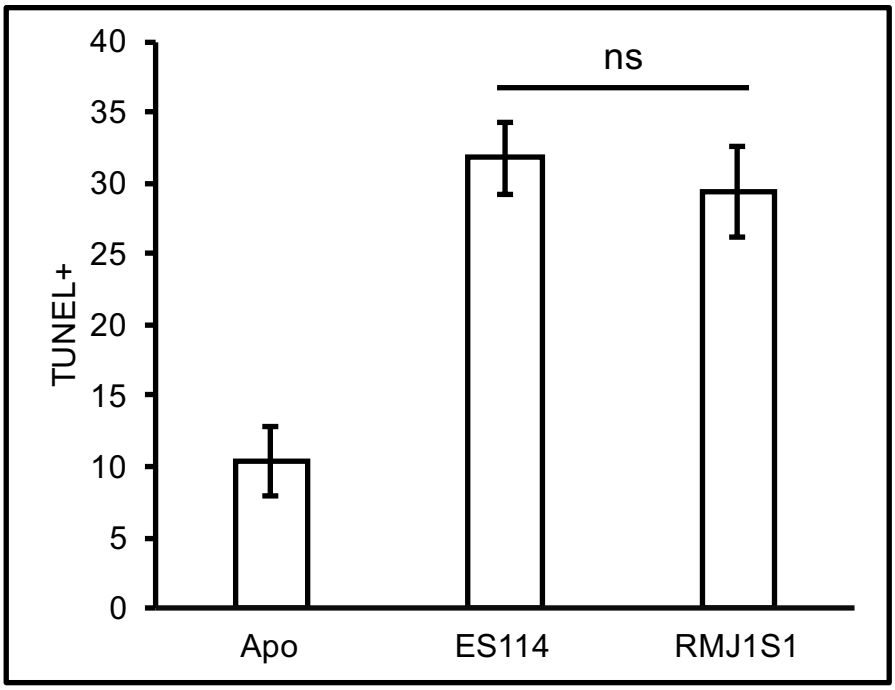


**Figure 3.5** Counts of TUNEL+ cells after exposure to wild-type and lanthionine-containing cell-surface factions. Freshly-hatched juvenile squid were exposed to cell-surface fractions isolated from strain ES114, RMJ1S1, or an mPBS control (Apo). Squid were fixed and TUNEL stained as described after 48h of exposure. TUNEL+ cells were counted per appendage set and averaged across treatments. Treatments with wild-type (ES114) or lanthionine-containing (RMJ1S1) CSFs were not significantly different (ns) when compared via a Student's T-Test ($p>0.1$). Both treatments were significantly different from untreated (Apo) ($p<0.01$).

the regression of infection-promoting ciliated epithelial appendages. This is a way for the host to "close the door" to further infection, preventing the acquisition of additional bacteria in the light organ. From the host perspective, this process could decrease the chance of acquiring deleterious bacteria (e.g. unwanted pathogens) in the light organ, and for the initial *V. fischeri* colonists stimulating this process may inhibit potential competition from subsequent *V. fischeri* strains (72). The PG-based signal TCT appears to be important in this process, as squid colonized by strains that release less TCT are more susceptible to superinfection by additional *V. fischeri* strains (72).

The selection of RMJ1S1 allowed us to present lanthionine-containing PG to juvenile squid, but the strain's sensitivity to salt prevented investigation of natural colonization. When PG was presented in cell-surface fractions, the lanthionine substitution did not appear to inhibit late-stage apoptosis (**Figure 3.5**). These results are consistent with studies of the capacity of lanthionine

and lanthionine-containing PG fragments to bind receptors and elicit responses in other hosts. In *Drosophila melanogaster*, peptidoglycan recognition proteins (PGRP) are specialized to recognize DAP- or Lys-type PG and coordinate an appropriate immune response (169). PG with DAP, lanthionine or cystathionine in the third position each triggered the DAP-PG-specific immune response (**Figure 3.6**) (170). Similarly, lanthionine, like DAP, binds to the immune protein NOD1 and induces immune signaling in human epithelial (171) and porcine (172) cells. Thus, it would not be unprecedented should lanthionine-containing PG function similarly to that of wild type.

However, it should be noted that the presentation of PG is different in CSFs than in the natural *V. fischeri-E. scolopes* symbiosis. The case may be that larger lanthionine-containing PG fragments in CSFs can still induce late-stage apoptosis yet lanthionine-containing PG monomers (i.e., TCT with DAP replaced by lanthionine) may be impaired in signaling. Additionally, the presentation as CSFs includes the immune adjuvant LPS, which acts synergistically with PG and may mask any subtle effects of pure PG (54). Eventually, it would be preferable to generate a strain with lanthionine-containing PG that is suitable for colonization studies.

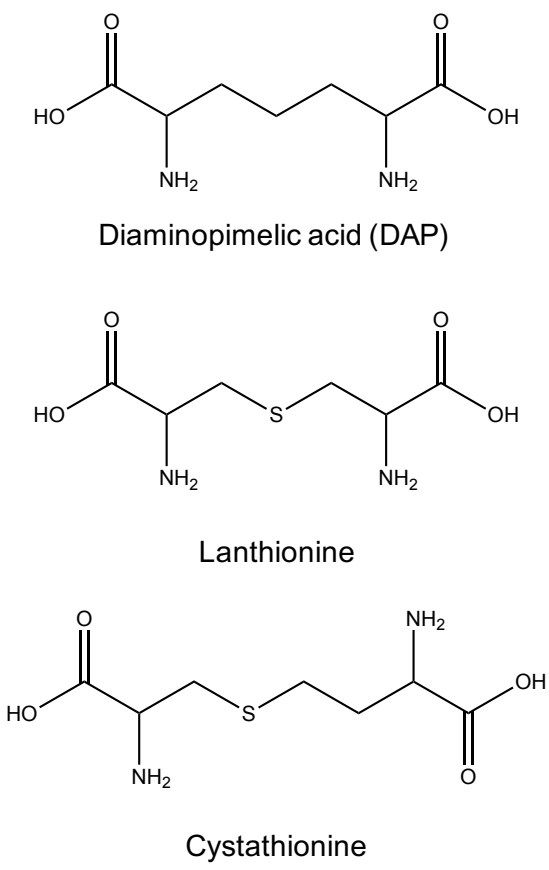


**Figure 3.6** Amino acids that can replace DAP in PG biosynthesis. Lanthionine has been found in PG of bacteria that evolved naturally (2) and experimentally (3). Cystathionine has been introduced into the PG of engineered E. coli (4). Both lanthionine and cystathionine can serve as substrates for E. coli MurE (5).

*Origins of suppressor mutant RMJS1*

We have shown that *V. fischeri* mutant RMJ1S1 has lanthionine-containing PG, and mutations in *cysK* and *yecC*; however, the origin of this suppressor remains unclear. As noted above, suppressors of DAP auxotrophy in RMJ1 were recovered at a frequency of ~$10^{-8}$, which seems high if both the *yecC* and *cysK* mutations were required. The fact that the *cysK* allele alone could restore DAP prototrophy to RMJ1 suggested that the *yecC* deletion may play a secondary role. We therefore probed our stocks to determine if they were mixed and contained any cells that remained wild type with respect to *cysK* or *yecC*. This led us to discover that the suppressor we initially stocked from cells scraped off a streak plate (RMJ1S0) was genetically distinct from the subsequent stock made from a broth culture (RMJ1S1). RMJ1S0 is wild type with respect to *yecC*, and although it has a mutation in *cysK* this allele is distinct from the *cysK* mutation in RMJ1S0. Both RMJ1S1 and RMJS0 can be traced to the same single colony, so their related but disparate genotypes are difficult to reconcile.

Perhaps the simplest explanation of these puzzling observations is that selection for suppression of auxotrophy in RMJ1 initially enriched a mutant with an amplification of *cysK*. Although wild-type *cysK* on a plasmid (~12 copies/cell (147)) did not restore robust growth to RMJ1 (**Figure 3.2**) amplification of the gene may have allowed some growth or survival and provided multiple copies of *cysK* as targets for mutation. If two growth-restoring *cysK* alleles arose, subsequent resolution of the amplified locus could have resulted in retention of different mutations in different lineages. The only other reasonable explanation would be that two cysK mutants arose very close to each other on a plate, perhaps one cross-feeding wild-type cells in a microcolony until another acquired a *cysK* mutation. We speculate that the *yecC* mutation was secondary, and by disrupting recycling of cystine into cysteine it might promote flux through the

cysteine biosynthetic pathway and thereby magnify the ability of the mutant CysK to produce lanthionine. The complementation experiment shown in **Figure 3.2** does not account or test for any role of *yecC*. The presence of a functional *yecC* gene in this assay may explain why complementing with the L140R allele *in trans* is not sufficient to restore grown of RMJ1 to the level of RMJ1S1. An alternative explanation for this observation is that the presence of wild-type *cysK* may diminish the effect of the *cysK* mutation. In the future, it would be interesting to determine whether deletion of *yecC* has any effect on RMJ1 alone or in combination with the *cysK* variants.

*Artificial evolution of lanthionine-containing PG*

Our study is similar to others that employed experimental evolution in generating lanthionine-containing PG. Richaud et al. overexpressed the *metB* gene while disrupting *metC* in an *E. coli* DAP auxotroph, which resulted in the incorporation of lanthionine and cystathionine thioethers in place of DAP in the PG (**Figure 3.6**) (4). Similarly, exogenous cystathionine or lanthionine could overcome the DAP auxotrophy of *E. coli dapA* mutants (5). In an approach more similar to ours, DAP-auxotrophs of *M. smegmatis* were used to select spontaneous suppressors that could grow in the absence of DAP (3). One such mutant replaced DAP with lanthionine, and had a mutation in the ribosome binding site of the cystathionine beta synthase gene (3), a gene that appears to be absent in *V. fischeri*. In *E. coli*, the MurE enzyme responsible for addition of DAP to the peptide side chain of PG (173) is able to use lanthionine as a substrate (5), and presumably this is true for MurE in *M. smegmatis* and *V. fischeri* as well. The mutations in *M. smegmatis* and *V. fischeri* that gave rise to lanthionine-containing PG occurred not in *murE* but in genes involved in cysteine biosynthesis and cystine transport, which may affect the intracellular pool of

lanthionine. It remains to be seen the extent to which MurE specificity and/or the available pool of suitable DAP replacements determines the natural evolution of variation at the third position in the PG peptide. Indeed, it is formally possible that many bacteria contain lanthionine in place of DAP, but do so in such a relatively small fraction of their PG that it remains undetected, owing to the limited pool of this substrate.

*A possible convergence of natural and artificial evolution*

As noted above, lanthionine can also be found naturally in the PG peptide of the oral bacterium *F. nucleatum* (2). A study of $H_2S$-producing enzymes in *F. nucleatum* revealed that this organism has a pair of paralogs homologous to CysK (82). One CysK homolog, Fn1220, can condense two cysteine residues to lanthionine, producing $H_2S$ (82). Though the researchers did not examine the effect of mutations in the gene on PG structure, the activity of this protein in *F. nucleatum* may be the source of lanthionine found in the PG. We now demonstrated that in a *V. fischeri* Δ*dapE* background, the expression of the L140R variant of *cysK* is sufficient to restore prototrophy in the absence of DAP **(Figure 3.2**). Our hypothesis is that both variants found in our screen have an increased capacity for lanthionine production compared to wild-type CysK. The purification and characterization of the CysK variants found in this study, as well as a comparison to Fn1220 from *F. nucleatum,* would help resolve whether CysK is directly responsible for lanthionine generation in our mutants.

*Long-term experimental evolution*

The isolation and characterization of mutant RMJ1S1 provides an opportunity to investigate how a model bacterium can accommodate a new cell wall structure. Given this strain's

relative attenuation in culture, a fertile area for future studies would be to grow RMJ1S1 in continuous culture to enrich for strains that grow better and/or better withstand NaCl. Such an experimental evolution approach would enable researchers to investigate what sorts of compensatory mutations arise, while also generating new more robust strains to investigate in this bacterium's symbiosis with *E. scolopes*.

## MATERIALS AND METHODS

**Bacterial strains and culture conditions**. The strains used in this study are listed in **Table 3.1**. When added to LB medium (135) for selection of *Escherichia coli*, kanamycin (Km) was used at a concentration of 40 μg $ml^{-1}$. For selection of *E. coli* with erythromycin (Em), 150 μg $ml^{-1}$ was added to BHI medium (Difco, Sparks, MD). *E. coli* was incubated at 37°C. *V. fischeri* was grown in LBS medium (137) or Tris-buffered minimal salts medium (72) with glycerol (rather than glucose) added to 0.3% final concentration and casamino acids added to 1 g/L. When added to LBS or minimal salts medium for selection of *V. fischeri*, Km, and Em were used at concentrations of 100 and 5 μg $ml^{-1}$ respectively. *V. fischeri* was grown at 28°C. DAP medium, which was used to isolate and grow the *V. fischeri* DAP auxotroph, was minimal salts medium with 40 mM DAP replacing ammonium chloride as a nitrogen source and with no casamino acids. Agar was added to a final concentration of 1.5% for solid media. Growth analysis was done by subculturing overnight cultures adjusted to an optical density at 595 nm ($OD_{595}$) of 1.0 1:100 in 200μL of media in 96-well plates (Costar). Cultures were grown shaking (200 RPM) at 28°C, and $OD_{595}$ was measured every hour using a BioTek Synergy 2 plate reader (BioTek. Winooski, VT).

**Molecular genetics and sequence analysis**. Plasmids (**Table 3.1**) were constructed using standard genetic techniques. Oligonucleotides used for PCR and cloning are listed in **Table 3.1** and were synthesized by Integrated DNA Technologies (Coralville, IA). DNA ligase and restriction enzymes were obtained from New England BioLabs (Beverly, MA). PCR was conducted with Phusion high-fidelity DNA polymerase (New England BioLabs, Beverly, MA). Plasmids used for cloning were isolated with the ZR Plasmid Miniprep kit (Zymo Research, Irvine, CA). DNA was repurified between cloning steps with the DNA Clean and Concentrator-5 kit (Zymo Research, Irvine, CA). Cloned PCR products were sequenced at the University of Michigan DNA Sequencing Core Facility, and sequences were analyzed using Geneious version 8.1 (148). Plasmids were generated in *E. coli* DH5αλ*pir* and conjugated into *V. fischeri* strains through triparental mating using CC118λ*pir* (150) carrying plasmid pEVS104 (140) as a conjugative helper. Genome resequencing was performed as described previously (149). Resulting assemblies were compared to the NCBI reference sequence using Geneious version 8.1 (148).

**Table 3.1:** Bacterial strains, plasmids, and oligonucleotides used in this study

| **Strain, plasmid, or oligonucleotide** | **Relevant characteristics**[a] | **Source or reference** |
|---|---|---|
| ***E. coli*** | | |
| CC118λ*pir* | Δ**(***ara-leu***)** *araD* Δ*lac74 galE galK phoA20 thi-1 rpsE rpsB argE(Am) recA λpir* | (140) |
| DH5α | φ80d*lacZ*ΔM15 Δ(*lacZYA-argF*)U169 *deoR supE44 hsdR17 recA1 endA1 gyrA96 thi-1 relA1* | (141) |

| | | |
|---|---|---|
| DH5α*λpir* | DH5α lysogenized with *λpir* | (142) |

| | | |
|---|---|---|
| ***V. fischeri*** | | |
| ES114 | Wild-type isolate from *E. scolopes* | (14) |
| RMJ1 | Δ*dapE* | This study |
| RMJ1S0 | Δ*dapE, cysK*(G232S) | This study |
| RMJ1S1 | Δ*dapE,* Δ*yecC* (97-437 bp, frameshift)*,* *cysK*(L140R) | This study |
| RMJ1S2 | Δ*dapE*, VF_1349 (G1144A) | This study |
| RMJ1S3 | Δ*dapE*, VFA_1086 (G484A/E162K) | This study |

| | | |
|---|---|---|
| **Plasmids**[b] | | |
| pCR-Blunt | *ori*$V_{ColE1}$, *kanR* | Thermo Fisher |
| pCR-Blunt-II-TOPO | *ori*$V_{ColE1}$, *kanR* | Thermo Fisher |
| pEVS94S | *ori*$V_{R6K}$ *ori*$T_{RP4}$*, ermR* | (140) |
| pEVS104 | conjugative helper plasmid; *ori*$V_{R6K}$, *ori*$T_{RP4}$, *kanR* | (140) |

| | | |
|---|---|---|
| pHK2 | *dapE* upstream fragment cloned into pCR-Blunt II TOPO and fused to pEVS94S | This study |
| pRMJ37 | *cysK* in pVSV104 | This study |
| pRMJ38 | *cysK*(L140R) in pVSV104 | This study |
| pRMJ39 | *cysK*(G232S) in pVSV104 | This study |
| pVSV104 | pES213, R6Kγ, $oriT_{RP4}$, *kanR*, *lacZ*α | (147) |
| pWC1 | Δ*dapE* deletion construct | This study |

| **Oligonucleotides**[c] | | |
|---|---|---|
| dapEupF | ATATCGCTAGCCCTTAATAACTCTTAACC TTAAAAGCTCTTAACTC | Anne Dunn |
| dapEupR | GCGTTAAATCACCTGTAGGAACAACAT | Anne Dunn |
| EVS131 | GCAATTGGATAAATTAGGGTTATGATGA GAGAGC | This study |
| EVS132 | GCCTAGGTAGTAGGATAGAAAATGAAAG TGAAGACTCGC | This study |
| RJ53 | TAAGCTAGCTGAAATGAAGGAACAGATC ATG | This study |
| RJ54 | AATGGTACCTGATTTGAACACATAGATGT TACA | This study |

[a] Drug resistance abbreviations used: *ermR*, erythromycin resistance; *kanR*, kanamycin resistance (*aph*).
[b] All alleles cloned in this study are from *V. fischeri* strain ES114. Replication origin(s) (*oriV*) on each vector are listed as R6Kγ, ColE1, and/or pES213. Plasmids based on pES213 are stable in *V. fischeri* and do not require antibiotic selection for maintenance (147).
[c] All oligonucleotides are shown 5' to 3'. Underlined regions highlight restriction enzyme recognition sites

**Construction of DAP auxotroph.** The region upstream of *dapE* along with the first 235 nucleotides of the gene was PCR amplified using primers dapEupF and dapEupR, the fragment was cloned into pCR-Blunt (Thermo Fisher, Waltham, MA), the resulting plasmid was linearized with NheI digestion and fused to SpeI-digested pEVS94S (140), and then deletion of an XbaI fragment removed most of the PCR-Blunt vector, resulting in pHK2. The region downstream of *dapE* was PCR amplified using primers EVS131 and EVS132, the fragment was cloned into pCR-Blunt-II-TOPO (Thermo Fisher, Waltham, MA), and the resulting plasmid was digested with MfeI and ligated to EcoRI-digested pHK2, yielding pWC1. The resulting allele on pWC1 contains a deletion in *dapE*, inserting proline and stop codons immediately after the first 78 residues of DapE, with regions flanking the gene allowing allelic exchange. This construct was conjugated into *V. fischeri* as described above. After initial incorporation of plasmid pWC1 by homologous recombination, cells were grown in DAP medium to allow exchange of the Δ*dapE* allele in place of the complete wild-type allele. Allelic exchange was confirmed by PCR and by screening for DAP auxotrophy.

**Construction of *cysK* complementation vectors**. To generate *cysK* complementation vectors pRMJ37, pRMJ38, and pRMJ39 the *cysK* gene was amplified from ES114, RMJ1S1 (L140R), or RMJ1S0 (G232S), respectively, using primers RJ53 and RJ54. The resulting PCR product was cloned into pCR-Blunt II-TOPO (Themo Fisher, Waltham, MA) and sequenced. The variants of *cysK* were subcloned by digestion with KpnI and ligation to pVSV104 linearized

with KpnI. The resulting transformants were directionally screened with SpeI digestion prior to final sequencing.

**Selection for spontaneous suppressors of DAP auxotrophy**. Strain RMJ1 was grown to an $OD_{595}$ of 0.5 in DAP medium, and 100 µL of culture was plated on minimal salts medium without DAP added. Cultures were plated in parallel on DAP plates to determine mutation frequency. Plates were incubated at 28°C and colonies were counted at 48h. Colonies were streak purified, PCR checked for the Δ*dapE* genotype, and stocked in minimal salts medium with glycerol added to 20% final concentration. Since the initial suppressor RMJ1S0 would not grow in liquid culture, colonies were scraped from a plate and resuspended to make a freezer stock.

**Analysis of PG amino acid and muropeptide content**. To isolate PG, cells were grown to an $OD_{595}$ of ~0.6 in minimal salts medium, chilled on ice for 10 min and centrifuged at 4°C and 15,000 x g for 10 min. After resuspension in 4 ml cold water, cell suspensions were dripped into 50 ml boiling, 4% SDS with continuous stirring, boiled for 30 min, and allowed to cool to room temperature. Samples were then centrifuged at 130,000 x g for 60 min at room temperature, resuspended in 20 ml 50°C water, and washed twice more in 20 mL water. The pellet was resuspended in 20 ml water, heated at 100°C for 2 min to dissolve precipitated SDS and washed twice more as above. Before resuspension, the supernatant was assayed for SDS using methylene blue and chloroform (156). When SDS was undetectable, the pellet was resuspended in 1 ml of 100 mM Tris HCl pH 7.5, and the suspension was subsequently treated with α-amylase (Sigma-Aldrich, St. Louis, MO), DNase I (Sigma-Aldrich, St. Louis, MO), RNase (Sigma-Aldrich, St. Louis, MO) and Trypsin (Worthington Biochemical, Lakewood, NJ). SDS was added to 1%, the solution was boiled for 15 min, diluted into 20 ml warm water, and centrifuged at 130,000 x g for 10 min at 20°C. The resulting pellet was washed twice in water, once in 8 M LiCl, and twice more

in water. The final pelleted PG was resuspended in 100 µl of water and stored at -80°C. Amino acid (157) and muropeptide analyses (158) were performed using HPLC as previously described. MALDI-TOF MS analysis was performed on the two major peaks (mono- and di-muropeptide) from ES114 and RMJ1S1. Additional fragmentation analysis was performed on each peak to determine the position of the molecular weight change.

**Microscopy.** Bacteria were grown to mid-log phase in minimal salts medium and viewed by phase-contrast microscopy using a Nikon (Melville, NY) Eclipse E600 microscope. Images were captured with a Nikon Coolpix 5000A camera and edited using the recolor, contrast, brighten, and sharpen features from Adobe Photoshop CC 2015 (Adobe Systems, San Jose, CA). Scale was determined by comparison to an imagen taken of a micrometer slide.

**Assaying effect of cell-surface fractions (CSFs) on *E. scolopes*.** CSFs were prepared as described previously (174). CSF doses were normalized based on protein content determined by a Bradford assay, and added directly to filter-sterilized Instant Ocean (Aquarium Systems, Mentor, Ohio) at a concentration of 100 µg protein $mL^{-1}$. Hatchling squid were exposed to CSF for 48 hr and fixed in 4% paraformaldehyde in mPBS. After fixing, TUNEL staining was performed using the DeadEnd$^{TM}$ Fluorometric TUNEL System (Promega, Madison, Wisconsin) as previously described (10). Stained animals were imaged using a Zeiss LSM 710 confocal microscope at the Biomedical Microscopy Core facility at the University of Georgia. TUNEL+ cells were counted per each set of appendages, and averaged per appendage set across treatments.

**ACKNOWLEGEMENTS**

We thank Anne Dunn, Zomary Flores-Cruz, Hank Kimbrough, and Warren Crabb for contributing to the construction of the Δ*dapE* mutant, and Glen Feller for assistance with NaCl assays.

# CHAPTER 4

# CONCLUSIONS AND FUTURE DIRECTIONS

The purpose of this dissertation was to investigate the role of peptidoglycan (PG) structure in the mutualistic *Vibrio fischeri – Euprymna scolopes* symbiosis while simultaneously exploring how the bacteria can evolve and accommodate a new PG structure. PG and its components have previously been shown to have roles as microbe-associated molecular patterns (MAMPs) in the squid-*Vibrio* symbiosis and other bacterial interactions with Eukaryotes. For example, the common PG-derived MAMP tracheal cytotoxin (TCT) is released in pathogenic and mutualistic interactions and triggers the apoptosis of ciliated cells in each of the systems where it has been studied, including the *V. fischeri*-squid symbiosis (166). The squid-*Vibrio* system provides a useful model for investigation of the intricacies of this and other PG-based MAMPs.

A *V. fischeri* mutant that does not release TCT would be a useful experimental tool, but previous attempts to generate such a strain were not successful. Specifically, an *ltgA ltgD ltgY* triple mutant, despite a ~90% reduction in extracellular TCT accumulation, still released enough TCT to trigger host light-organ morphogenesis (72). For my dissertation work, I took a different approach to disrupting this signal, aiming to alter the PG structure of the bacterial symbiont through the selection of spontaneous mutants. The strategy involved generating strains auxotrophic for three PG-specific D-amino acids: D-Ala, D-Glu, and diaminopimelic acid (DAP). These auxotrophs were then used to select spontaneous mutations that suppressed

auxotrophy (i.e., restored prototrophy) to the parent strains. The ability to overcome D-Glu, D-Ala, or DAP auxotrophy could be accomplished in two general ways: 1) the strain could induce or develop a novel biosynthetic route to the amino acid required by the auxotrophic parent, or 2) the strain could replace or omit that amino acid in its PG side chain. The goals for my research were to investigate what effects both types of mutations had on *V. fischeri*, and whether structural alterations had effects on PG's role as a signal in the symbiosis. Successful manipulation of PG using this approach also provides us with a strain of a model Gram-negative organism with atypical PG that can be studied further.

**DISCOVERY OF A D-ASP-ASSOCIATED LTTR**

In Chapter 2, I showed how a cell could suppress D-Glu auxotrophy by inducing a cryptic alternative route to D-Glu biosynthesis. In the mutants I analyzed, the PG was wild type, and the genome was altered through a single point mutation in an uncharacterized LysR-type transcriptional regulator (LTTR). The genetic organization of this regulator in *V. fischeri* (**Figure 2.2**) led me to postulate that it was regulating a divergently transcribed operon annotated as encoding a transporter and an aspartate racemase, RacD. The data in Chapter 2 show that this LTTR, DarR, binds upstream of the transporter-racemase operon and increases its transcription in response to D-Asp. The most likely explanation for my data are that RacD can also work as a Glu racemase, and when RacD is expressed at high levels it generates enough D-Glu to support PG biosynthesis. In the initial suppressor, mutation of *darR* led to a hyperactive DarR variant, which activates transcription of the *racD* promoter regardless of whether D-Asp is present.

Notably, *darR* is often linked to *racD* or other genes related to Asp metabolism in a variety of Proteobacteria (**Figure 2.6**). Thus, the serendipitous discovery of DarR may shed light

on metabolic responses to D-Asp in a wide range of bacteria. *V. fischeri* ES114 and *A. baylyi* ADP1 can both grow using D-Asp, whereas mutants lacking *darR* or *racD* in these organisms are impaired in their growth (**Figure 2.7**). This suggests that the normal function of DarR in these organisms is to direct a catabolic response to available D-Asp through the activity of RacD. In the context of the squid-*Vibrio* symbiosis, it is tempting to suggest the light organ as a potential source of D-Asp for *V. fischeri,* as D-Asp has been found in other animal tissues, potentially as a neuro-signal or osmolyte (95). However, initial attempts to view the $P_{racD}$-*gfp* reporter in the squid light organ did not reveal observable induction of the *gfp*-based reporter in symbiotic cells (data not shown). This approach merits further study, and could benefit from a more sensitive method to detect the reporter, perhaps using confocal rather than epifluorescence microscopy to assay for *gfp* expression. Using qPCR to probe expression of *darR* and *racD* genes throughout the course of host colonization would provide an alternative avenue to assess the role of this locus during symbiosis.

Some *darR* homologs can be found proximal to iso-aspartyl dipeptidase genes (**Figure 2.6 B**), and this includes *V. fischeri* which has a DarR paralog, VF_1510, that is divergently transcribed from a putative iso-aspartyl dipeptidase gene. Previous studies have described the function of one of these proteins in *E. coli*, HypT. This LTTR activates transcription of a target promoter in the presence of hypochlorite (132) and its activity is modulated upon methionine oxidation (133). I hypothesize hypochlorite addition leads to protein damage and accumulation of iso-Asp-X dipeptides, which could serve as the effector for HypT and its orthologs. Purification and binding analyses of HypT, VF_1510, and related proteins could be used to determine binding constants of each potential signal, including hypochlorite and iso-Asp-X dipeptides. If hypochlorite does directly or indirectly activate VF_1510, this information could

prove relevant to the symbiosis, as HOCl is produced by the host and encountered by *V. fischeri* upon colonization (41, 134).

A large-scale investigation of the effector-binding domains (EBD) of DarR and its homologs could also prove interesting. Divergence of the EBD may to some degree be indicative of different effectors, and intermediate conservation of the EBD may therefore reflect LTTRs with similar but distinct effectors. If, say, one set of DarR-like proteins instead evolved the ability to recognize and respond to L-Asp, a structural analysis of the range of changes necessary to recognize otherwise identical isomers could be of interest to the field of structural biology. Broad analyses of full-length DarR homolog protein and EBD sequences have not yielded any particularly striking results. For example, one might expect that if either the full length or EBD sequences from the homologs in various groups are aligned and treed, they might group such that branches of the tree reflected similar genetic contexts (e.g. *darR* homologs near mandelate racemase genes might have a distinct effector and might cluster in an analysis of the EBD). Though there is some grouping of DarR homologs consistent with their proximity to racemase or iso-aspartyl-dipeptidase genes, this association is not absolute in trees generated from either set of sequences (EBD or full length) (data not shown). A more detailed and careful bioinformatic analysis could reveal more subtle trends. For example, conserved residues or motifs within EBDs may be more predictive of function than the homology over the entire length of the EBD.

The initial suppressor mutation in *darR* ultimately led to not only an investigation into the function of the LTTR itself, but also the *racD* gene it regulates. With respect to the initial selection, the most relevant finding is that when expressed at high levels, the putative Asp racemase RacD apparently is able to function as a Glu racemase. Although RacD activity has not been assessed, its overexpression restored wild-type cell wall structure to a *murI* (Glu racemase)

mutant, which strongly suggests promiscuity for Glu as a substrate. As shown in Chapter 2, *racD* is essential for growth on D-Asp in both *V. fischeri* ES114 and *A. baylyi* strain ADP1 (**Figure 2.7**), suggesting that RacD normally functions in these bacteria to interconvert D-Asp and L-Asp as part of D-Asp catabolism.

Neidle and colleagues have begun to analyze how the RacD protein from *V. fischeri* might evolve as a more optimal Glu racemase. By placing this *racD* in a gene duplication system in *A. baylyi* ADP1 and using a *murI* deletion background strain that could not generate D-Glu through normal MurI activity, the organism is forced to rely on the Glu racemase activity of RacD to maintain its cell wall structure. In preliminary studies, as few as four copies of the evolved *racD* gene from *V. fischeri* have been able to support growth in the absence of exogenous D-Glu (unpublished data, C. Moxley). Future studies aim to grow the strain in continuous culture with a goal of generating a lineage with only one copy of the *racD* gene and investigating how the strain has evolved. The hypothesis is that the RacD protein will accommodate a more "Glu friendly", MurI-like biochemistry, and its activity on L-Glu will be sufficiently higher than the native RacD, although mutants leading to higher expression of RacD per copy are also possible.

Perhaps most germane to our initial goal, the knowledge gained from careful study of DarR and RacD will enable the selection of new D-Glu auxotroph suppressors in a *racD murI* background. By eliminating both racemases with demonstrated capacity to provide D-Glu, selective pressure may lead to the replacement of D-Glu residues in the peptide side chain and strains with novel PG structure. This iterative approach toward blocking biosynthesis of wild-type PG allows the research to continue moving in the direction of novel PG, which will provide insights to the bacterium's ability to evolve and accommodate such structures.

## GENERATION OF A LANTHIONINE-CONTAINING PG MUTANT

In Chapter 3, I discussed the selection and characterization of a spontaneous mutant that suppresses DAP auxotrophy in a Δ*dapE* background, and I showed that this mutant of *V. fischeri* replaces the DAP in its PG with lanthionine. Such a change in the context of the cell wall can have major effects. In this instance, the lanthionine-containing mutant strain RMJ1S1 grew relatively slowly, had large rounded cells, and displayed increased sensitivity to NaCl. Whole-genome sequencing revealed two changes in the strain, a point mutation in the *cysK* gene, and a partial deletion of the *yecC* gene encoding a cystine transporter. This creation of a *V. fischeri* strain with novel PG structure offers a new avenue for research into the symbiotic role of PG.

The PG monomer TCT is shed from *V. fischeri* in unusually high amounts and can trigger light-organ morphogenesis alone or synergistically with LPS (54), sparking interest in how this PG is recognized by the host and elicits responses. PG recognition proteins (PGRPs) are immune components involved in coordinating recognition and response to PG in many hosts, and PGRPs have been identified and partially characterized in *E. scolopes* (10, 11). However, as mentioned above, a TCT-null strain was not constructed and may not be possible with wild-type PG structure. With the generation of strain RMJ1S1, we now have a strain that makes no bona fide TCT. Because RMJ1S1 is impaired in its ability to survive in seawater, I isolated and tested the ability of cell-surface fractions to trigger one hallmark of symbiotic light-organ morphogenesis; the induction of late-stage apoptosis in ciliated epithelial cells on the organ's surface (**Figure 3.5**). When hatchling squid were investigated 48h after exposure to cell-surface fractions, such fractions from wild type and RMJ1S1 were indistinguishable in their ability to trigger apoptosis in host light organ epithelia. These data could suggest that the PGRPs (or other receptors) used to recognize and respond to PG in *E. scolopes* do not have the ability to discern subtle differences

in PG side chain structure when it is presented in the form of cell-surface fractions, although alternative explanations for this result are possible. The presentation of PG in CSF is probably different from how it would be encountered in the symbiosis, and would, for example, lack PG monomers akin to extracellular TCT. It would therefore be valuable to generate a more symbiosis-proficient mutant strain with altered PG for future animal studies.

The initial characterization of the lanthionine-containing mutant RMJ1S1 provides an opportunity to use a model organism to investigate how a bacterium can accommodate a new cell wall structure. Moving forward, it will be interesting to grow this strain in increasing concentrations of NaCl, using an experimental evolution approach to enrich the best growing strains for future analysis. My hypothesis is that some genes involved in PG synthesis and turnover will acquire mutations to accommodate lanthionine-containing PG and allow for quicker PG turnover, increased PG crosslinking and higher tolerance for salt. Additionally, other genetic alterations could increase the available lanthionine pool or make lanthionine a better substrate for enzymes involved in PG biosynthesis and remodeling. Re-sequencing the genomes of evolved strains would reveal mutations that have allowed for faster growth, and isolation and HPLC analysis of PG can ensure the maintenance of lanthionine-type PG. Eventually, a strain can be selected to use in squid colonization assays, either alone or in competition with wild type. The case may be that while lanthionine-containing cell-surface fractions can still trigger late-stage apoptosis, a strain with lanthionine-type PG is impaired in its ability to colonize and/or signal the host.

The generation of strain RMJ1S1 serves as a proof-of-concept for our overall approach to alter PG structure in *V. fischeri*. Now that we have shown that the third position in the peptide stem can be changed in *V. fischeri*, it will be exciting to select more DAP auxotroph suppressors,

including selecting in a Δ*cysK* background. The selection and screening of more DAP-independent suppressors will shed light on other modifications that can replace wild-type PG structure of *V. fischeri*. Additionally, experiments outlined above will reveal how this model marine bacterium accommodates such new cell wall structures. Combined with analysis of any effects on the symbiosis, future studies using this approach should be fruitful.

**D-ALA AUXOTROPH SUPPRESSORS**

In addition to the results described in Chapters 2 and 3, three suppressors of D-Ala auxotrophy were also subjected to PG structure analysis and whole-genome resequencing (data not shown). All three of the suppressors displayed wild-type PG, and two of the three contained nonsense mutations in the *spoT* gene (VF_0104), which encodes a protein that is involved in responses to nutrient-starvation stresses (175). My working hypothesis is that these *spoT* mutations activate a broad spectrum racemase (*bsrV*), which can use Ala as a substrate and is induced during stationary phase in *Vibrio cholerae* (91). In these studies of BsrV from *V. cholerae*, cells entered stationary phase and activated *bsrV* when they depleted nutrients from the medium, and it seemed plausible that mutations in *spoT* might mimic the underlying regulatory response described. In an attempt to test whether there is up-regulation of the *bsrV* promoter in these *spoT* mutants, I generated a *bsrV* transcriptional reporter to *gfp*. In both *spoT* mutant strains, there was no apparent effect on expression of the *bsrV* reporter (data not shown). However, *V. cholerae* BsrV does act as an alanine racemase (91), and so moving forward any suppressors of D-Ala auxotrophy should be selected in a Δ*bsrV* background. Initial analysis of a *alr*::Tn5 Δ*bsrV* double mutant suppressor suggested that it may contain a 1:1:1 ratio of Ala:Glu:DAP rather than the canonical 2:1:1 ratio, which is consistent with preservation of the

L-Ala but loss of the D-Ala in the PG peptide chain. However, this result needs to be confirmed and the PG structure elucidated more precisely.

## CONCLUSIONS

The bacterial cell wall has long been an important area of study, especially for its crucial role as a target for antibiotics. It is clear that while the overall structure of the PG layer is conserved, it can be changed. By relying on the inherent ability of bacteria to adapt through spontaneous mutations, we were able to develop an approach to alter the peptide side chain of *V. fischeri*'s PG. Because of the iterative nature of this approach, even suppressor mutants that regain wild-type PG provide information that broadens our understanding of PG biosynthesis and D-amino acid metabolism in *V. fischeri* and by elucidating alternative pathways to wild-type PG they suggest additional pathways to block in attempts to find mutants with novel PG. Future studies will continue to use this approach. With advances in sequencing technology making whole-genome resequencing to reveal the genetic basis of suppressors more cost-effective, these sorts of approaches could also be applied creatively to help address a number of scientific questions.

## REFERENCES


1. **Vollmer W, Blanot D.** 2008. Peptidoglycan structure and architecture. FEMS Microbiol Rev **32:**149-167.
2. **Vasstrand EN, Jensen HB, Miron T, Hofstad T.** 1982. Composition of peptidoglycans in *Bacteroidaceae*: determination and distribution of lanthionine. Infect Immun **36:**114-122.
3. **Consaul SA, Wright LF, Mahapatra S, Crick DC, Pavelka MS, Jr.** 2005. An unusual mutation results in the replacement of diaminopimelate with lanthionine in the peptidoglycan of a mutant strain of *Mycobacterium smegmatis*. J Bacteriol **187:**1612-1620.
4. **Richaud C, Mengin-Lecreulx D, Pochet S, Johnson EJ, Cohen GN, Marlière P.** 1993. Directed evolution of biosynthetic pathways. Recruitment of cysteine thioethers for constructing the cell wall of *Escherichia coli*. J Biol Chem **268:**26827-26835.
5. **Mengin-Lecreulx D, Blanot D, van Heijenoort J.** 1994. Replacement of diaminopimelic acid by cystathionine or lanthionine in the peptidoglycan of *Escherichia coli*. Journal Bacteriol **176:**4321-4327.
6. **Ruby EG.** 1996. Lessons from a cooperative, bacterial-animal association: the *Vibrio fischeri-Euprymna scolopes* light organ symbiosis. Annu Rev Microbiol **50:**591-624.
7. **Boettcher KJ, and E. G. Ruby.** 1994. Occurence of plasmid DNA in the sepiolid squid symbiont *Vibrio fischeri*. Curr Micriobiol **29:**279-286.
8. **Goodson MS, Kojadinovic M, Troll JV, Scheetz TE, Casavant TL, Soares MB, McFall-Ngai MJ.** 2005. Identifying components of the NF-kappaB pathway in the beneficial *Euprymna scolopes-Vibrio fischeri* light organ symbiosis. Appl Environ Microbiol **71:**6934-6946.

9. **Krasity BC, Troll JV, Lehnert EM, Hackett KT, Dillard JP, Apicella MA, Goldman WE, Weiss JP, McFall-Ngai MJ.** 2015. Structural and Functional Features of a Developmentally Regulated Lipopolysaccharide-Binding Protein. mBio **6:**15.

10. **Troll JV, Adin DM, Wier AM, Paquette N, Silverman N, Goldman WE, Stadermann FJ, Stabb EV, McFall-Ngai MJ.** 2009. Peptidoglycan induces loss of a nuclear peptidoglycan recognition protein during host tissue development in a beneficial animal-bacterial symbiosis. Cell Microbiol **11:**1114-1127.

11. **Troll JV, Bent EH, Pacquette N, Wier AM, Goldman WE, Silverman N, McFall-Ngai MJ.** 2009. Taming the symbiont for coexistence: a host PGRP neutralizes a bacterial symbiont toxin. Environ Microbiol **12:**2190-2203.

12. **McFall-Ngai MJ, Ruby EG.** 1991. Symbiont recognition and subsequent morphogenesis as early events in an animal-bacterial mutualism. Science **254:**1491-1494.

13. **Wei SL, Young RE.** 1989. Development of sybiotic bacterial bioluminescence in a nearshore cephalopod, *Euprymna scolopes*. Mar Biol **103:**541-546.

14. **Boettcher KJ, Ruby EG.** 1990. Depressed light emission by symbiotic *Vibrio fischeri* of the sepiolid squid *Euprymna scolopes*. J Bacteriol **172:**3701-3706.

15. **Jones BW, Nishiguchi MK.** 2004. Counterillumination in the Hawaiian bobtail squid, *Euprymna scolopes* Berry (Mollusca: Cephalopoda). Mar Biol **144:**1151-1155.

16. **Ruby EG, McFall-Ngai MJ.** 1992. A squid that glows in the night: development of an animal-bacterial mutualism. J Bacteriol **174:**4865-4870.

17. **Stabb E, Millikan D.** 2009. Is the *Vibrio fischeri-Euprymna scolopes* Symbiosis a Defensive Mutualism?, Defensive Mutualism in Microbial Symbiosis. CRC Press.

18. **McFall-Ngai MJ.** 1994. Animal-bacterial interactions in the early life history of marine invertebrates: The *Euprymna scolopes*/*Vibrio fischeri* symbiosis. Am Zool **34:**554-561.

19. **McFall-Ngai MJ, and E. G. Ruby.** 1998. *Sepiolids* and *Vibrios*: When first they meet. BioScience **48:**257-265.

20. **Nyholm SV, Stabb EV, Ruby EG, McFall-Ngai MJ.** 2000. Establishment of an animal-bacterial association: recruiting symbiotic vibrios from the environment. Proc Natl Acad Sci U S A **97:**10231-10235.

21. **Nyholm SV, Deplancke B, Gaskins HR, Apicella MA, McFall-Ngai MJ.** 2002. Roles of *Vibrio fischeri* and nonsymbiotic bacteria in the dynamics of mucus secretion during symbiont colonization of the *Euprymna scolopes* light organ. Appl Environ Microbiol **68:**5113-5122.

22. **Nyholm SV, McFall-Ngai MJ.** 2003. Dominance of *Vibrio fischeri* in secreted mucus outside the light organ of *Euprymna scolopes*: the first site of symbiont specificity. Appl Environ Microbiol **69:**3932-3937.

23. **Sycuro LK, Ruby EG, McFall-Ngai M.** 2006. Confocal microscopy of the light organ crypts in juvenile *Euprymna scolopes* reveals their morphological complexity and dynamic function in symbiosis. J Morphol **267:**555-568.

24. **Kremer N, Philipp E, Carpentier M-C, Brennan CA, Kraemer L, Altura MA, Augustin R, Häsler R, Heath-Heckman E, Peyer SM, Schwartzman J, Rader BA, Ruby EG, Rosenstiel P, McFall-Ngai MJ.** 2013. Initial Symbiont Contact Orchestrates Host-Organ-wide Transcriptional Changes that Prime Tissue Colonization. Cell Host Microbe **14**.

25. **Graf J, Dunlap PV, Ruby EG.** 1994. Effect of transposon-induced motility mutations on colonization of the host light organ by *Vibrio fischeri*. J Bacteriol **176:**6986-6991.

26. **DeLoney-Marino CR, Wolfe AJ, Visick KL.** 2003. Chemoattraction of *Vibrio fischeri* to serine, nucleosides, and N-acetylneuraminic acid, a component of squid light-organ mucus. Appl Environ Microbiol **69:**7527-7530.

27. **Deloney-Marino CR, Visick KL.** 2012. Role for *cheR* of *Vibrio fischeri* in the *Vibrio*-squid symbiosis. Can J Microbiol **58:**29-38.

28. **Brennan CA, Mandel MJ, Gyllborg MC, Thomasgard KA, Ruby EG.** 2013. Genetic determinants of swimming motility in the squid light-organ symbiont *Vibrio fischeri*. Microbiologyopen **2:**576-594.

29. **Millikan DS, Ruby EG.** 2004. *Vibrio fischeri* flagellin A is essential for normal motility and for symbiotic competence during initial squid light organ colonization. J Bacteriol **186:**4315-4325.

30. **Millikan DS, Ruby EG.** 2002. Alterations in *Vibrio fischeri* motility correlate with a delay in symbiosis initiation and are associated with additional symbiotic colonization defects. Appl Environ Microbiol **68:**2519-2528.

31. **Ruby EG, Asato LM.** 1993. Growth and flagellation of *Vibrio fischeri* during initiation of the sepiolid squid light organ symbiosis. Arch Microbiol **159:**160-167.

32. **Nyholm SV, McFall-Ngai MJ.** 2004. The winnowing: establishing the squid-*vibrio* symbiosis. Nat Rev Microbiol **2:**632-642.

33. **Canesi L, Gallo G, Gavioli M, Pruzzo C.** 2002. Bacteria-hemocyte interactions and phagocytosis in marine bivalves. Microsc Res Tech **57:**469-476.

34. **Marmaras VJ, Lampropoulou M.** 2009. Regulators and signalling in insect haemocyte immunity. Cell Signal **21:**186-195.

35. **Koropatnick TA, Kimbell JR, McFall-Ngai MJ.** 2007. Responses of host hemocytes during the initiation of the squid-*Vibrio* symbiosis. Biol Bull **212:**29-39.

36. **Montgomery MK, McFall-Ngai M.** 1994. Bacterial symbionts induce host organ morphogenesis during early postembryonic development of the squid *Euprymna scolopes*. Development **120:**1719-1729.

37. **Nyholm SV, Stewart JJ, Ruby EG, McFall-Ngai MJ.** 2009. Recognition between symbiotic *Vibrio fischeri* and the haemocytes of *Euprymna scolopes*. Environ Microbiol **11:**483-493.

38. **Schleicher TR, VerBerkmoes NC, Shah M, Nyholm SV.** 2014. Colonization state influences the hemocyte proteome in a beneficial squid-*Vibrio* symbiosis. Mol Cell Proteomics **13:**2673-2686.

39. **Collins AJ, Schleicher TR, Rader BA, Nyholm SV.** 2012. Understanding the role of host hemocytes in a squid/*Vibrio* symbiosis using transcriptomics and proteomics. Front Immunol **3:**91.

40. **Lamarcq LH, McFall-Ngai MJ.** 1998. Induction of a gradual, reversible morphogenesis of its host's epithelial brush border by *Vibrio fischeri*. Infect Immun **66:**777-785.

41. **Weis VM, Small AL, McFall-Ngai MJ.** 1996. A peroxidase related to the mammalian antimicrobial protein myeloperoxidase in the *Euprymna-Vibrio* mutualism. Proc Natl Acad Sci U S A **93:**13683-13688.

42. **Small AL, McFall-Ngai MJ.** 1999. Halide peroxidase in tissues that interact with bacteria in the host squid *Euprymna scolopes*. J Cell Biochem **72:**445-457.

43. **Davidson SK, Koropatnick TA, Kossmehl R, Sycuro L, McFall-Ngai MJ.** 2004. NO means 'yes' in the squid-vibrio symbiosis: nitric oxide (NO) during the initial stages of a beneficial association. Cell Microbiol **6:**1139-1151.

44. **Foster JS, McFall-Ngai MJ.** 1998. Induction of apoptosis by cooperative bacteria in the morphogenesis of host epithelial tissues. Dev Genes Evol **208:**295-303.

45. **Doino JA, McFall-Ngai MJ.** 1995. A transient exposure to symbiosis-competent bacteria induces light organ morphogenesis in the host squid. Biol Bull **189:**347-355.

46. **Aschtgen M-SS, Wetzel K, Goldman W, McFall-Ngai M, Ruby E.** 2015. *Vibrio fischeri*-derived outer membrane vesicles trigger host development. Cell Microbiol doi:10.1111/cmi.12525.

47. **Ellis TN, Kuehn MJ.** 2010. Virulence and immunomodulatory roles of bacterial outer membrane vesicles. Microbiol Mol Biol Rev **74:**81-94.

48. **Ionescu M, Zaini PA, Baccari C, Tran S, da Silva AM, Lindow SE.** 2014. *Xylella fastidiosa* outer membrane vesicles modulate plant colonization by blocking attachment to surfaces. Proc Natl Acad Sci U S A **111**.

49. **Jones HE, Copland A, Hamstra H, Cohen J, Brown J, Klein N, Ley P, Dixon G.** 2014. LOS oligosaccharide modification enhances dendritic cell responses to meningococcal native outer membrane vesicles expressing a non-toxic lipid A. Cell Microbiol **16:**519-534.

50. **Lappann M, Otto A, Becher D, Vogel U.** 2013. Comparative proteome analysis of spontaneous outer membrane vesicles and purified outer membranes of *Neisseria meningitidis*. J Bacteriol **195:**4425-4435.

51. **Sjöström AE, Sandblad L, Uhlin BE, Wai SN.** 2015. Membrane vesicle-mediated release of bacterial RNA. Sci Rep **5:**15329.

52. **Vanhove A, Duperthuy M, Charrière GM, Roux F, Goudenège D, Gourbal B, Kieffer-Jaquinod S, Couté Y, Wai S, Destoumieux-Garzón D.** 2015. Outer membrane vesicles are vehicles for the delivery of *Vibrio tasmaniensis* virulence factors to oyster immune cells. Environ Microbiol **17:**1152-1165.

53. **Foster JS, Apicella MA, McFall-Ngai MJ.** 2000. *Vibrio fischeri* lipopolysaccharide induces developmental apoptosis, but not complete morphogenesis, of the *Euprymna scolopes* symbiotic light organ. Dev Biol **226:**242-254.

54. **Koropatnick TA, Engle JT, Apicella MA, Stabb EV, Goldman WE, McFall-Ngai MJ.** 2004. Microbial factor-mediated development in a host-bacterial mutualism. Science **306:**1186-1188.

55. **Luker KE, Collier JL, Kolodziej EW, Marshall GR, Goldman WE.** 1993. *Bordetella pertussis* tracheal cytotoxin and other muramyl peptides: distinct structure-activity relationships for respiratory epithelial cytopathology. Proc Natl Acad Sci U S A **90:**2365-2369.

56. **Steimle A, Autenrieth IB, Frick J-SS.** 2016. Structure and function: Lipid A modifications in commensals and pathogens. Int J Med Microbiol doi:10.1016/j.ijmm.2016.03.001.

57. **Kim JK, Park HY, Lee BL.** 2016. The symbiotic role of O-antigen of *Burkholderia* symbiont in association with host *Riptortus pedestris*. Dev Comp Immunol **60:**202-208.

58. **Busset N, De Felice A, Chaintreuil C, Gully D, Fardoux J, Romdhane S, Molinaro A, Silipo A, Giraud E.** 2016. The LPS O-Antigen in Photosynthetic *Bradyrhizobium* Strains Is Dispensable for the Establishment of a Successful Symbiosis with *Aeschynomene* Legumes. PloS one **11**.

59. **Erbs G, Newman MA.** 2012. The role of lipopolysaccharide and peptidoglycan, two glycosylated bacterial microbe-associated molecular patterns (MAMPs), in plant innate immunity. Mol Plant Pathol **13:**95-104.

60. **Guo L, Lim KB, Poduje CM, Daniel M, Gunn JS, Hackett M, Miller SI.** 1998. Lipid A acylation and bacterial resistance against vertebrate antimicrobial peptides. Cell **95:**189-198.

61. **Adin DM, Phillips NJ, Gibson BW, Apicella MA, Ruby EG, McFall-Ngai MJ, Hall DB, Stabb EV.** 2008. Characterization of *htrB* and *msbB* mutants of the light organ symbiont *Vibrio fischeri*. Appl Environ Microbiol **74:**633-644.

62. **Phillips NJ, Adin DM, Stabb EV, McFall-Ngai MJ, Apicella MA, Gibson BW.** 2011. The lipid A from *Vibrio fischeri* lipopolysaccharide: a unique structure bearing a phosphoglycerol moiety. J Biol Chem **286:**21203-21219.

63. **Brennan CA, Hunt JR, Kremer N, Krasity BC, Apicella MA, McFall-Ngai MJ, Ruby EG.** 2014. A model symbiosis reveals a role for sheathed-flagellum rotation in the release of immunogenic lipopolysaccharide. eLife **3**.

64. **Cookson BT, Cho HL, Herwaldt LA, Goldman WE.** 1989. Biological activities and chemical composition of purified tracheal cytotoxin of *Bordetella pertussis*. Infect Immun **57:**2223-2229.

65. **Melly MA, McGee ZA, Rosenthal RS.** 1984. Ability of monomeric peptidoglycan fragments from *Neisseria gonorrhoeae* to damage human fallopian-tube mucosa. J Infect Dis **149:**378-386.

66. **Holtje JV, Mirelman D, Sharon N, Schwarz U.** 1975. Novel type of murein transglycosylase in *Escherichia coli*. J Bacteriol **124:**1067-1076.

67. **Goodell EW.** 1985. Recycling of murein by *Escherichia coli*. J Bacteriol **163:**305-310.

68. **Jacobs C, Huang LJ, Bartowsky E, Normark S, Park JT.** 1994. Bacterial cell wall recycling provides cytosolic muropeptides as effectors for beta-lactamase induction. EMBO J **13:**4684-4694.

69. **Lyon RS.** 2001. Tracheal cytotoxin production by the *Bordetellae*. Ph.D. Washington University, St. Louis, MO.

70. **Mielcarek N, Debrie A-SS, Raze D, Bertout J, Rouanet C, Younes AB, Creusy C, Engle J, Goldman WE, Locht C.** 2006. Live attenuated *B. pertussis* as a single-dose nasal vaccine against whooping cough. PLoS Pathog **2**.

71. **Cloud-Hansen KA, Hackett KT, Garcia DL, Dillard JP.** 2008. *Neisseria gonorrhoeae* uses two lytic transglycosylases to produce cytotoxic peptidoglycan monomers. J Bacteriol **190:**5989-5994.

72. **Adin DM, Engle JT, Goldman WE, McFall-Ngai MJ, Stabb EV.** 2009. Mutations in *ampG* and lytic transglycosylase genes affect the net release of peptidoglycan monomers from *Vibrio fischeri*. J Bacteriol **191:**2012-2022.

73. **Vollmer W.** 2008. Structural variation in the glycan strands of bacterial peptidoglycan. FEMS Microbiol Rev **32**.

74. **Snowden MA, Perkins HR.** 1990. Peptidoglycan cross-linking in *Staphylococcus aureus*. Eur J Biochem **191**.

75. **Glauner B, Höltje JV, Schwarz U.** 1988. The composition of the murein of *Escherichia coli*. J Biol Chem **263:**10088-10095.

76. **Lemaitre B, Hoffmann J.** 2007. The host defense of Drosophila melanogaster. Annu Rev Immunol **25:**697-743.

77. **Kaneko T, Yano T, Aggarwal K, Lim J-H, Ueda K, Oshima Y, Peach C, Erturk-Hasdemir D, Goldman WE, Oh B-H, Kurata S, Silverman N.** 2006. PGRP-LC and PGRP-LE have essential yet distinct functions in the drosophila immune response to monomeric DAP-type peptidoglycan. Nat Immunol **7:**715-723.

78. **Lemaitre B, Hoffmann J.** 2007. The host defense of *Drosophila melanogaster*. Annu Rev Immunol **25:**697-743.

79. **Han YW.** 2015. *Fusobacterium nucleatum*: a commensal-turned pathogen. Curr Opin Microbiol **23C:**141-147.

80. **Colucci F.** 2015. An Oral Commensal Associates with Disease: Chicken, Egg, or Red Herring? Immunity **42:**208-210.

81. **Fukamachi H, Nakano Y, Yoshimura M, Koga T.** 2002. Cloning and characterization of the l-cysteine desulfhydrase gene of *Fusobacterium nucleatum*. FEMS Microbiol Lett **215:**75-80.

82. **Yoshida Y, Ito S, Kamo M, Kezuka Y, Tamura H, Kunimatsu K, Kato H.** 2010. Production of hydrogen sulfide by two enzymes associated with biosynthesis of homocysteine and lanthionine in *Fusobacterium nucleatum* subsp. *nucleatum* ATCC 25586. Microbiology **156:**2260-2269.

83. **Awano N, Wada M, Mori H, Nakamori S, Takagi H.** 2005. Identification and functional analysis of *Escherichia coli* cysteine desulfhydrases. Appl Environ Microbiol **71:**4149-4152.

84. **Turner RD, Vollmer W, Foster SJ.** 2014. Different walls for rods and balls: The diversity of peptidoglycan. Mol Microbiol **91:**862-874.

85. **Schleife.Kh, Kandler O.** 1972. Peptidoglycan Types of Bacterial Cell-Walls and Their Taxonomic Implications. Bacteriol Rev **36:**407-477.

86. **He W, Li C, Lu C-D.** 2011. Regulation and characterization of the *dadRAX* locus for d-amino acid catabolism in *Pseudomonas aeruginosa* PAO1. J Bacteriol **193:**2107-2115.

87. **He W, Li G, Yang C-K, Lu C-D.** 2014. Functional characterization of the *dguRABC* locus for d-Glu and d-Gln utilization in *Pseudomonas aeruginosa* PAO1. Microbiology **160:**2331-2340.

88. **Cava F, Lam H, de Pedro MA, Waldor MK.** 2011. Emerging knowledge of regulatory roles of D-amino acids in bacteria. Cell Mol Life Sci **68:**817-831.

89. **Radkov AD, Moe LA.** 2014. Bacterial synthesis of D-amino acids. Appl Microbiol Biotechnol **98:**5363-5374.

90. **Espaillat A, Carrasco-López C, Bernardo-García N, Pietrosemoli N, Otero LH, Álvarez L, de Pedro MA, Pazos F, Davis BM, Waldor MK, Hermoso JA, Cava F.** 2013. Structural basis for the broad specificity of a new family of amino-acid racemases. Acta Crystallogr D Biol Crystallogr **70:**79-90.

91. **Lam H, Oh D-CC, Cava F, Takacs CN, Clardy J, de Pedro MA, Waldor MK.** 2009. D-amino acids govern stationary phase cell wall remodeling in bacteria. Science **325:**1552-1555.

92. **Ota N, Shi T, Sweedler JV.** 2012. d-Aspartate acts as a signaling molecule in nervous and neuroendocrine systems. Amino Acids **43:**1873-1886.

93. **Errico F, Napolitano F, Nisticò R, Centonze D, Usiello A.** 2008. D-aspartate: an atypical amino acid with neuromodulatory activity in mammals. Reviews in the neurosciences **20:**429-440.

94. **D'Aniello A.** 2007. D-Aspartic acid: an endogenous amino acid with an important neuroendocrine role. Brain research reviews **53:**215-234.

95. **Katane M, Homma H.** 2011. D-Aspartate--an important bioactive substance in mammals: a review from an analytical and biological point of view. J Chromatogr B Analyt Technol Biomed Life Sci **879:**3108-3121.

96. **Errico F, Rossi S, Napolitano F, Catuogno V, Topo E, Fisone G, D'Aniello A, Centonze D.** 2008. D-aspartate prevents corticostriatal long-term depression and attenuates schizophrenia-like symptoms induced by amphetamine and MK-801. J Neurosci **28:**10404 –10414.

97. **Kim PM, Molliver ME, Blackshaw S, Young SG.** 2006. Behavioural alterations in male mice lacking the gene for D-aspartate oxidase. Behav Brain Res **171:**295-302.

98. **Nørregaard-Madsen M, McFall E, Valentin-Hansen P.** 1995. Organization and transcriptional regulation of the *Escherichia coli* K-12 D-serine tolerance locus. J Bacteriol **177:**6456-6461.

99. **Moritz RL, Welch RA.** 2006. The *Escherichia coli argW-dsdCXA* genetic island is highly variable, and E. coli K1 strains commonly possess two copies of *dsdCXA*. J Clin Microbiol **44:**4038-4048.

100. **Hryckowian AJ, Baisa GA, Schwartz KJ, Welch RA.** 2015. *dsdA* Does Not Affect Colonization of the Murine Urinary Tract by *Escherichia coli* CFT073. PloS one **10**.

101. **Connolly JP, Gabrielsen M, Goldstone RJ, Grinter R, Wang D, Cogdell RJ, Walker D, Smith DG, Roe AJ.** 2016. A Highly Conserved Bacterial D-Serine Uptake System Links Host Metabolism and Virulence. PLoS Pathog **12**.

102. **Connolly JPR, Goldstone RJ, Burgess K, Cogdell RJ, Beatson SA, Vollmer W, Smith DGE, Roe AJ.** 2015. The host metabolite D-serine contributes to bacterial niche specificity through gene selection. ISME J **9:**1039-1051.

103. **Steen AD, Jørgensen BB, Lomstein BA.** 2013. Abiotic racemization kinetics of amino acids in marine sediments. PloS one **8**.

104. **Man EH, Bada JL.** 1987. Dietary D-amino acids. Annu Rev Nutr **7:**209-225.

105. **Yoshimura T, Esak N.** 2003. Amino acid racemases: functions and mechanisms. J Biosci Bioeng **96:**103-109.

106. **Tanaka-Hayashi A, Hayashi S, Inoue R, Ito T, Konno K, Yoshida T, Watanabe M, Yoshimura T, Mori H.** 2015. Is D-aspartate produced by glutamic-oxaloacetic transaminase-1 like 1 (Got1ll): a putative aspartate racemase? Amino Acids **47:**79-86.

107. **Raucci F, Fiore M.** 2011. D-Asp: a new player in reproductive endocrinology of the amphibian *Rana esculenta*. J Chromatogr B Analyt Technol Biomed Life Sci **879:**3268-3276.

108. **Uda K, Abe K, Dehara Y, Mizobata K, Sogawa N, Akagi Y, Saigan M, Radkov AD, Moe LA.** 2015. Distribution and evolution of the serine/aspartate racemase family in invertebrates. Amino Acids **48:**387–402.

109. **Wang L, Ota N, Romanova EV, Sweedler JV.** 2011. A novel pyridoxal 5'-phosphate-dependent amino acid racemase in the *Aplysia californica* central nervous system. J Biol Chem **286:**13765-13774.

110. **Hernández SB, Cava F.** 2016. Environmental roles of microbial amino acid racemases. Environ Microbiol **18:**1673-1685.

111. **Hanby WE, Rydon HN.** 1946. The capsular substance of *Bacillus anthracis*. Biochem J **40:**297-309.

112. **Moe LA.** 2013. Amino acids in the rhizosphere: From plants to microbes. Am J Bot **100:**1692-1705.

113. **Sasabe J, Miyoshi Y, Rakoff-Nahoum S, Zhang T, Mita M, Davis BM, Hamase K, Waldor MK.** 2016. Interplay between microbial D-amino acids and host D-amino acid oxidase modifies murine mucosal defence and gut microbiota. Nat Microbiol **1:**16125.

114. **Azúa I, Goiriena I, Baña Z, Iriberri J, Unanue M.** 2013. Release and consumption of D-amino acids during growth of marine prokaryotes. Microb Ecol **67:**1-12.

115. **Teira E, van Aken H, Veth C, Herndl GJ.** 2006. Archaeal uptake of enantiomeric amino acids in the meso- and bathypelagic waters of the North Atlantic. Limnol Oceanogr **51:**60-69.

116. **Pèrez MT, Pausz C, Herndl GJ.** 2003. Major shift in bacterioplankton utilization of enantiomeric amino acids between surface waters and the ocean's interior. Limnol Oceanogr **48:**755-763.

117. **Schleife K, Kandler O.** 1972. Peptidoglycan types of bacterial cell-walls and their taxonomic implications. Bacteriol Rev **36:**407-477.

118. **Chesnokova ON, McPherson SA, Steichen CT, Turnbough CL, Jr.** 2009. The spore-specific alanine racemase of *Bacillus anthracis* and its role in suppressing germination during spore development. J Bacteriol **191:**1303-1310.

119. **Lyell NL, A. N. Septer, A.K. Dunn, D. Duckett, Stoudenmire and E.V. Stabb.** 2017. An expanded transposon-mutant library reveals that *Vibrio fischeri* δ-aminolevulinate auxotrophs can colonize *Euprymna scolopes*. Appl Environ Microbiol **(In Press)**.

120. **Schell MA.** 1993. Molecular biology of the LysR family of transcriptional regulators. Annu Rev Microbiol **47:**597-626.

121. **Fulton DL, Li YY, Laird MR, Horsman BGS, Roche FM, Brinkman FSL.** 2006. Improving the specificity of high-throughput ortholog prediction. BMC Bioinformatics **7:**1-16.

122. **Alanazi AM, Neidle EL, Momany C.** 2013. The DNA-binding domain of BenM reveals the structural basis for the recognition of a T-N11-A sequence motif by LysR-type transcriptional regulators. Acta Crystallogr D Struct Biol **69:**1995-2007.

123. **Craven SH, Obidimma C. Ezeika, Cory Momany and Ellen L. Neidle.** 2008. LysR Homologs in *Acinetobacter*: Insights into a Diverse and Prevalent Family of Transcriptional Regulators, p 163-202. *In* Gerischer U (ed), *Acinetobacter* Molecular Biology. Horizon Press, Norwich, U.K.

124. **Verzijl D, Riedl T, Parren PWHI, Gerritsen AF.** 2017. A novel label-free cell-based assay technology using biolayer interferometry. Biosens Bioelectron **87:**388-395.

125. **Furuchi T, Suzuki T, Sekine M, Katane M, Homma H.** 2009. Apoptotic inducers activate the release of D-aspartate through a hypotonic stimulus-triggered mechanism in PC12 cells. Arch Biochem Biophys **490:**118-128.

126. **Ahn J-WW, Chang JH, Kim K-JJ.** 2015. Structural basis for an atypical active site of an L-aspartate/glutamate-specific racemase from *Escherichia coli*. FEBS Lett **589:**3842-3847.

127. **Clarke S.** 2003. Aging as war between chemical and biochemical processes: protein methylation and the recognition of age-damaged proteins for repair. Ageing Res Rev **2:**263-285.

128. **Aswad DW, Paranandi MV, Schurter BT.** 2000. Isoaspartate in peptides and proteins: formation, significance, and analysis. J Pharm Biomed Anal **21:**1129-1136.

129. **Fu JC, Ding L, Clarke S.** 1991. Purification, gene cloning, and sequence analysis of an L-isoaspartyl protein carboxyl methyltransferase from *Escherichia coli*. J Biol Chem **266:**14562-14572.

130. **Hicks WM, Kotlajich MV, Visick JE.** 2005. Recovery from long-term stationary phase and stress survival in *Escherichia coli* require the L-isoaspartyl protein carboxyl methyltransferase at alkaline pH. Microbiology **151:**2151-2158.

131. **Kumawat M, Pesingi P, Agarwal R, Goswami T, Mahawar M.** 2016. Contribution of protein isoaspartate methyl transferase (PIMT) in the survival of *Salmonella typhimurium* under oxidative stress and virulence. Int J Med Microbiol **306:**222-230.

132. **Gebendorfer KM, Drazic A, Le Y, Gundlach J, Bepperling A, Kastenmüller A, Ganzinger KA, Braun N, Franzmann TM, Winter J.** 2012. Identification of a hypochlorite-specific transcription factor from *Escherichia coli*. J Biol Chem **287:**6892-6903.

133. **Drazic A, Miura H, Peschek J, Le Y, Bach NC, Kriehuber T, Winter J.** 2013. Methionine oxidation activates a transcription factor in response to oxidative stress. Proc Natl Acad Sci U S A **110:**9493-9498.

134. **Visick KL, Ruby EG.** 1998. The periplasmic, group III catalase of *Vibrio fischeri* is required for normal symbiotic competence and is induced both by oxidative stress and by approach to stationary phase. J Bacteriol **180:**2087-2092.

135. **Miller J.** 1992. A short course in bacterial genetics. Cold Spring Harbor Laboratory Press, New York, NY.

136. **Ornston LNaRYS.** 1966. The conversion of catechol and protocatechuate to beta-ketoadipate by Pseudomonas putida. . J Biol Chem **241:**3787-3794.

137. **Stabb EV, Reich KA, Ruby EG.** 2001. *Vibrio fischeri* genes *hvnA* and *hvnB* encode secreted NAD(+)-glycohydrolases. J Bacteriol **183:**309-317.

138. **Juni E, Janik A.** 1969. Transformation of *Acinetobacter calco-aceticus* (*Bacterium anitratum*). J Bacteriol **98:**281-288.

139. **Vaneechoutte M, Young DM, Ornston NL, Baere T, Nemec A, Reijden T, Carr E, Tjernberg I, Dijkshoorn L.** 2006. Naturally Transformable *Acinetobacter sp.* Strain ADP1 Belongs to the Newly Described Species *Acinetobacter baylyi*. Appl Environ Microbiol **72:**932-936.

140. **Stabb EV, Ruby EG.** 2002. RP4-based plasmids for conjugation between *Escherichia coli* and members of the *Vibrionaceae*. Methods Enzymol **358:**413-426.

141. **Hanahan D.** 1983. Studies on transformation of *Escherichia coli* with plasmids. J Mol Biol **166:**557-580.

142. **Dunn AK, Martin MO, Stabb EV.** 2005. Characterization of pES213, a small mobilizable plasmid from *Vibrio fischeri*. Plasmid **54:**114-134.

143. **Galloway NR, Toutkoushian H, Nune M, Bose N, Momany C.** 2013. Rapid cloning for protein crystallography using type IIS restriction enzymes. Cryst Growth Des **13:**2833-2839.

144. **Colton DM, Stoudenmire JL, Stabb EV.** 2015. Growth on glucose decreases cAMP-CRP activity while paradoxically increasing intracellular cAMP in the light-organ symbiont *Vibrio fischeri*. Mol Microbiol **97:**1114-1127.

145. **Jones RM, Williams PA.** 2003. Mutational analysis of the critical bases involved in activation of the AreR-regulated sigma54-dependent promoter in *Acinetobacter sp.* strain ADP1. Appl Environ Microbiol **69:**5627-5635.

146. **Yanisch-Perron C, Vieira J, Messing J.** 1985. Improved M13 phage cloning vectors and host strains: nucleotide sequences of the M13mp18 and pUC19 vectors. Gene **33:**103-119.

147. **Dunn AK, Millikan DS, Adin DM, Bose JL, Stabb EV.** 2006. New rfp- and pES213-derived tools for analyzing symbiotic *Vibrio fischeri* reveal patterns of infection and *lux* expression *in situ*. Appl Environ Microbiol **72:**802-810.

148. **Kearse M, Moir R, Wilson A, Stones-Havas S, Cheung M, Sturrock S, Buxton S, Cooper A, Markowitz S, Duran C, Thierer T, Ashton B, Meintjes P, Drummond A.** 2012. Geneious Basic: an integrated and extendable desktop software platform for the organization and analysis of sequence data. Bioinformatics **28:**1647-1649.

149. **Kimbrough JH, Stabb EV.** 2015. Antisocial *luxO* mutants provide a stationary-phase aurvival advantage in *Vibrio fischeri* ES114. J Bacteriol **198:**673-687.

150. **Herrero M, de Lorenzo V, Timmis KN.** 1990. Transposon vectors containing non-antibiotic resistance selection markers for cloning and stable chromosomal insertion of foreign genes in Gram-negative bacteria. J Bacteriol **172:**6557-6567.

151. **Sambrook J, Fritsch EF, Maniatis T.** 1989. Molecular cloning, vol 2. Cold spring harbor laboratory press, New York.

152. **Horton RM, Cai ZL, Ho SN, Pease LR.** 1990. Gene splicing by overlap extension: tailor-made genes using the polymerase chain reaction. Biotechniques **8:**528-535.

153. **Neidle EL, Hartnett C, Ornston LN.** 1989. Characterization of *Acinetobacter calcoaceticus catM*, a repressor gene homologous in sequence to transcriptional activator genes. J Bacteriol **171:**5410-5421.

154. **Reams AB, Neidle EL.** 2003. Genome plasticity in *Acinetobacter*: new degradative capabilities acquired by the spontaneous amplification of large chromosomal segments. Mol Microbiol **47:**1291-1304.

155. **Seaton SC, Elliott KT, Cuff LE, Laniohan NS, Patel PR, Neidle EL.** 2012. Genome-wide selection for increased copy number in *Acinetobacter baylyi* ADP1: locus and context-dependent variation in gene amplification. Mol Microbiol **83:**520-535.

156. **Hayashi K.** 1975. A rapid determination of sodium dodecyl sulfate with methylene blue. Anal Biochem **67:**503-506.

157. **González-Castro MJ, López-Hernández J, Simal-Lozano J, Oruña-Concha MJ.** 1997. Determination of amino acids in green beans by derivatization with phenylisothiocianate and high-performance liquid chromatography with ultraviolet detection. J Chromatogr Sci **35:**181-185.

158. **Popham DL, Helin J, Costello CE, Setlow P.** 1996. Analysis of the peptidoglycan structure of *Bacillus subtilis* endospores. J Bacteriol **178:**6451-6458.

159. **Studier FW.** 2005. Protein production by auto-induction in high density shaking cultures. Protein Expr Purif **41:**207-234.

160. **Solovyev VaS, A.** 2011. Automatic Annotation of Microbial Genomes and Metagenomic Sequences. Nova Science Publishers.

161. **Mrázek J, Xie S.** 2006. Pattern locator: a new tool for finding local sequence patterns in genomic DNA sequences. Bioinformatics **22:**3099-3100.

162. **Aziz RK, Bartels D, Best AA, DeJongh M, Disz T, Edwards RA, Formsma K, Gerdes S, Glass EM, Kubal M, Meyer F, Olsen GJ, Olson R, Osterman AL, Overbeek RA, McNeil LK, Paarmann D, Paczian T, Parrello B, Pusch GD, Reich C, Stevens R, Vassieva O, Vonstein V, Wilke A, Zagnitko O.** 2008. The RAST Server: rapid annotations using subsystems technology. BMC genomics **9:**75.

163. **McCoy AJ, Adams NE, Hudson AO, Gilvarg C, Leustek T, Maurelli AT.** 2006. L,L-diaminopimelate aminotransferase, a trans-kingdom enzyme shared by *Chlamydia* and plants for synthesis of diaminopimelate/lysine. Proc Natl Acad Sci U S A **103:**17909-17914.

164. **Karita M, Etterbeek ML, Forsyth MH, Tummuru MK, Blaser MJ.** 1997. Characterization of *Helicobacter pylori dapE* and construction of a conditionally lethal *dapE* mutant. Infect Immun **65:**4158-4164.

165. **Brooks JF, Gyllborg MC, Cronin DC, Quillin SJ, Mallama CA, Foxall R, Whistler C, Goodman AL, Mandel MJ.** 2014. Global discovery of colonization determinants in the squid symbiont *Vibrio fischeri*. Proc Natl Acad Sci U S A **111:**17284-17289.

166. **Cloud-Hansen KA, Peterson SB, Stabb EV, Goldman WE, McFall-Ngai MJ, Handelsman J.** 2006. Breaching the great wall: peptidoglycan and microbial interactions. Nat Rev Microbiol **4:**710-716.

167. **Sinha RK, Rosenthal RS.** 1980. Release of Soluble Peptidoglycan from Growing Gonococci: Demonstration of Anhydro-Muramyl-Containing Fragments. Infect Immun **29:**914-925.

168. **Lyell NL, A. N. Septer, A.K. Dunn, D. Duckett, Stoudenmire and E.V. Stabb.** 2017. An expanded transposon-mutant library reveals that *Vibrio fischeri* δ-aminolevulinate auxotrophs can colonize *Euprymna scolopes*. Appl Environ Microbiol **83**.

169. **Kurata S.** 2014. Peptidoglycan recognition proteins in *Drosophila* immunity. Dev Comp Immunol **42:**36-41.

170. **Stenbak CR, Ryu J-HH, Leulier F, Pili-Floury S, Parquet C, Hervé M, Chaput C, Boneca IG, Lee W-JJ, Lemaitre B, Mengin-Lecreulx D.** 2004. Peptidoglycan molecular requirements allowing detection by the *Drosophila* immune deficiency pathway. J Immunol **173:**7339-7348.

171. **Uehara A, Fujimoto Y, Kawasaki A, Kusumoto S, Fukase K, Takada H.** 2006. *Meso*-diaminopimelic acid and *meso*-lanthionine, amino acids specific to bacterial peptidoglycans, activate human epithelial cells through NOD1. J Immunol **177:**1796-1804.

172. **Tohno M, Shimazu T, Aso H, Uehara A, Takada H, Kawasaki A, Fujimoto Y, Fukase K, Saito T, Kitazawa H.** 2008. Molecular cloning and functional characterization of porcine nucleotide-binding oligomerization domain-1 (NOD1) recognizing minimum agonists, *meso*-diaminopimelic acid and *meso*-lanthionine. Mol Immunol **45:**1807-1817.

173. **Kouidmi I, Levesque RC, Paradis-Bleau C.** 2014. The biology of Mur ligases as an antibacterial target. Mol Microbiol **94:**242-253.

174. **Post DM, Ketterer MR, Phillips NJ, Gibson BW, Apicella MA.** 2003. The *msbB* mutant of *Neisseria meningitidis* strain NMB has a defect in lipooligosaccharide assembly and transport to the outer membrane. Infect Immun **71:**647-655.

175. **Hauryliuk V, Atkinson GC, Murakami KS, Tenson T, Gerdes K.** 2015. Recent functional insights into the role of (p)ppGpp in bacterial physiology. Nat Rev Microbiol **13:**298-309.